

CRANFIELD UNIVERSITY

Junguo Zhao

Areal Artefact Manufacturing Using SPDT

SATM
Cranfield University

MRes in Manufacturing
Academic Year: 2017 - 2018

Supervisor: Dr. Claudiu Giusca Dr. Saurav Goel
August 2018

CRANFIELD UNIVERSITY

Cranfield University
Precision Engineering

MRes in Manufacturing

Academic Year 2017 - 2018

Junguo Zhao

Areal Artefact Manufacturing Using SPDT

Supervisor: Dr. Claudiu Giusca Dr. Saurav Goel

August 2018

This thesis is submitted in partial fulfilment of the requirements for
the degree of MRes

***(NB. This section can be removed if the award of the degree is
based solely on examination of the thesis)***

© Cranfield University 2018. All rights reserved. No part of this
publication may be reproduced without the written permission of the
copyright owner.

ABSTRACT

With the increasing importance of the surface engineering, surface topography measuring instrument has been used in wider range of applications, which requires trustworthy calibration process to deliver traceability so that the instrument is able to give comparable and reliable measurement. The calibration standard / artefact is designed to transfer traceability easily and reliably. In current market, the feature of the artefact used for evaluation the surface topography measuring process are not sufficiently accurate. This insufficiency may be solved by using certain types of calibration standard specified in ISO standard however they are not commercially produced. In this project, one of the desired types called 'radial sinusoidal shape' was produce by SPDT (single point diamond turning) manufacturing method. The feature parameters of the artefact are designed to meet the instrument measurement requirement and the machining path is generated with consideration of the tooling geometry. To assess the repeatability in z direction of the turning machine, a step height experiment was designed and conducted. The measurement result indicates that the repeatability of the machine is unsatisfactory when the feed distance smaller than 100 nm. The wavelength and the amplitude of machined radial sinusoidal shape was measured by stylus profiler, followed by the measurement uncertainty analysis. The measurement result was compared with the design to evaluate quality of the manufacturing process. To estimate the systematic error of the profiler, CCI was used to measure the machined radial sinusoidal shape. The measurement result was also compared with the design.

Keywords:

Surface topography measuring instrument, calibration, SPDT, measurement uncertainty.

ACKNOWLEDGEMENTS

I would firstly thank my supervisors Dr. Claudiu Giusca and Dr. Saurav Goel. They have been helping me with understanding the project and the knowledge since very beginning. They encourage me to explore the unknown independently, which cultivates me to transform from a student to an independent researcher.

I would like to thank the technique support Mr. Alan Heaume. He trained me the safe operation of the measuring instruments. Most importantly, without his years' experience on diamond turning, this project would not have physical output. I also would like to thank Dr. Christopher Shaw who showed me how to operation DektakXT profiler.

I would like to thank the examiner of my internal review Dr. Jafar Jamshidi. He pointed out the inadequacies of my progress and the presentation with full patience and even explained the concept that I was confused at that time.

I would like to thank my classmates in CDT, who are also my friends. We had unforgettable time during modules, conferences, industry tour and individual project.

Then I would like to thank my boyfriend Peter Polak for encouraging me throughout the entire year, especially during the occasionally hard time. Moreover, I would like to thank him for guiding me with studying Matlab. I would not be able to have big progress without him.

Finally, I would like to express my profound gratitude to my parents for supporting me for years studying and the coming PhD. They are always there to encourage me to pursue uphill of my life and guide me to be an upright person. I would not have any accomplishment without them.

TABLE OF CONTENTS

ABSTRACT	i
ACKNOWLEDGEMENTS.....	ii
LIST OF FIGURES.....	v
LIST OF TABLES	ix
LIST OF ABBREVIATIONS.....	x
1 Introduction.....	11
1.1 Calibration standard.....	12
1.2 Aim of project.....	14
2 Literature review.....	15
2.1 'Material measures'	15
2.2 'Stedman diagram'	18
2.3 Artefacts.....	20
2.3.1 Type AIR	21
2.3.2 Type PGR	24
2.3.3 Type PPT	28
2.3.4 Type PCS.....	30
2.3.5 Type ASG.....	31
2.3.6 Type PPS	33
2.3.7 Type AFL.....	34
2.3.8 Type ACG, combine with type PRB or type ASP	35
2.3.9 Type PPR.....	39
2.4 Manufacturing methods for artefacts.....	40
2.5 Knowledge gap	43
2.6 Objectives	44
2.7 Research questions	45
2.8 Hypotheses.....	45
3 Methodology.....	45
4 Results and discussions.....	48
4.1 Feature and machining process design	48
4.2 Performance verification of SPDT in z direction.....	52
4.2.1 Introduction	52
4.2.2 Experiments	53
4.3 Product measurement.....	63
4.3.1 Method	63
4.3.2 Results	65
5 Measurement uncertainty	78
6 Application of the product.....	84
7 Summary	87
8 Conclusion.....	87
9 Future work	88

REFERENCES.....	89
APPENDICES	97
Appendix A G-code for radial sinusoidal shape	97

LIST OF FIGURES

Figure 1. Calibration and traceability pyramid	12
Figure 2. Surface topography measuring process.....	13
Figure 3. Typical constraints in traditional AW space plots [13].....	19
Figure 4. Stedman diagram sketch [17].....	20
Figure 5. Left: Fabricated roughness specimen by grayscale EBL. Right: Fabricated roughness specimen by DLW. For both: (a) Design surface. The inset shows the corresponding 3D view plot. (b) Typical measured AFM image of the topography. [25]	22
Figure 6. Bandwidth distribution of irregular artefact and example instruments (CCI: Coherence Correlation Interferometer, stands for non-contact measuring instrument; Dektak XT: stands for contact measuring instrument)	23
Figure 7. Different step on artefact [28].....	25
Figure 8. Possible implementation of a profile for an Sq calibration standard. A simple rectangular profile where the upper and lower terraces have equal area result in an Sq value that is half the height difference between the levels.[29]	25
Figure 9. Scheme of the fabrication processes [31]	26
Figure 10. AFM image of a silicon single atom stepped surface [32]	26
Figure 11. Depth-setting standard developed by PTB (source: https://www.ptb.de/cms/en/ptb/fachabteilungen/abt5/fb-51/ag-5110/mikromesstechniknormale0/tiefeneinstellnormale00.html)	27
Figure 12. Bandwidth distribution of step height artefact and example instruments	28
Figure 13. AFM / SPM calibration grating, undercut edges (source: https://www.microtonano.com/AFM-XYZ-calibration-standard-for-calibrated-measurements-and-dimensions.php?currency=pounds#a34030100B).....	29
Figure 14. AFM / SPM calibration grating, trapezoid structure (source: https://www.microtonano.com/AFM-XYZ-calibration-standard-for-calibrated-measurements-and-dimensions.php?currency=pounds#a34030100B).....	29
Figure 15. A Micro-Artefact for Fringe Projection (source: https://www.ptb.de/cms/fileadmin/internet/fachabteilungen/abteilung_5/5.3_koordinatenmesstechnik/Messgeraete_Bilder/5.3/uPK-Flyer-engl.pdf)	30
Figure 16. Cross grating and star shape artefact [39]	31
Figure 17. NPL areal standard [40]	32

Figure 18. Bandwidth distribution of star shape artefact and example instruments	32
Figure 19. Confocally scanned 3D data set of the chirp standard of a μ_{surf} explorer microscope by NanoFocus AG. [41]	33
Figure 20. Bird's eye view of profiles measured by LSM. [43]	34
Figure 21. Bandwidth distribution of chirp artefact and example instruments...	34
Figure 22. Bandwidth distribution of flat artefact and example instruments.....	35
Figure 23. AFM image of cross grating. (source: http://www.tedpella.com/calibration_html/afm_spm_calibration.htm.aspx#677-AFM).....	36
Figure 24. Pyramid feature grating (source: https://anfatec-shop.de/p/tgt1).....	37
Figure 25. Hemisphere feature grating [49]	37
Figure 26. Diamond feature grating (source: https://www.emsdiasum.com/microscopy/products/sem/standards.aspx) .	37
Figure 27. Combined shapes grating (source: https://www.thorlabs.com/newgrouppage9.cfm?objectgroup_id=7502).....	38
Figure 28. Letters 'AR' grating (source: https://www.asylumresearch.com/Products/CalStd/CalStd.shtml)	38
Figure 29. Bandwidth distribution of cross grating artefact and example instruments	39
Figure 30. Line grating. (source: https://anfatec-shop.de/p/tdg01)	40
Figure 31. Bandwidth distribution of combination of all types of artefact and example instruments	43
Figure 32. Radial sinusoidal geometry	48
Figure 33. Illustration of the tool path generation of radial sinusoidal shape in small scale.....	51
Figure 34. Tool path in real machining condition	51
Figure 35. Moore nanotech 350UPL ultra-precision turning machine outside-look (top picture) and inside structure (bottom picture)	53
Figure 36. Depth of cut copper sample	54
Figure 37. Talysurf Series 2 profilometer	55
Figure 38. The arrows are the approximate measurement positions and directions	55

Figure 39. Data analysis on TalyMap Gold 4.1.....	55
Figure 40. Error and standard uncertainty of programmed vs measured depths. First to third cut corresponds to cutting direction. Left: cutting from edge to the centre; right: cutting from centre to the edge.	57
Figure 41. Possible error sources during the SPDT process.....	58
Figure 42. Calibrated step height artefact	59
Figure 43. Calibrated optical flat standard.....	60
Figure 44. Assessment of flatness effect on step height measurement	61
Figure 45. Histogram showing heights distribution. Around value of 44.5 nm owns most of the calculated step height	61
Figure 46. DektakXT overview	64
Figure 47. DektakXT close view	64
Figure 48. Extract profiles	65
Figure 49. Striped-scans	65
Figure 50. 60° profile measured on DektakXT.....	66
Figure 51. 60° profile, left waves	66
Figure 52. 60° profile, right waves	66
Figure 53. 60° profile, left waves, levelled	67
Figure 54. 60° profile, left waves, levelled, and morphological filtered	67
Figure 55. Subtraction between DektakXT measured 0° profile, left waves (blue) and designed waves (red).	67
Figure 56. Above: subtraction between CCI measured profile, left waves (blue) and designed waves (red). Below: residual profile. (Ra 14.1nm, Rq 17nm)	68
Figure 57. 120° profile, left waves fitting result. Black curve: data points; blue curve: fitting curve; red curve: excluded data points.....	69
Figure 58. Above: subtraction between measured 0° profile, left waves (blue) and best fitting result (red). Below: residual profile.....	72
Figure 59. Above: subtraction between measured 0° profile, right waves (blue) and best fitting result (red). Below: residual profile.....	72
Figure 60. Subtraction between measured 120° profile, second measurement, left waves (blue) and best fitting result (red).....	73
Figure 61. Subtraction between measured 120° profile, second measurement, right waves (blue) and best fitting result (red).....	73

Figure 62. Subtraction between measured 60° profile, left waves (blue) and best fitting result (red).....	73
Figure 63. Subtraction between measured 60° profile, right waves (blue) and best fitting result (red).....	74
Figure 64. Subtraction of 120° profile, left waves, first and second measurements.	75
Figure 65. Above: subtraction between measured 0° profile, right waves (blue) and 60° profile, right waves (red). Below: residual profile.....	75
Figure 66. Above: subtraction between measured 0° profile, left waves (blue) and 60° profile, left waves (red). Below: residual profile.....	76
Figure 67. Residual profile of subtraction between 0° profile, left waves and 60° profile, left waves measured by CCI. (Ra 1.71 nm; Rq 2.06 nm).....	76
Figure 68. Subtraction of two profiles extracted from two repeated measurement of CCI. Geometry influence in the middle was thresholded. (Ra 1.82 nm, Rq 2.36 nm).....	77
Figure 69. Periodical sinusoidal shape (Type PPS) [9]. p: period; d: amplitude.	81
Figure 70. Cross grating (Type ACG) [9]. l_x, l_y : pitch in x and y axis; θ : angle between x and y axes; d : depth of the pits.	82
Figure 71. Taylor Hobson CCI 6000.....	84
Figure 72. Example of measurement from CCI.....	85
Figure 73. Extracted area of repeated measurement from CCI.....	85
Figure 74. Designed radial sinusoidal shape, imported in Talymap.	85

LIST OF TABLES

Table 1. List of metrological characteristics for surface texture measurement methods [7].....	13
Table 2. Types of profile material measure and evaluated metrological characteristics and parameters [10][11].....	15
Table 3. Types of areal material measure and evaluated metrological characteristics and parameters [10][11].....	16
Table 4. Graphical profile type of material measures	17
Table 5. Graphical areal type of material measures	17
Table 6. Measurement on first sample: cutting from edge to centre.....	56
Table 7. Measurement on second sample: cutting from centre to edge.....	57
Table 8. Measurement results of calibrated step height on different position of z working range (25%, 50% and 75% of working range representatively) Unit: nm	60
Table 9. Uncertainty contributed to step height measurements	63
Table 10. Fitting results of measured profiles (unit: mm).....	69
Table 11. Fitting results of 120 degree measured profiles (unit: mm).....	70
Table 12. Repeated measurement of wavelength and amplitude.....	71
Table 13. Roughness parameters of residual profiles between residual profiles and best fitting result	74
Table 14. Residual of subtractions between different measurements	77
Table 15. Uncertainty sources of measurement	78
Table 16. Flatness measurements	80
Table 17. Step height measurement and uncertainty contribution.....	80
Table 18. Repeated measurement results of the product on CCI.....	86

LIST OF ABBREVIATIONS

DLW	Direct laser writing
EBL	Electron beam lithography
EDM	Electric discharge machining
FIB	Focus ion beam
MC	Metrological characteristics
SPDT	Single point diamond turning
WLI/CCI	White light interferometer

1 Introduction

In the past 20 years surface texture has been used to enhance the functionality of the manufactured parts. Hence measurement of surface texture plays an important role in the production quality control and assurance [1].

Three methods are used to measure surface texture: line-profiling method, areal-topography method and areal-integrating method [2]. By using line-profiling method, two-dimensional graph of the surface geometry is produced, which could be expressed as a height function $z(x)$. By applying areal-topography method, three-dimensional image of the surface irregularity is generated, which may be defined as a height function $z(x, y)$ of two independent variables x and y , or a series parallel two-dimension profiles are juxtaposed, which is explained as $z(x)$ as a function of y . Areal-integrating method measures a representative area of the surface, and provides a numerical result, neither profiling data $z(x)$ nor areal-topography data $z(x, y)$. For instance, total integrated scatter [3] and angle-resolved scatter [4] methods collect the light scattered from the surface to calculate surface roughness; pneumatic measuring system detects the resistance to the gas flow that go over a rough surface to determine a roughness parameter [2].

The probe systems for techniques of the surface texture measuring methods are mainly distinguished by the way to detect surface irregularity. The contact stylus measures surface topography by continuously moving probe and contacting the surface with sphere tip. The non-contact probe system measures surface by shooting light beam on the surface and detecting reflected / scattered light from the surface. Also, a probe determines secondary electron emission intensity by using electron beam exciting the surface to measure surface topography. Among them, the contact profiling method is the first and widely used surface texture measurement method [5] and areal-topography method becomes now most prevalent technique in surface texture measuring application.

To ensure the surface topography measurement provides reliable, repeatable, reproducible and comparable results, metrological traceability [6] to the

international standard is essential to be guaranteed (traceability chain is shown in Figure 1). Calibration [6] transfers the traceability from the international units through the unbroken chain to the user instruments, followed by the measurement uncertainty [6] contributing to the calibration. To deliver the traceability easily and reliably to the industry, calibration standards (or artefacts) are produced and calibrated by primary metrology institute to be used for instrument calibration.

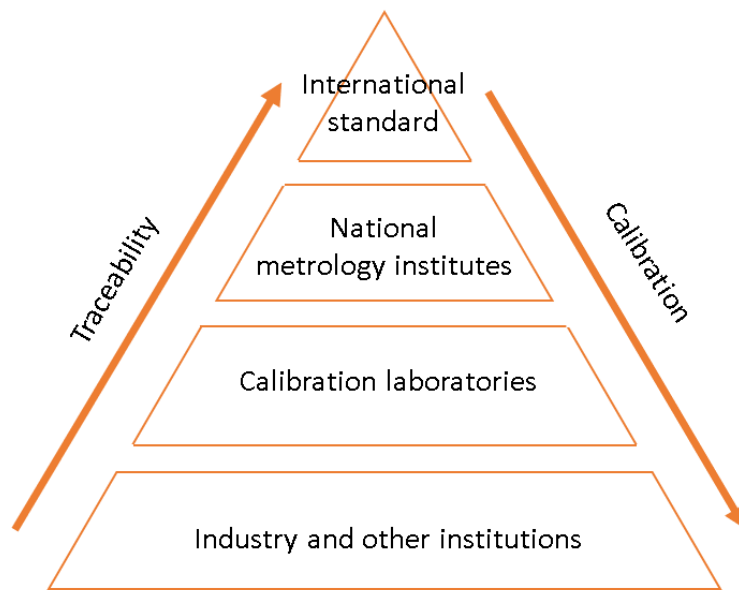


Figure 1. Calibration and traceability pyramid

1.1 Calibration standard

According to the different usage, calibration standards realise different calibration functions. In the measurement process, surface topography information was collected as form of raw data points (step 1). Height is expressed as a function of x and y (step 2). Then the raw data is processed by specialised software (step 3). Eventually surface roughness parameters are calculated accordingly (step 4). The process is illustrated in Figure 2.

Some of the artefacts are used for calibrating the measuring equipment. International standard [7] recommends by determining 8 metrological characteristics (seen Table 1). MCs estimate the combined effect of various influence factors and most importantly they can be quantified by measuring

specified features of calibration standards. Other calibration standards are used for checking surface roughness parameters, hence these artefacts are used to evaluate overall measuring process of the instrument.

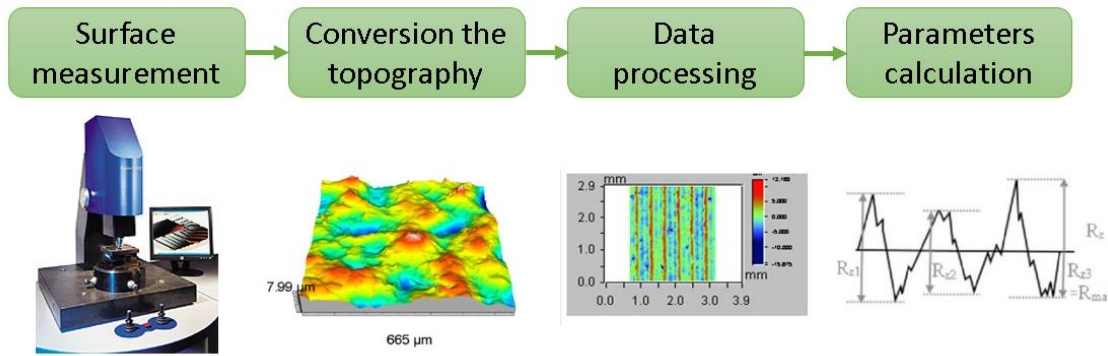


Figure 2. Surface topography measuring process

Table 1. List of metrological characteristics for surface texture measurement methods [7]

Metrological characteristic	Symbol	Main potential error along
Amplification coefficient	$\alpha_x \alpha_y \alpha_z$	x,y,z
Linearity deviation	$l_x l_y l_z$	x, y, z
Flatness deviation	Z_{FLT}	z
Measurement noise	N_M	z
Topographic spatial resolution	W_R	z
x-y perpendicularity deviation	Δ_{PER}	x, y
Topography fidelity	T_{FI}	x, y, z
Maximum measurable local slope	ϕ_{MS}	z

Measurement noise assess the noise from measuring process that is added in the result. Flatness deviation indicates the quality of the areal reference of

instruments. Amplification coefficient and linearity deviation evaluate instrument response function that describes the relation between the actual quantity and the measured value. X-Y perpendicularity (also calling it 'squareness' on 3D areal measuring instruments [8]) assesses orthogonality between x and y axis of instrument coordinate. The spatial resolution indicates the smallest lateral distance or feature that could be detected. Topography fidelity is defined as closeness of agreement between a measured surface profile or measured topography and one whose uncertainties are insignificant by comparison. Maximum measurable local slope is the greatest measurable slope.

1.2 Aim of project

This project aims to manufacturing calibration standard that is capable to evaluate overall performance of the surface topography instruments, which the process includes assessment of the functionality of the artefact and evaluation of the manufacturing process.

2 Literature review

2.1 'Material measures'

ISO 25178-70 [9] defines 13 profile types and 11 areal types of material measures, i.e. calibration standard. Each material measure has measurand that is intended to be measured [6]. The measurands of material measures should be calibrated before they are used for calibration. By measuring the measurand of chosen artefact, associated MC or surface roughness parameters are tested. The types of material measure and the evaluated MCs are listed in Table 2 and Table 3. Graphics of each material measures are shown in Table 4 and Table 5.

Table 2. Types of profile material measure and evaluated metrological characteristics and parameters [10][11]

Type	Name	Measurand	Target
PPS	Periodic sinusoidal shape	Ra(Sa) / Rq(Sq), RSm	Parameters
PPT	Periodic triangular shape	Ra(Sa) / Rq(Sq), RSm	Parameters
PPR	Periodic rectangular shape	Ra(Sa) / Rq(Sq), RSm	Parameters
PPA	Periodic arcuate shape	Ra(Sa) / Rq(Sq), RSm	Parameters
PGR	Groove, rectangular	Depth d	α_z
PGC	Groove, circular	Depth d	α_z
PRO	Irregular profile	Ra, Rz	Parameters, Z_{FLT}
PCR	Circular irregular profile	Ra, Rz	Parameters, Z_{FLT}
PRI	Prism	Angle between face, Pz of faces	α

PRB	Razor blade	Stylus condition (R)	Tip radius
PAS	Approximated sinusoidal shape	Ra, RSm	N_M
PCS	Contour standard	R, angles, distances, heights	Overall
PDG	Double groove	Depth d, spacing l	$\alpha_x \alpha_y \alpha_z$

Table 3. Types of areal material measure and evaluated metrological characteristics and parameters [10][11]

Type	Name	Measurand	Target
AGP	Grooves, perpendicular	Spacing l, depth d, angle	$\alpha_x \alpha_y \alpha_z, \Delta_{PER}$
AGC	Groove, circular	Diameter D, depth d	$\alpha_x \alpha_y \alpha_z, \Delta_{PER}$
ASP	Hemisphere	Radius R	α
APS	Plane – sphere	Distance d, radius R, diameters D	$\alpha_x \alpha_y \alpha_z, \Delta_{PER}$
ACG	Cross grating	Pitches l, angle, average depth D	$\alpha_x \alpha_y \alpha_z, \Delta_{PER}$
ACS	Cross sinusoidal	Sa, Sq	Parameters
ARS	Radial, sinusoidal	Sa, Sq	Parameters
ASG	Star-shape grooves	Depth d	α, W_R
AIR	Irregular	Sa, Sq, Sz, Ssk, Sku	Parameters
AFL	Flat plane	Pt, Pq(Sq), Rq, Rz(Sz), STRt, FLTt	Parameters, Z_{FLT}
APC	Photochromic pattern	Various depending on pattern	Intensity

Table 4. Graphical profile type of material measures

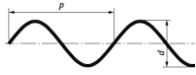
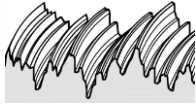
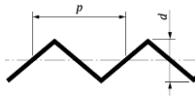

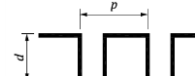
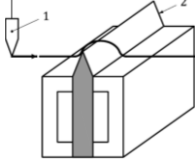



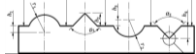

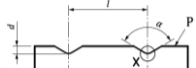
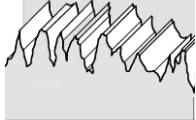
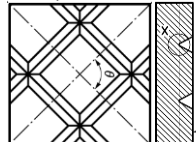

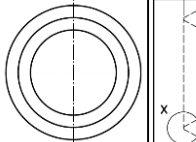
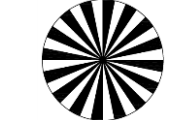
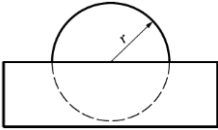
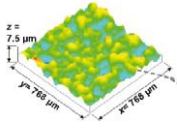
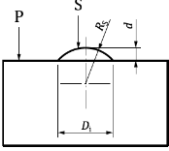

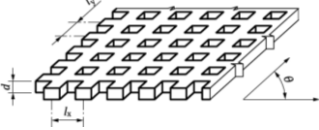
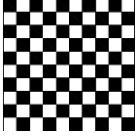
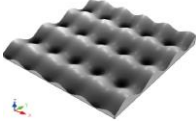
Type	Feature	Type	Feature
PPS		PCR	
PPT		PRI	
PPR		PRB	
PPA		PAS	
PGR		PCS	
PGC		PDG	
PRO			

Table 5. Graphical areal type of material measures

Type	Feature	Type	Feature
AGP		ARS	
AGC		ASG	

ASP		AIR	
APS		AFL	
ACG		APC	
ACS			

The performance of areal surface texture measuring instruments is demonstrated in amplitude – wavelength space by Stedman [12], called ‘Stedman diagram’. In this thesis, it is used to illustrate gap of artefact products. The derivation principle of the diagram is explained in next section.

2.2 ‘Stedman diagram’

A 2D coordinate system consisted of wavelength and amplitude was introduced by Stedman to demonstrate working range and limitations of the areal surface texture measuring instruments [12]. The horizontal and vertical boundary constrains working range of the instrument and sloped borders present the measurement limitations of the instrument. An example is shown in Figure 3.

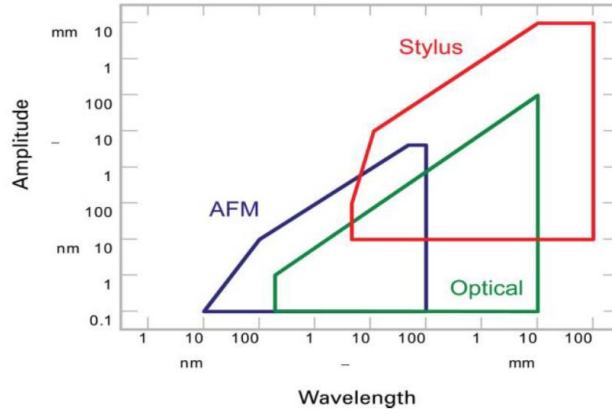


Figure 3. Typical constraints in traditional AW space plots [13]

The slopes of the borders are derived from a sinusoidal perturbation of A and W that is defined by:

$$y = A \sin\left(\frac{2\pi x}{W}\right) \quad (1)$$

In terms of the limitations of contact measurement method, stylus radius constrains the smallest interval of surface feature that could be detected. For the light-based measurement methods, the steepness of the surface feature decides detectable reflected light from the surface. Relating to characteristics of sinusoidal wave, the maximum slope S_{\max} and minimum radius R_{\min} express limitations mathematically, by deriving first and second differentiation of the sinusoidal perturbation, equation (1), which are:

$$y' = \frac{2\pi A}{W} \cos\left(\frac{2\pi x}{W}\right) \quad (2)$$

$$y'' = -\frac{4\pi^2 A}{W^2} \sin\left(\frac{2\pi x}{W}\right) \quad (3)$$

When $\cos\left(\frac{2\pi x}{W}\right)$ and $\sin\left(\frac{2\pi x}{W}\right)$ equal 1 respectively, y' and y'' have maximum and minimum value, which are maximum slope S_{\max} and minimum radius R_{\min} respectively. Substitute S_{\max} and R_{\min} in equations (2) (3) and apply logarithm to each parameters, the equation (2) and (3) evolve to:

$$\log A = \log \frac{S_{max}}{2\pi} + \log W \quad (4)$$

$$\log A = \log \frac{R_{min}}{4\pi^2} + 2 * \log W \quad (5)$$

Hence, according to equations (4) and (5), in log A-W space, limitations of maximum measurable slope is expressed by a straight line with slope of 1 and limitations of minimum measurable radius is expressed by a straight line with slope of 2.

As practical examples of application of Stedman diagram, capability of optical instruments [14] and stylus instrument [15] and the limitations of both techniques were analysed comprehensively. Also, many surface texture measuring instruments were compared by applying Stedman diagram[16]. Some of examples are showed in Figure 4.

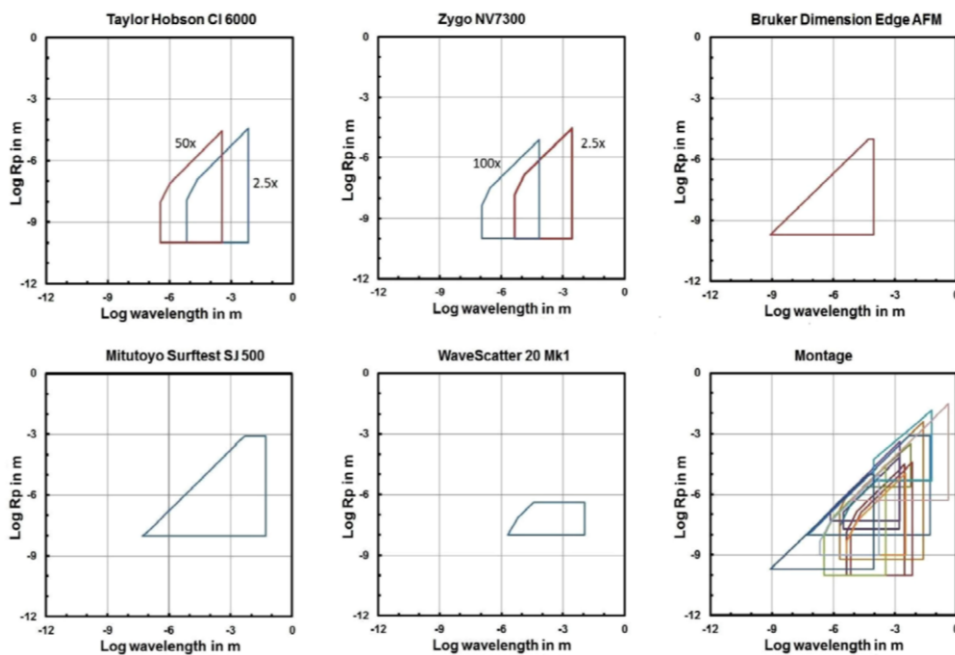


Figure 4. Stedman diagram sketch [17]

2.3 Artefacts

Contact and non-contact instruments are usually used for measuring areal surface topography. Initially, the ISO standard defines few primary types of

material measure for surface texture using *profile* method [18]. They are Type A (depth measurement standard), type B (tip condition measurement standard), type C (spacing measurement standard), type D (roughness measurement standard) and type E (profile coordinate measurement standard). Theoretically the principle of the standard classification is suitable for areal method as well because the contact method could be used to obtain areal surface topography (eg. instrument AFM or 3D mapping technique that parallelly measures multiple profiles that intervals are small enough to reflect true surface geometry). Then GPS published calibration standards classification for areal surface texture measuring with contact instruments [10], which are type ER (groove standard), type ES (sphere/plane measurement standard), type CS (contour standard) and type CG (cross-grating measurement standard). Most recent specification for measuring areal surface texture [9] defines the material measure type, which are not specified for contact or non-contact method, with clarified measurand. Furthermore, in the same document, the profile material measures were re-defined with more detailed division. Both areal and profile material measures are covered evaluation of depth, tip condition, spacing, roughness and instrument coordinate.

2.3.1 Type AIR

'Irregular' (Type AIR) consists of a limited range of wavelength components on the surface. The associated measurands are a series of surface roughness parameters S_a (arithmetic mean height of the surface), S_q (root mean square height of the surface), S_z (maximum height of the surface), S_{sk} (skewness of the surface) and S_{ku} (kurtosis of the surface). Type AIR is used for evaluating overall performance of areal surface texture measuring instrument.

Type AIR is mainly manufactured by mechanical means. Diamond ball end milling was adopted [19][20], which have auto-correlation length 70 μm and 40 μm respectively and S_q of 1.0 μm in both research. Lapping [21] and Nano-grinding [22] are widely used for fabrication due to constant removing the material over the time, so that the roughness value could achieve subnanometer level. In [21], specimens with 5 different nominal values of S_a have been designed, which are

50 nm, 100 nm, 250 nm, 500 nm and 1000 nm respectively. In [22], nanogrinding and ultraprecision turning profile standard specimens were fabricated, which the roughness range R_z within 150 nm to 450 nm for samples from turning process and range R_z within 1 μm to 15 μm for samples from nanogrinding. Diamond turning process also were used somewhere else for fabrication of profile roughness standard specimen [23][24] with R_k value 0.4 μm and R_q value about 1.77 μm respectively in each research. It is suggested that conventional manufacturing method has properties that suitable to produce irregular surface.

Non-conventional methods were attempted to applied. Several roughness specimens were made by electron beam lithography (EBL) and direct laser writing (DLW) to test areal roughness measuring instrument [25]. Auto-correlation length designed in this research was 0.89 μm with effective fabrication dimension of 10 μm * 10 μm . Peak to valley height S_z of 0.84 μm for EBL sample and 1.18 μm for DLW sample, rms height S_q of 0.15 μm for EBL sample and 0.11 μm for DLW sample. The measuring results for each fabricated surface show that the typical root-mean-square residuals of the surface fabricated by EBL and DLW are approximately 43.5 nm and 195.3 nm respectively.

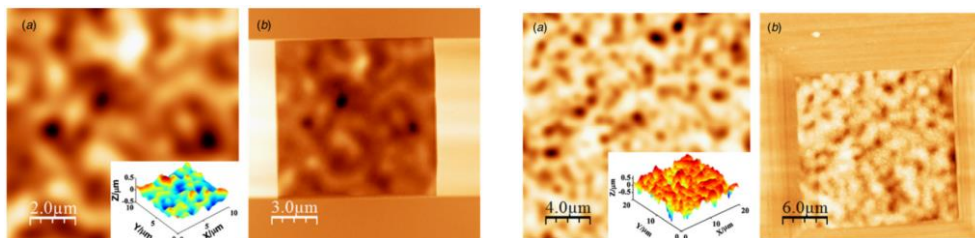


Figure 5. Left: Fabricated roughness specimen by grayscale EBL. Right: Fabricated roughness specimen by DLW. For both: (a) Design surface. The inset shows the corresponding 3D view plot. (b) Typical measured AFM image of the topography. [25]

In the market, VLSI Standards Incorporated produced a series irregular standards with pitch from 6 μm to 200 μm and amplitude from 9 nm to 470 nm [26]. NPL has produced calibration standard with autocorrelation length 40 μm and 70 μm by electroform manufacturing method.

Irregular calibration standard with different dimensions are made to use on different type of instrument. To achieve clear illustration and to be easy comparing measuring capability with instruments, Stedman diagram A-W space is adopted. In the artefact-instrument map of the irregular artefact, amplitude value is the distance between peak to valley, wavelength is the auto-correlation length. The map can be found in Figure 6.

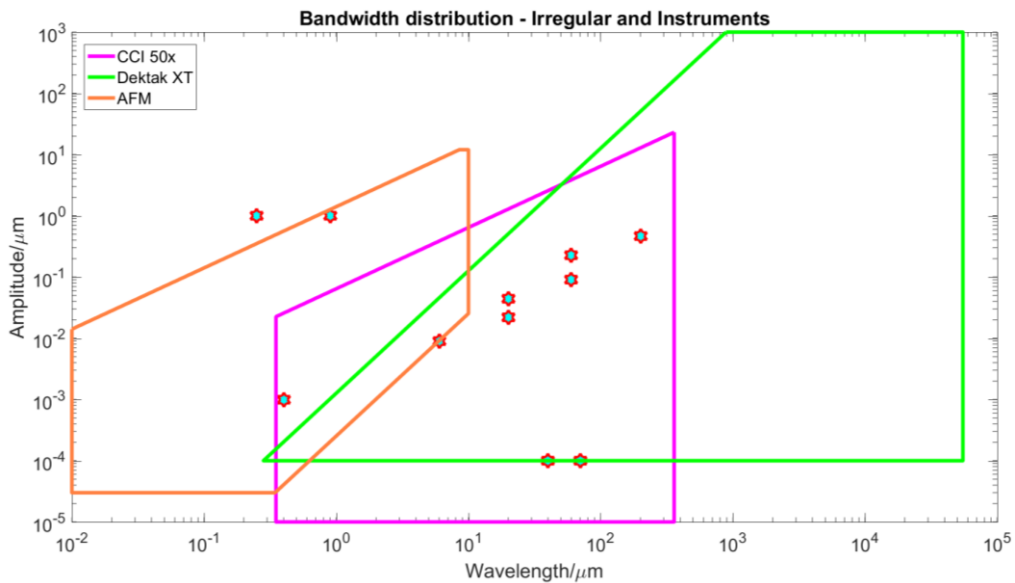


Figure 6. Bandwidth distribution of irregular artefact and example instruments (CCI: Coherence Correlation Interferometer, stands for non-contact measuring instrument; Dektak XT: stands for contact measuring instrument)

It is noticed that one of the markers is outside of any instrument polygons. The reason is that the polygons draw in the map does not stand for the performance of entire family of this kind of instrument.

To assess overall performance of instrument, irregular surface is the only product being commercialized. However, the comparison between designed surface and manufactured surface lacks reliability since the two surfaces are not likely the same, which this issue could be eliminated by using type ACS (cross sinusoidal) and ARS (radial sinusoidal) that are the types been defined in standard but not commercialized until now.

2.3.2 Type PGR

'Groove, rectangular' (type PGR) material measure has a wide groove with a flat bottom. The groove is wide enough not to be affected by lateral resolution and lateral limitations of the instrument. Sometimes it could be a series separate grooves with same or different depth. The material measure is design for determining amplification coefficient, α_z , and linearity I_z in vertical direction. Multiple step heights with different height are used more often than a single step height to establish the relation between ideal response curve and instrument response curve [27].

The height of the groove is usually only few micros. Electric discharge machining (EDM) was adopted [28] to fabricate multiple height calibration artefact (seen Figure 7). Two series of specimens were made with three step values that are 2, 5 and 7 μm and 20, 50 and 70 μm respectively and same width that is 0.7 mm. Also, a dedicated virtual calibration standard designed for nanoscale surface texture measurements was developed (seen Figure 8), generation by using an electrical signal generator and a piezo [29] with S_q (root mean square height) measured value about 2 nm. NPL fabricated a set of step heights with height values varying from 50 nm to 2 μm using electroform technique [30]. Combination of e-beam lithography and etch was used [31] (process is illustrated in Figure 9). In the process, E-beam is applied for constructing the structure of the pattern. Etching provides the depth feature on Si substrate. After removing the e-beamed mask the final product finishes. The trenches have width 300 nm and depth 1.25 μm . Furthermore, the height of step has been pushed to the extremely small scale. A stepped silicon single atom specimen was made to realise sub-nanometre level of height calibration standard that owns the height 300-340 pm (seen Figure 10) [32]. All the products indicates that type PGR standard could be fabricated by wide range of choices, which could be mechanical, physical beam or chemical methods.

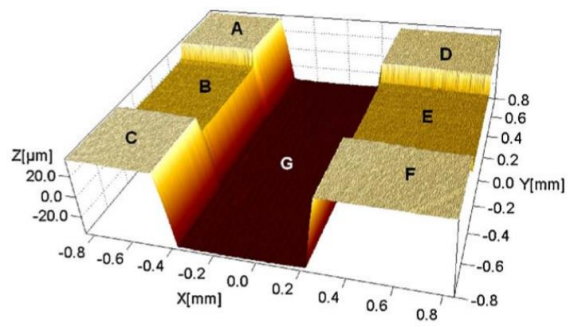


Figure 7. Different step on artefact [28]

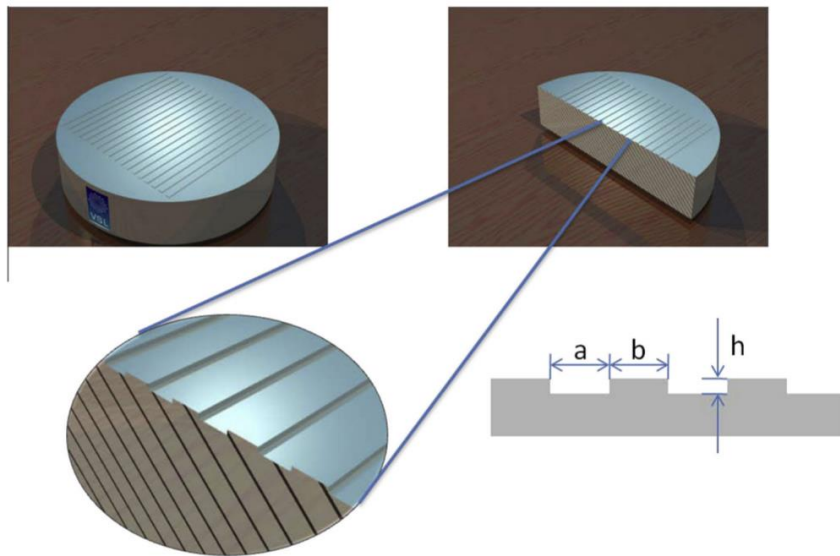


Figure 8. Possible implementation of a profile for an Sq calibration standard. A simple rectangular profile where the upper and lower terraces have equal area result in an Sq value that is half the height difference between the levels.[29]

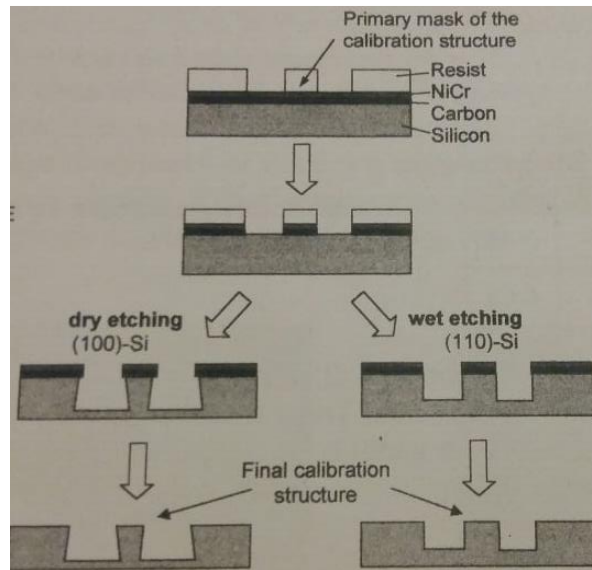


Figure 9. Scheme of the fabrication processes [31]

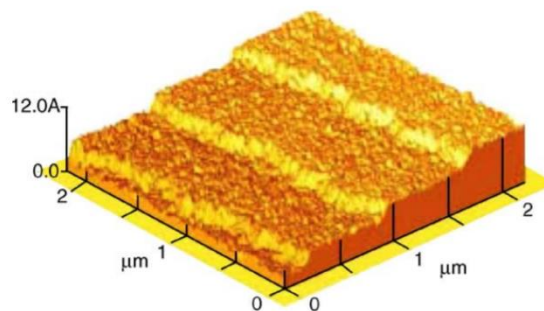


Figure 10. AFM image of a silicon single atom stepped surface [32]

This type of calibration artefact has one of the biggest possessions in the artefact market. VLSI Standards produced multiple step heights with the same width 100 μm and various depths from 8 nm to 940 nm, and another series of step heights having width 1000 μm and depth varying from 1.8 μm to 50 μm [26]. A Germany company 'Anfatec Instrument AG' has step height product with width in the range 2 μm – 50 μm along with height of step in the range 21 nm – 25 μm [33]. PELCO INTERNATIONAL produced single step on Mica with heights 5 nm, 15 nm and 30 nm [34]. A series of steps were made by Veeco with width 100 μm and heights 20 nm to 10 μm [35]. MikroMasch has rectangular and trapezoidal step height shape, with pitch 3 μm and 10 μm for rectangular shape and 10 μm for trapezoidal shape, which value of height has changing from 20 nm to 1500 nm for rectangular and constant value 1750 nm for trapezoidal [36]. Japan NTT

Advanced Technology Corporation fabricated 10 steps within 1 μm and 10 μm distance respectively with depth 0.31 nm of nominal value [37]. PTB developed a depth-setting standard [38] manufactured by diamond turning that has discrete depth of grooves 5 μm , 50 μm , 450 μm , 1 mm, 2 mm and 5 mm (seen Figure 11).

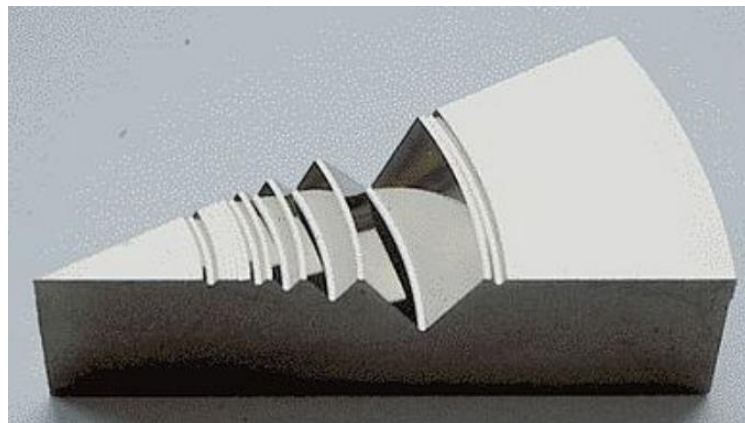
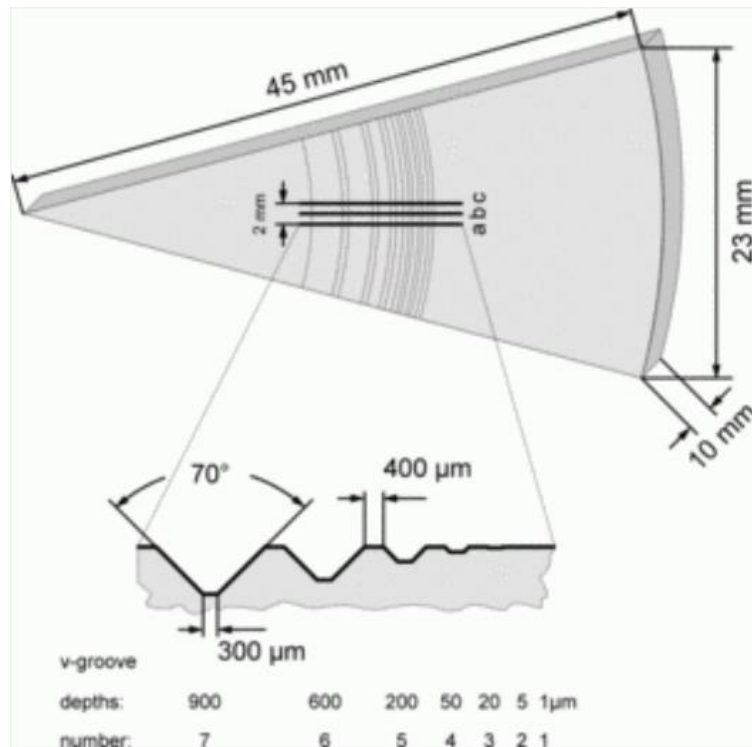


Figure 11. Depth-setting standard developed by PTB (source: <https://www.ptb.de/cms/en/ptb/fachabteilungen/abt5/fb-51/ag-5110/mikromesstechniknormale0/tiefeneinstellnormale00.html>)

The bandwidth distribution of step height artefact and the instrument polygons in A-W space are illustrated in Figure 12. Wavelength took the value of the groove

width and amplitude has the value of depth of the groove. The map indicates that the step height artefact product has mature development so that their products are sufficient to test the performance of contact, non-contact and AFM equipment.

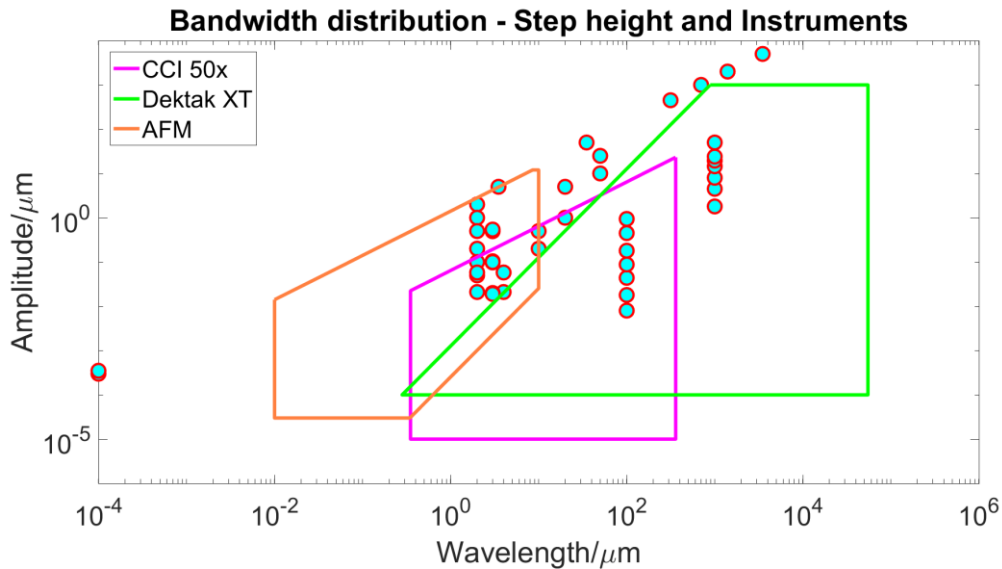


Figure 12. Bandwidth distribution of step height artefact and example instruments

2.3.3 Type PPT

Periodic triangular shape (type PPT) produces triangular shape along a direction. This type of material measure is defined by pitch and height of the triangular or the height and the angle between two adjacent flanks. Type PPT is used for testing tip condition of probing system or the spacing measurement [18].

In standard, there are other type of material measures that could be used for tip condition evaluation (such as type PRB, i.e. razor blade). In market, this type of calibration artefact also realise other functions at the same time by cleverly design the feature. For example, one of the products is available on supplier 'micro to nano' (seen Figure 13), which has 1x1 mm² effective working area with grating manufactured by etching on silicon. Its pitch is about 3 μm with 0.1 μm accuracy and the height is about 1 μm. The edge radii are about 5 nm and the angle of flanks is 54.74°. It is stated to be used on determination of tip aspect ratio and the lateral calibration of AFM or SPM. The other grating for AFM/SPM calibration (seen Figure 14) has active area of 3x3 mm², 10 μm pitch with 0.1 μm accuracy

and 1.75 μm height. It is claimed to be useful for the linearity of the scanner of probe system in the vertical direction.

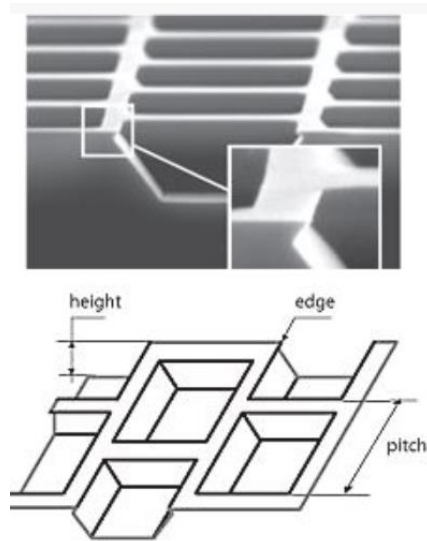


Figure 13. AFM / SPM calibration grating, undercut edges (source: <https://www.microtonano.com/AFM-XYZ-calibration-standard-for-calibrated-measurements-and-dimensions.php?currency=pounds#a34030100B>)

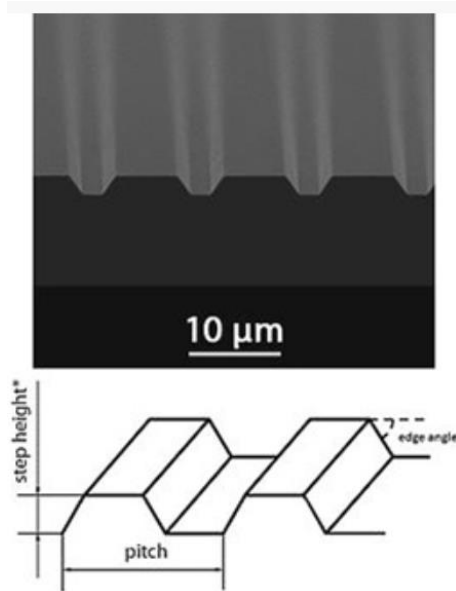


Figure 14. AFM / SPM calibration grating, trapezoid structure (source: <https://www.microtonano.com/AFM-XYZ-calibration-standard-for-calibrated-measurements-and-dimensions.php?currency=pounds#a34030100B>)

2.3.4 Type PCS

Contour standard (type PCS) is consisted of different surface geometries and is specified at least two arcs of circle and two wedges are required. The radius of the arcs, depth of the wedge and angle between two flanks of the wedge can be measured. Amplification coefficient and linearity in vertical direction will be evaluated by applying the artefact. For contact measuring method, stylus tip also can be evaluated.

PTB electro-eroded (EDM) a micro artefact using stainless steel for fringe projection (dimensions being seen in Figure 15). This product provides multiple dimension for each feature so that a wide range of probes could be evaluated.

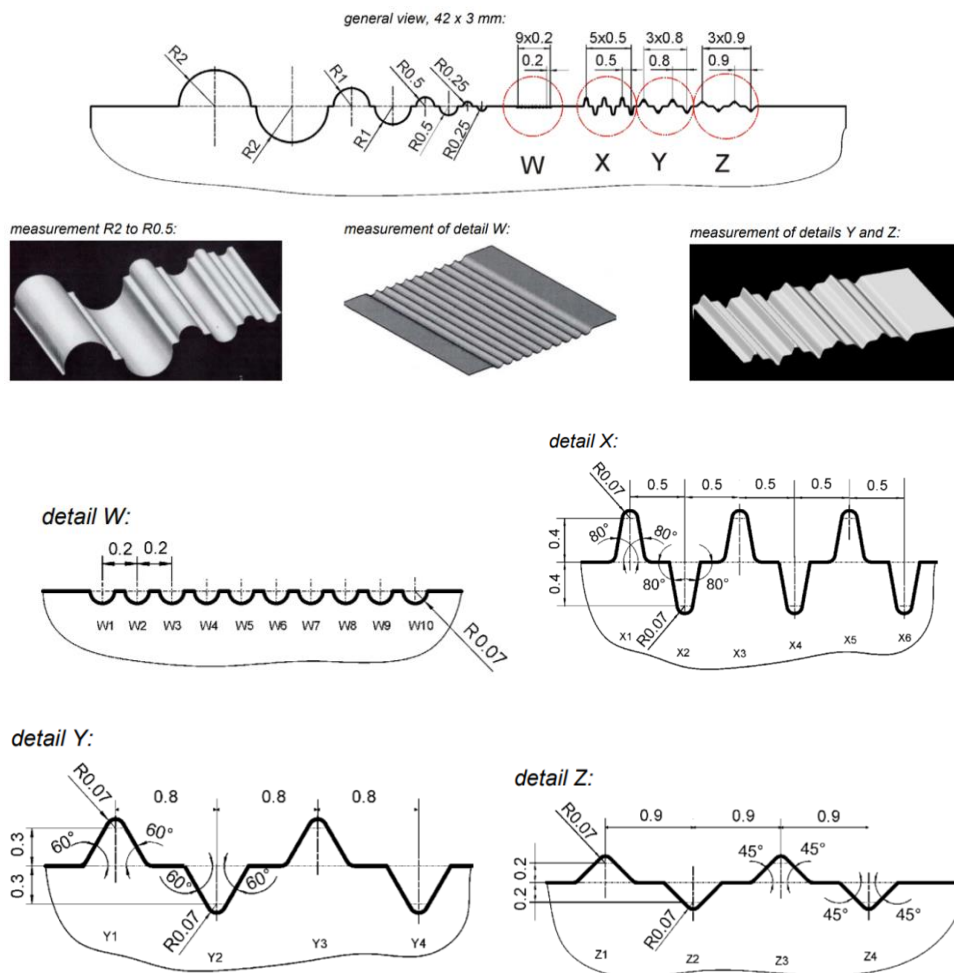


Figure 15. A Micro-Artifact for Fringe Projection (source:

https://www.ptb.de/cms/fileadmin/internet/fachabteilungen/abteilung_5/5.3_koordinatenmesstechnik/Messgeraete_Bilder/5.3/uPK-Flyer-engl.pdf)

2.3.5 Type ASG

Star shape groove (type ASG) has a series of grooves arranged in the circumferential direction independently. It is usually used for evaluating lateral resolution or topographic spatial resolution due to the continuous changing spatial wavelength along the radius direction with constant depth of grooves.

NPL developed a standard set that has multiple star shape (seen Figure 16) with radius 70 μm and 40 μm , 18 upper petals and 18 lower petals. Chosen manufacturing process reduced the entire production cost [39]: a master specimen was fabricated by e-beam writing and electroforming on a nickel shim and the duplications were made by electroforming.

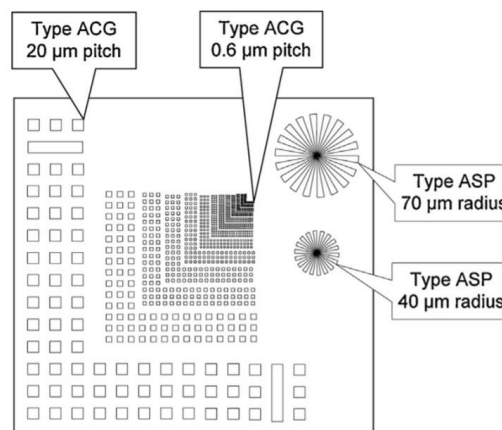


Figure 16. Cross grating and star shape artefact [39]

The mature product that has star shape has been commercialized by NPL [40] (seen Figure 17). The star shapes (selected by blue rectangular) with various dimensions are electroformed on the chip. Two of them have width range from 700 nm - 50 μm , 700 nm - 25 μm with 200 nm depth of grooves and the other two have width range from 700 nm - 25 μm , 200 nm - 6 μm with 50 nm depth of grooves.

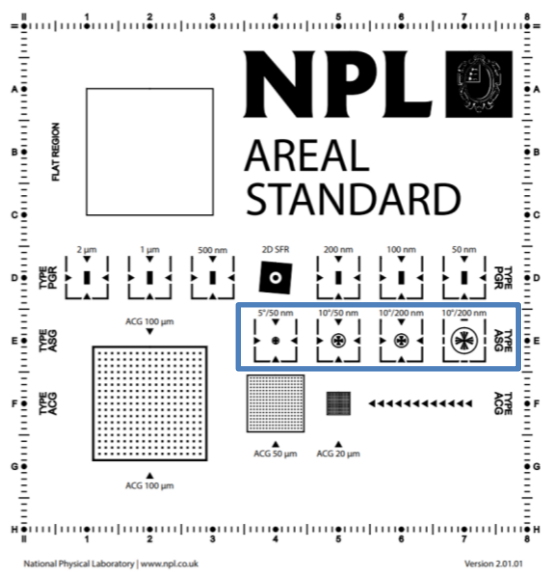


Figure 17. NPL areal standard [40]

The artefact-instrument map for star shape artefact is shown in Figure 18. The markers connected by horizontal lines stand for the lower and higher width limit of the grooves. Even though there are not many products of type ASG standard been made in the market, the figure shows that the current artefacts are capable to be used for all three types of instrument.

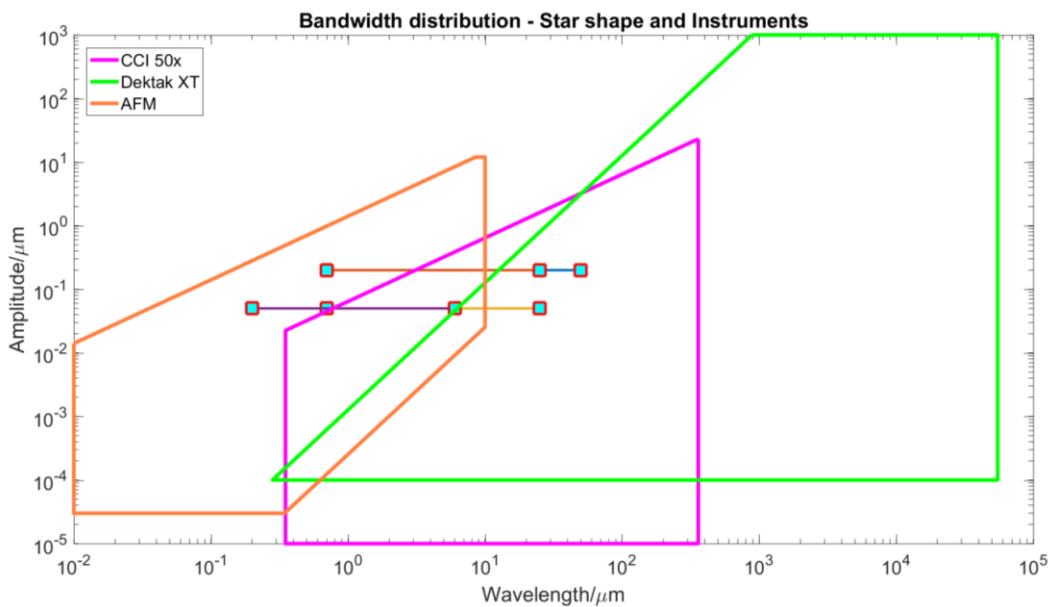


Figure 18. Bandwidth distribution of star shape artefact and example instruments

2.3.6 Type PPS

Periodical sinusoidal shape (type PPS) has sinusoidal wave forming along the x or y direction. Depending on different designs, the wavelength and amplitude of the product can be discretely changing along the feature forming direction, which is the reason why it is usually called ‘chirp’ standard. It is originally designed to evaluate lateral resolution, similar with star shape artefact.

Ultra-precision diamond turning was used in [41] (seen Figure 19) and [42] to fabricate chirp features that has constant value of amplitude that is 1 μm and gradually varying of wavelength from 91 to 10 μm . FIB technique was also used [43], which the sample has varying amplitude and wavelength (seen Figure 20). Considering the maximum measurable slope and diffraction limit wavelength, authors set wavelength from 0.2 μm to 2 μm with 15 wavelengths in geometry and the slope up to 45 degrees. By using this sample, instrument response to the different wavelengths and angles can be studied without changing artefact.

However, this type of artefact is active in research development but not in the market, which may due to the complicated manufacturing program and the delivered functions could be realised by applying other several artefacts.

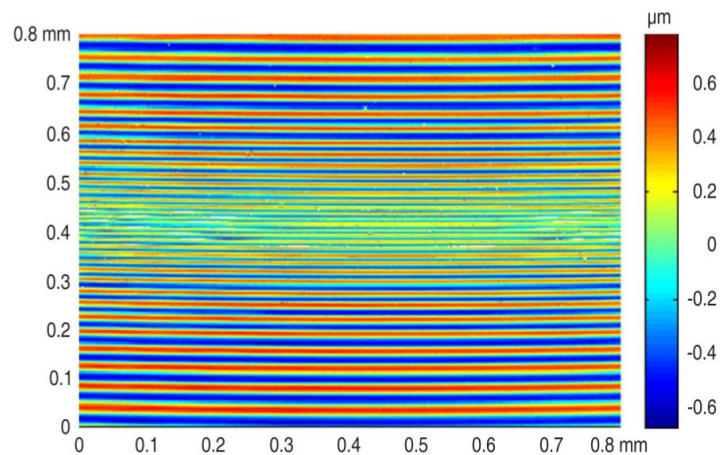


Figure 19. Confocally scanned 3D data set of the chirp standard of a μ_{surf} explorer microscope by NanoFocus AG. [41]

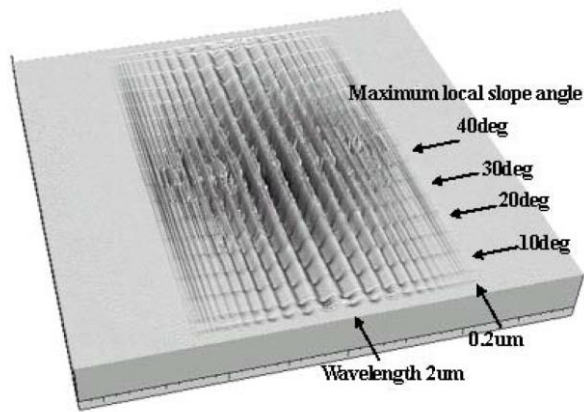


Figure 20. Bird's eye view of profiles measured by LSM. [43]

The artefact-instrument map for chirp artefact is shown in Figure 21. The markers connected by lines stand for the lower and higher wavelengths and the amplitudes of the sinusoidal wave.

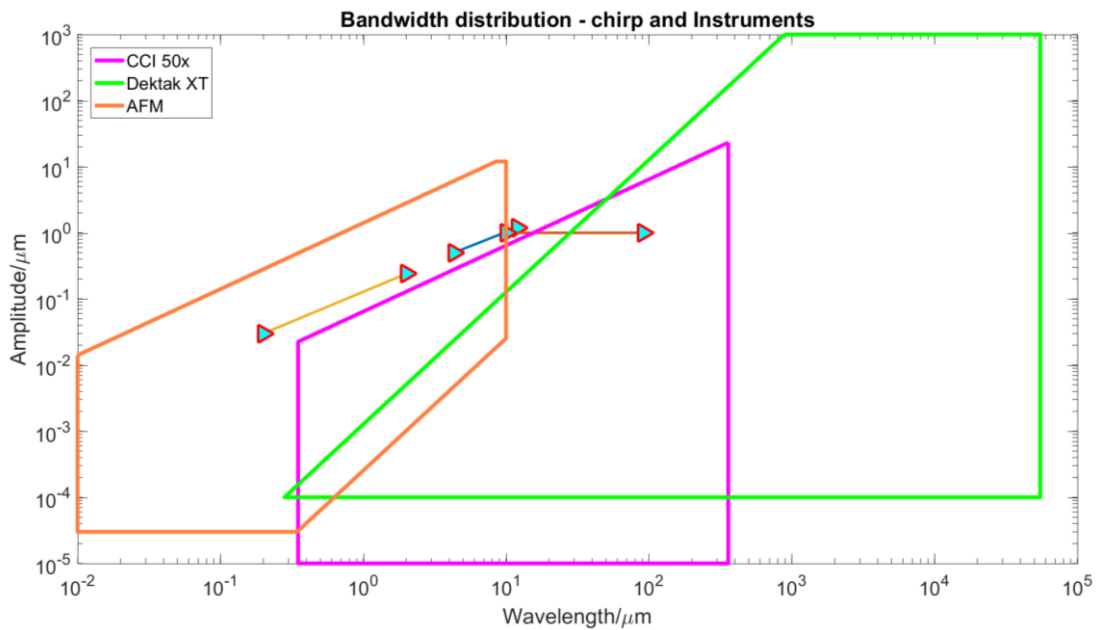


Figure 21. Bandwidth distribution of chirp artefact and example instruments

2.3.7 Type AFL

Flat (type AFL) is a flat plane with form deviation with neglectable roughness. It is designed to determine measurement noise and residual flatness. Usually it is made by polished glass [9].

NPL made a flat calibration standard that has Sz (maximum height) less than 20 nm by e-beam (seen Figure 17). EU project ‘Transfer Standards for Calibration of SPMs’ developed a flat standard using Quartz with peak to valley distance less than 10 nm [44]. Taylor Hobson produced a tungsten carbide optical flat calibration standard that has roughness less than 5 nm.

Artefact map for flat standard and the instrument example polygon is shown in Figure 22. Amplitude is given by maximum peak to valley height. Wavelength has the same value of auto-correlation length.

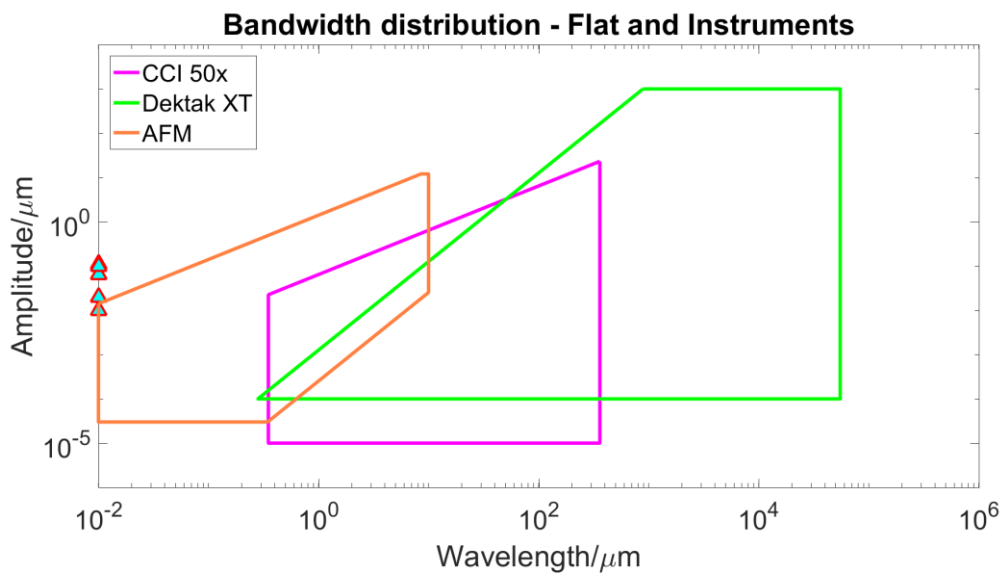


Figure 22. Bandwidth distribution of flat artefact and example instruments

2.3.8 Type ACG, combine with type PRB or type ASP

Cross grating (type ACG) consists of two-dimensional array pattern. It is used for determination in lateral direction of amplification and linearity by locating centre of gravity of the square holes, and squareness by measuring angle between orthogonal fitting lines through centre of the square.

The cross gratings used in [45] have pitch 100 μm and 30 μm. NPL made cross grating in calibration standard set having pitch 100 μm, 50 μm and 20 μm (seen Figure 17).

There are many commercialized cross grating in the market. One of them is shown in Figure 23, which has less 500 nm pitch. VLSI [26] and MikroMasch [36]

have grating standard produced with pitch around 2 μm to 10 μm and height of feature from around 20 nm to 180 nm. NanoSensors has pyramids array produced with 200 nm pitch and 70 nm depth [46]. Pelco [34] made waffle grating with about 463 nm pitch. SIS made waffle pattern on glass with pitch 1500 nm and height 100 nm [47].

There is even more product that not only used as cross grating but also used as other type material measure realising different function by designing different feature in grating instead of typical square shape. For example, a grating product introduced pyramid (Figure 24) that has 2.12 μm tip to tip distance to be able to test tip geometry of instruments, which the pyramid shape is similar as type PRB (i.e. razor blade). Also type ASP (hemisphere) was introduced in grating (Figure 25) to enable probe tip checking. Furthermore, diamond shape (Figure 26), combined features (Figure 27) or even letters (Figure 28) are used and more different measurand are defined. EU project 'Transfer Standards for Calibration of SPMs' has pyramids array making on the Pt coated Si substrate with pitch 100 nm, 300 nm [46] and 1000 nm, 3000 nm and 10000 nm [48] respectively. Anfattec Instruments AG manufactured a series of grating products with pitch range within 500 nm to 10000 nm and depth in the range of about 20 nm to 500 nm [33].

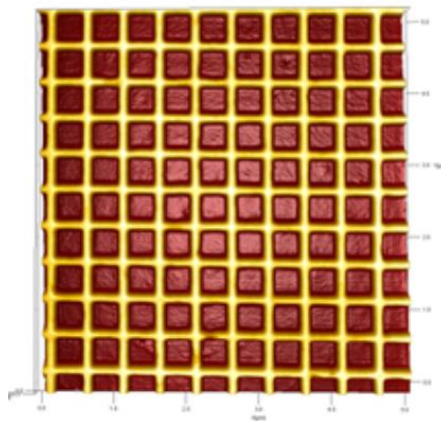


Figure 23. AFM image of cross grating. (source: http://www.tedpella.com/calibration_html/afm_spm_calibration.htm.aspx#677-AFM)

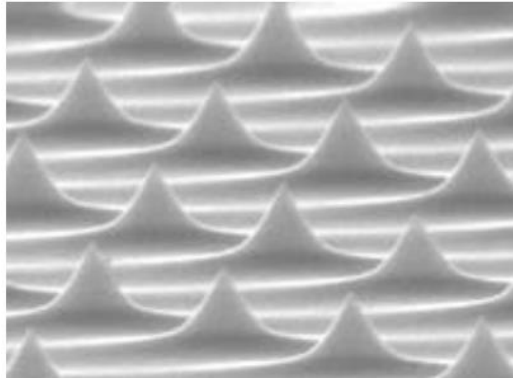


Figure 24. Pyramid feature grating (source: <https://anfatec-shop.de/p/tgt1>)

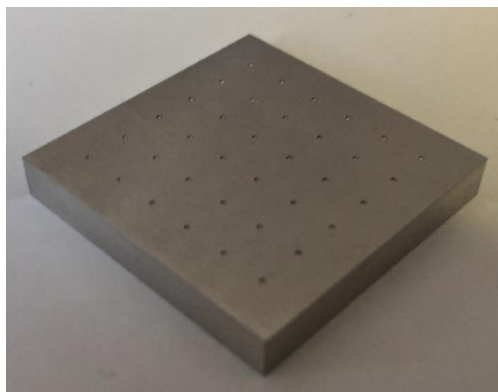


Figure 25. Hemisphere feature grating [49]

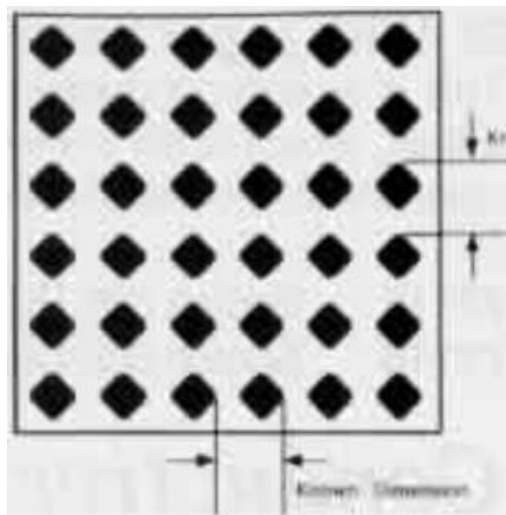


Figure 26. Diamond feature grating (source: <https://www.emsdiasum.com/microscopy/products/sem/standards.aspx>)

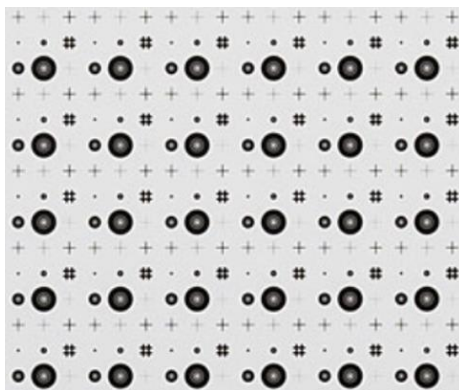


Figure 27. Combined shapes grating (source: https://www.thorlabs.com/newgrouppage9.cfm?objectgroup_id=7502)

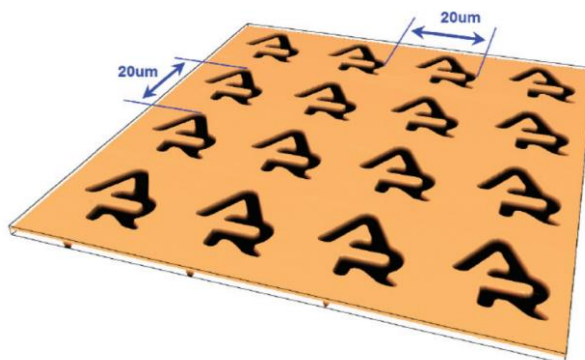


Figure 28. Letters 'AR' grating (source: <https://www.asylumresearch.com/Products/CalStd/CalStd.shtml>)

Artefact-instrument map for cross grating standard is shown in Figure 29. Amplitude is given by the height of small square. Wavelength is given by the pitch. Cross grating has been maturely developed in market. The covered area by markers cross through three polygons, which implies that the current products are sufficient to be used for calibration various surface texture measuring instruments.

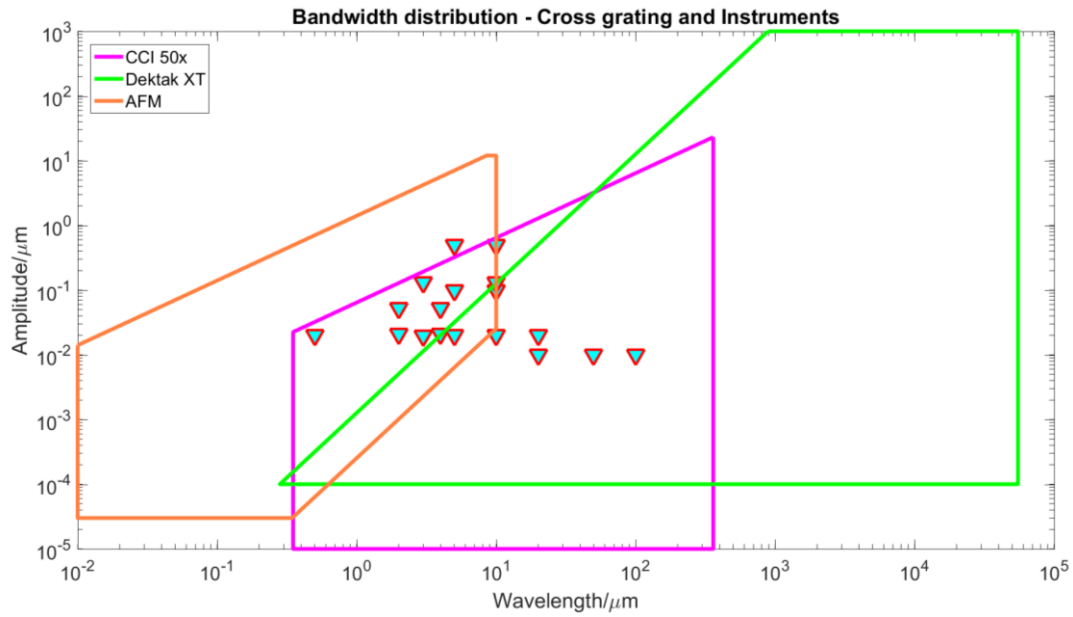


Figure 29. Bandwidth distribution of cross grating artefact and example instruments

2.3.9 Type PPR

Line grating (type PPR) is developed for lateral direction performance evaluation in one dimension. It can be used for determination of amplification and linearity of the tested lateral direction.

In Figure 30, the line grating characterizes 3600 lines/mm (i.e. pitch 278 nm) and the height is about 55 nm. Advanced Surface Microscopy Inc. has replica line grating having pitch 750 nm and height 100 nm [50] using Ni. MikroMasch [36] produced line grating on Si substrate with 3000 nm pitch and 1800 nm depth of the feature. Optical manufacturer company Moxtek produced line gratings on Si substrate coated by tungsten, which they have pitch 300 nm and 700 nm with feature height 100 nm [51]. Comparing with cross grating, it only evaluates one direction property of instrument and no ability to check squareness. Hence the market of line grating is not as big as cross grating.

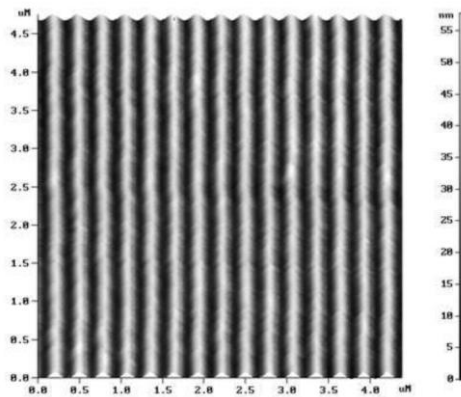


Figure 30. Line grating.

(source: <https://anfatec-shop.de/p/tdg01>)

2.4 Manufacturing methods for artefacts

Manufacturing artefact has been conducted by various methods. Summarily, they are chemical or physical reaction method such as etching [31], physical beam methods such as E-beam machining [39], DLM (direct laser machining) [11][25], electroform [39][52], FIB (focus ion beam) [43][53], EDM (electrical discharge machining) [28], lithography [25][31], and mechanical methods such as grinding [22], milling [49][19], lapping [21] and turning [22][41][24].

Etching is a process that remove material from substrate by taking advantage of reaction between workpiece and chemical solution (wet etch) or plasma (dry etch). Research [54] has proved that one of the biggest advantage of this approach is suitable for many material types. However, it was also indicated that some of the sample materials had quite slow reaction speed (<2 nm/min). Also, for the specific form (such as sinusoidal shape targeted in this project), this method is not a good choice.

FIB applying for material milling is realised by using high ion current beam scanning the surface of substrate. The arbitrary shape can be etched. The main benefits of this technique are the flexibility of the shape forming, high machining resolution and useable for any material erosion. However, the processing time is the main drawback [55]. Although assisted gas could be used to speed up the

processing time, the extra cost spent on gas and anti-leak equipment etc. will be high. It is not economic on artefact manufacturing.

Lithography uses a beam to project on a large-area, patterned mask to remove material on substrate. Comparing with FIB, lithology can fabricate much faster and due to the masked property, mass production is achievable [56]. However, for the artefact requiring large volume material removing (dimension usually around few hundred micros), the reasonable consumed time cannot be achieved easily.

EDM is an excellent technique by using thermal energy to machine complex geometry and remove material that has electrical conducted property regardless of hardness. Due to the high thermal energy generating in the process, carbon is intended to penetrate into the outer layer of the machined surface [57], resulting in the high micro-hardness of the new surface, which may cause micro crack and other unpredictable condition on the surface.

Electroforming is a metal forming process that makes parts by electrodeposition. It has advantage on producing complex shape, detail reproduction and processing on the thin wall component. The mass production could be achieved due to the electrolyte bath could be used for multiple parts at the same time. But one of the main drawbacks is the limitation of availability of material types, i.e. the conductive property of the material is required. Also, the deposition consumes long time to have desired thickness of layer. Most importantly, the quality of surface finishing is hard to control [58].

Direct laser machining in 3D application can realise turning/milling operation on brittle [59]. It requires properties of rapid heating, melting and evaporating in substrate material. Advantages of the technique are the property of simple programming and processing flexibility, while the disadvantages are that thermal effect may need to take into account and that speed limit requires consideration due to the characteristics of scan head [60].

E-beam machining removes material by using high velocity electron beam to strike material surface over small spot (about 10-100 micros) [61]. The process

requires vacuum environment. This technique is able to process almost any material regardless of material properties and provide good surface finishing. However, the vacuum environment is not easy to create, and the equipment maintains costly. Comparing with conventional machining process, it has lower material removal rate [62]. The recast layer cannot be avoided after processing [61].

Lapping and grinding process take advantage of the abrasive between rubbing surfaces. The surfaces are grinding wheel and workpiece for grinding process and for lapping process, the two surfaces could be the workpiece and a brittle material or the workpiece and a material softer than workpiece. Surfaces made by these techniques could obtain high finishing quality. They are mainly used for roughness standard in artefact production.

Milling is the cutting process by using rotary cutter to remove material from workpiece. It produces workpiece fast by mounting multiple tool. The material removal rate is high due to the milling tool has multiple cutting edge. For the feature such as pocket, trench or hole on the surface, this is the best technique to use. But it is not suitable for the feature such as sinusoidal wave that have curved edge and periodical changing.

SPDT (single point diamond turning) is an ultraprecision cutting process that employs diamond as the tool on a precise lathe under the precise control. The machined surface can achieve high quality of surface finishing and desired form accuracy, under the premise of having accurate tool motion and friendly material properties of workpiece [63]. Also, it is one of the techniques that have capability to produce free form surface. Depending on the tool radius and machine motion accuracy, SPDT has capability to manufacturing most of the artefact (seen the blue rectangular in Figure 31). As one of a representative of the ultra-precision manufacturing technique, SPDT has been studied comprehensively through decades. Any element that could potentially affect cutting surface roughness and form accuracy has been experimented to find the optimum machining condition. For example, reaction between diamond tool and workpiece [64], material microstructure [65] and tool geometry [65] [66] has been explored. On the other

hand, from mechanical point of view, new servo system was also developed to enhance accuracy of the device [67]. Furthermore, the characterization of surface by SPDT was also developed [68]. Contributions of tuning process to the surface characters were studied, which potentially provides directions that could push the surface engineering even below nanometre level.

In this project, sinusoidal wave is the major surface feature to obtain, which requires highly smooth surface and excellent accuracy of the form. The research on SPDT has been developed for decades, which provides the technique comprehensive understanding to application. Hence SPDT is the best choice to manufacture the chosen artefact.

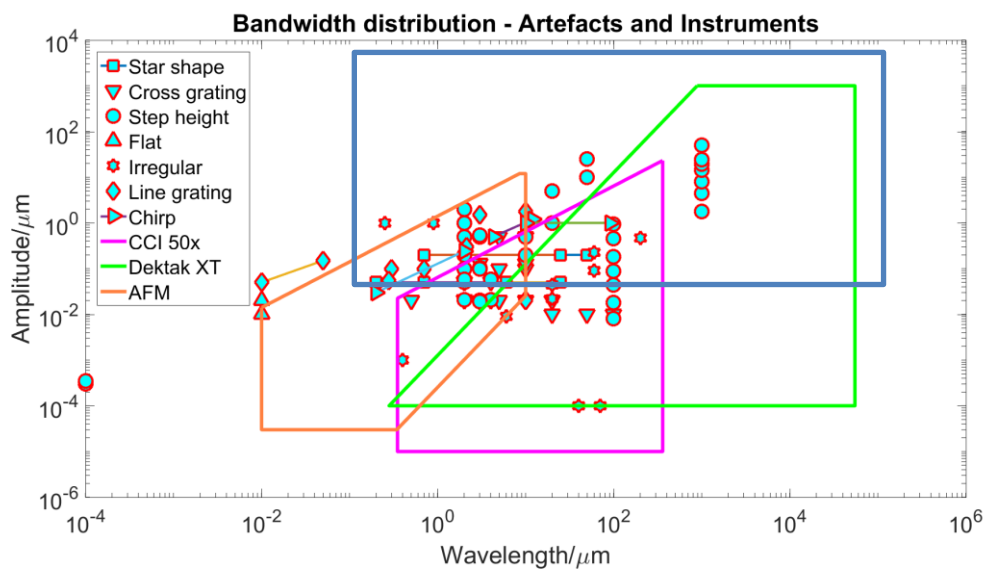


Figure 31. Bandwidth distribution of combination of all types of artefact and example instruments

2.5 Knowledge gap

Looking at the current market of artefacts, the types that could be used for evaluating overall performance of instrument is not sufficient. Currently only the irregular surface calibration standard (Type AIR) with calibrated surface roughness parameters are available in the market. However, for the optical instruments, slope on the surface is crucial to be seen since the reaction of the light and surface could affect measuring result. Moreover, the irregular surface does not have designed form so that the surface roughness parameters could not

be determined from design. In fact, in ISO standard for areal surface texture, two types of roughness material measures designed by function with known local slope are not yet commercialized. They are type ARS (radial sinusoidal) and type ACS (cross sinusoidal). The value of their roughness parameters can be calculated based on designed dimension of product, which provides higher reliability and confidence when compare designed value and measured value of roughness parameters.

Besides, there is large gap located in the big wavelength and small amplitude area for all instruments, shown in Figure 31, which would also need calibration standard to be produced.

In terms of manufacturing process, variety of them have been used to produce artefacts. All processes are belonging to subtractive manufacturing, which display huge potential on producing artefact with additive manufacturing (AM) process. However, considering the requirement of accuracy of the artefact, AM process cannot provide satisfactory of surface finishing, which it would be expected long time improvement and study on accuracy of the technique until it could give high quality surface of product.

2.6 Objectives

Manufacturing type ARS and type ACS challenge differently on SPDT technique. To produce type ARS artefact, which is rotational symmetric shape, need control of 3 axis of the machine: x, y and z. To manufacture type ACS, which is non-rotational symmetric shape, need control not only x, y and z, but also c axis that takes over spindle rotary. Moreover, the radial sinusoidal shape would also test the cooperation of the turning machine on x, y and z axis, which could be a valuable assessment before testing the machine cooperation with forth axis.

Hence, the objective of this project is: 1) to manufacture the type ARS material measure by using SPDT (single point diamond turning) technique that is defined in ISO standards but not produced commercially, 2) to evaluate the machining process so as to verify the performance of the chosen diamond turning machine, 3) assess the quality and functionality of the final product.

2.7 Research questions

In terms of feature parameter and tool path design:

1. What are the suitable dimensions of the artefact?

In terms of the manufacturing:

2. How accurate SPDT machine could achieve on z direction?

In terms of the product measurement:

3. What is the best technique to certify the quality of the product?
4. How to quantify the quality of the manufacturing process?

2.8 Hypotheses

According to the research questions, hypotheses are proposed:

1. To evaluate the measuring instrument effectively, the feature dimension may be at micro level.
2. For the specific material such as copper, which has good machining properties on diamond turning process, the depth of cut in z direction could repeatably achieve a hundred of nanometres.
3. Contact measuring method may be more accurate and be able to deliver traceability than non-contact measuring method.
4. For the diamond-turning-friendly material, the form of the machining result could achieve sub-micrometre accuracy.

3 Methodology

1. *Parameters design of the artefact dimension.*

The feature dimension is designed to capable of applying on chosen optical surface texture measuring instrument: white light interferometer with highest magnification lens, which has 0.36mm x 0.36 mm field of view, within $\pm 22^\circ$ detectable slope. ISO standard [69] recommends that standard number of five sampling lengths are needed to calculate roughness parameters. Hence five sine waves should be seen in one field of view Moreover, the smallest diamond tool

currently available has nose radius 0.114 mm, which constrains the machinable smallest wavelength and deepest amplitude.

2. *Performance verification of chosen diamond turning machine on z direction.*

In this project, Moore nanotech 350UPL is chosen to undertake machining process, which is ultra-precision machining systems for single point diamond turning. To test repeatability on z axis, three replicated cuts were performed at different radii of a copper workpiece continuously with constant spindle speed. The workpiece was cut from edge to centre. Each replicated depth consists of a series value of feed that are 50 nm, 150 nm, 250 nm and 500 nm respectively to estimate the repeatable smallest depth of cut of the machine. Each feed generated a 2 mm wide plateau for the step height calculation. The other sample was designed to be cut from centre to the edge of the workpiece with same parameter setting to verify the possible effects from cutting direction.

3. *Best technique to measure the product.*

Two measuring method could be chosen for measuring the product: contact (DektakXT profiler and Taylor Hobson Series 2 profilometer) and non-contact (Taylor Hobson CCI) measuring technique. Comparing with contact method, non-contact method may give fake points responding to spikes on surface. For the turning product, issue usually appears in the centre of the workpiece. The geometry of the centre after machining may be a peak with high slope or a sag. The non-contact measuring method may provide wrong measuring response due to the inappropriate reflection and receiving of the light. Moreover, contact method delivers more reliable traceability to the measurement. Comparing two profilers, Taylor Hobson has laser inspection on the motional stage, while DektakXT does not have the inspection, which former instrument may give more stable sampling spacing in scanning than latter one. However, Taylor Hobson does not have motional stage on slow axis. It requires assisted device to undertake the work, which introduces larger measurement uncertainty. In this case, to evaluate wavelengths of the product, the stylus needs to go through the centre of the workpiece. By using 'map scan' function of DektakXT, profile

scanning through the centre could be easier to find without extra device. Also, DektakXT has smallest sampling spacing among three instruments. Hence the product was measured by DektakXT stylus profiler.

4. *Quality of manufacturing process.*

This could be evaluated by comparing the designed sinusoidal shape with manufactured product. The difference between them would be caused by manufacturing process and the measuring process. The contribution of measuring process would be assessed by evaluating instrumental and measurement uncertainty.

4 Results and discussions

4.1 Feature and machining process design

Feature parameter design:

The radial sinusoidal shape (seen Figure 32) was designed to be fabricated in 0.5 mm diameter circular area. To meet the requirement of 5 sinusoidal waves visual in one field of view under CCI 50x magnification lens, it is designed to have 4 sinusoidal waves along radial distance, which each of the wave has wavelength/pitch 62.5 μm .

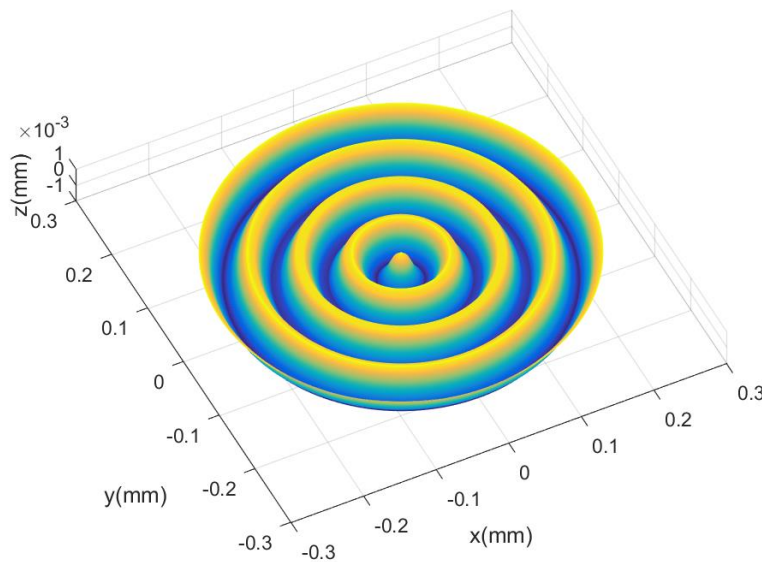


Figure 32. Radial sinusoidal geometry

Designed radial sinusoidal shape has wavelength 62.5 μm , depth of the wave 1.7 μm . Hence the function of the sine wave could be expressed as:

$$y = 0.0008604 * \cos(100.5 * x) \quad (6)$$

where: depth of the wave is two times of the amplitude of the function, and wavelength equals $2\pi/100.5$.

Measurand of the radial sinusoidal shape are surface roughness parameters Sa and Sq, which are Average Roughness and Root Mean Square Roughness respectively that stand for the overall measure of the texture over the entire evaluated surface area.

Surface texture parameter Sa (arithmetical mean height) is given by [70]:

$$Sa = \frac{1}{A} \iint |z(x, y)| dx dy \quad (7)$$

Surface texture parameter Sq (root mean square height) is given by:

$$Sq = \sqrt{\frac{1}{A} \iint z(x, y)^2 dx dy} \quad (8)$$

Tool path generation:

The smallest diamond tool available on Moore machine in Cranfield precision lab is 0.114 mm nominal tool radius, which is even much larger than the pitch of the wave. Hence the tool radius needs to be considered in the calculation of amplitude. The determination of feasible amplitude value is demonstrated below.

The tool radius determines the smallest machinable curvature that could be calculated by:

$$R = \frac{[1 + (\frac{dy}{dx})^2]^{1.5}}{|\frac{d^2y}{dx^2}|} \quad (9)$$

where, R is radius of smallest curvature, which here the values should be larger than tool radius. y is the function of x . To make sure that the chosen tool radius could be used in the case that the optical tool radius measurement contributes measurement error, the value 0.115 mm is used in program.

The function of the curve is a relation of cosine:

$$y = A * \cos(P * x) \quad (10)$$

The reason why applies cosine function instead of sine function is that for turning process, cosine function starts with the highest point rather than middle point of sine function, which is good for tool cutting into the material during turning process.

In equation (9), the $\frac{dy}{dx}$ estimate tangent value of the curve slope, $\tan \alpha$, derived by first differentiation of the cosine function in equation (10).

$$\tan \alpha = \frac{dy}{dx} \quad (11)$$

The tool cutting the surface is the same as a ball with the radius as same as the tool rolling over the desired shape. Hence to obtain each point on the tool moving path, the normal relation between them should be established (seen Figure 33). Each point on tool moving path corresponds to the desired curve perpendicularly.

The slope of each perpendicular line, $\tan \alpha_{nor}$, could be expressed as:

$$\tan \alpha_{nor} = -\frac{1}{\tan \alpha} \quad (12)$$

The distance d between the points on tool moving path and corresponding points on the desired curve equals to the tool radius, determined by equation (13) below. The value is measured by optical measurement lens, which is 0.11392 mm.

$$d = \sqrt{(x_2 - x_1)^2 + (y_2 - y_1)^2} \quad (13)$$

Where: (x_1, y_1) are the points on desired curve and (x_2, y_2) are points on tool path.

The relation between y_2 and x_2 is expressed as:

$$\tan \alpha_{nor} = \frac{y_2}{x_2} \quad (14)$$

Replace y_2 in equation (13) with the relation in equation (14), with the known curve function, the tool path coordinates (x_2, y_2) series could be derived.

The illustration of desired curve, normal lines and the tool moving path is shown in Figure 33. To clearly demonstrate relations, tool path (red curve in the feature) has been moved down to be close to the arrows. The real situation of the desired curve and the tool path is illustrated in Figure 34.

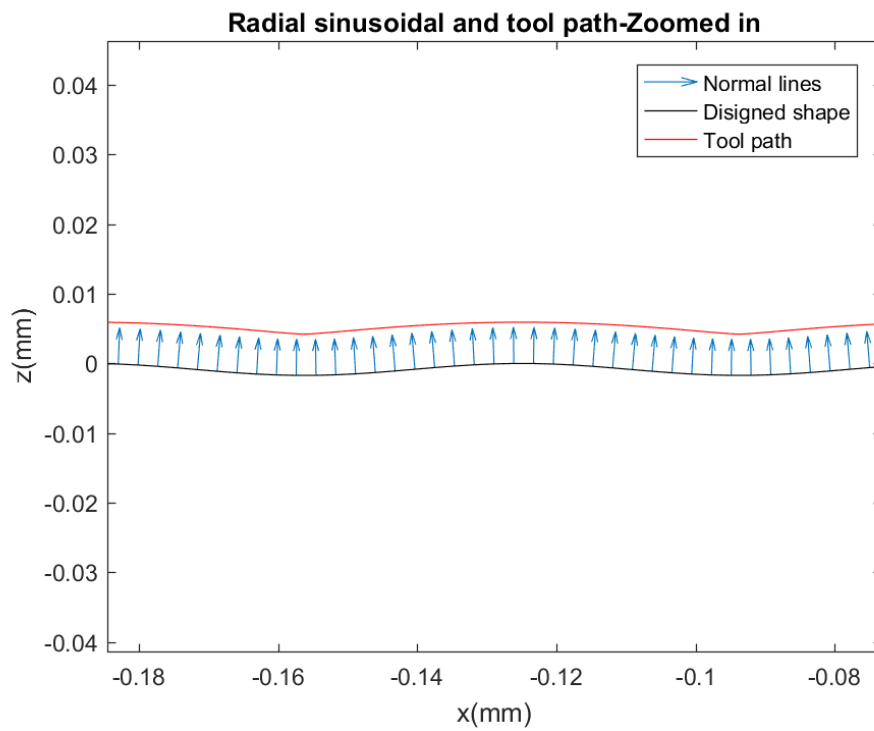


Figure 33. Illustration of the tool path generation of radial sinusoidal shape in small scale

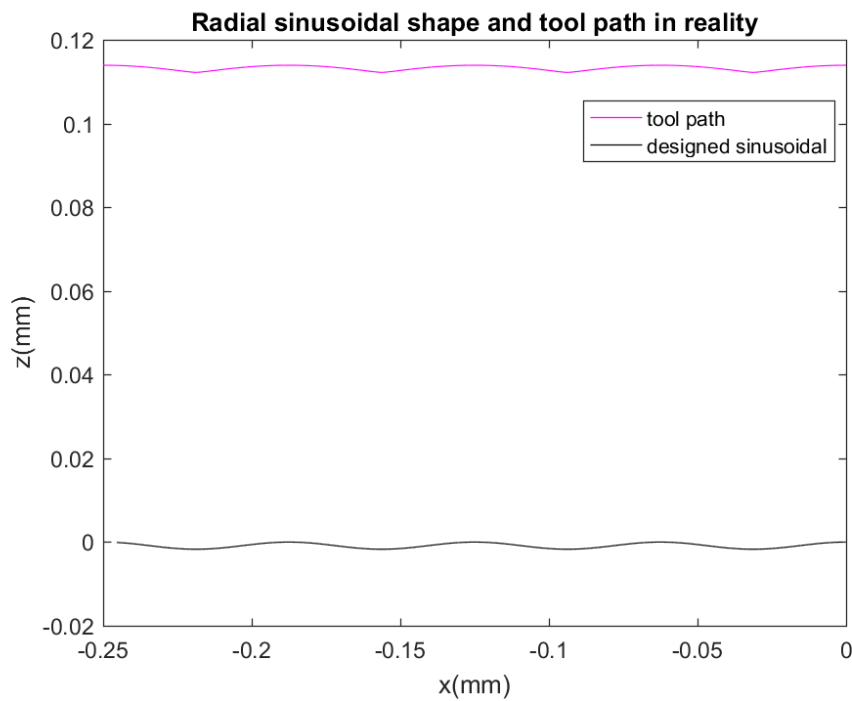


Figure 34. Tool path in real machining condition

In program, feed rate was set as 0.03 mm/min. Spindle speed was 2000 RPM. The program code is shown in Appendix A. The shape was cut in the centre of a copper workpiece that has diameter about 50 mm. The entire feature was finished by one cut. Rough cut was conducted before cutting the designed shape.

4.2 Performance verification of SPDT in z direction

4.2.1 Introduction

SPDT, i.e. 'single point diamond turning', is turning process with diamond as the cutting tool. Due to the natural qualities of diamond (high hardness, high wear resistance, low friction coefficient, high modulus of elasticity, high thermal conductivity, low coefficient of thermal expansion, and low affinity with non-ferrous metals), It can be used for precision machining of non-metallic hard and brittle materials, high wear resistant materials, composite materials and other ductile non-ferrous materials [63].

Moore Nanotech 350 UPL SPDT centre (seen Figure 35) is chosen to machine workpiece. The slideway is supported by oil bearing and spindle is supported by air bearing. It has a liquid cooling system for spindle with aerostatic bearings having motion error of less than 50 nm. The resolution of the driving system can achieve up to 0.034 nm [71]. The advantage of using vacuum clamping system in this machine instead of physical fixture is that minimizes the deformation of workpiece in diametric direction. The granite support of spindle provides the thermal stability and stiffness during machining process. Tool inspection adopts advanced optical tool setting system that provides clear image of possible tool wear or contamination on the cutting surface of the tool tip.

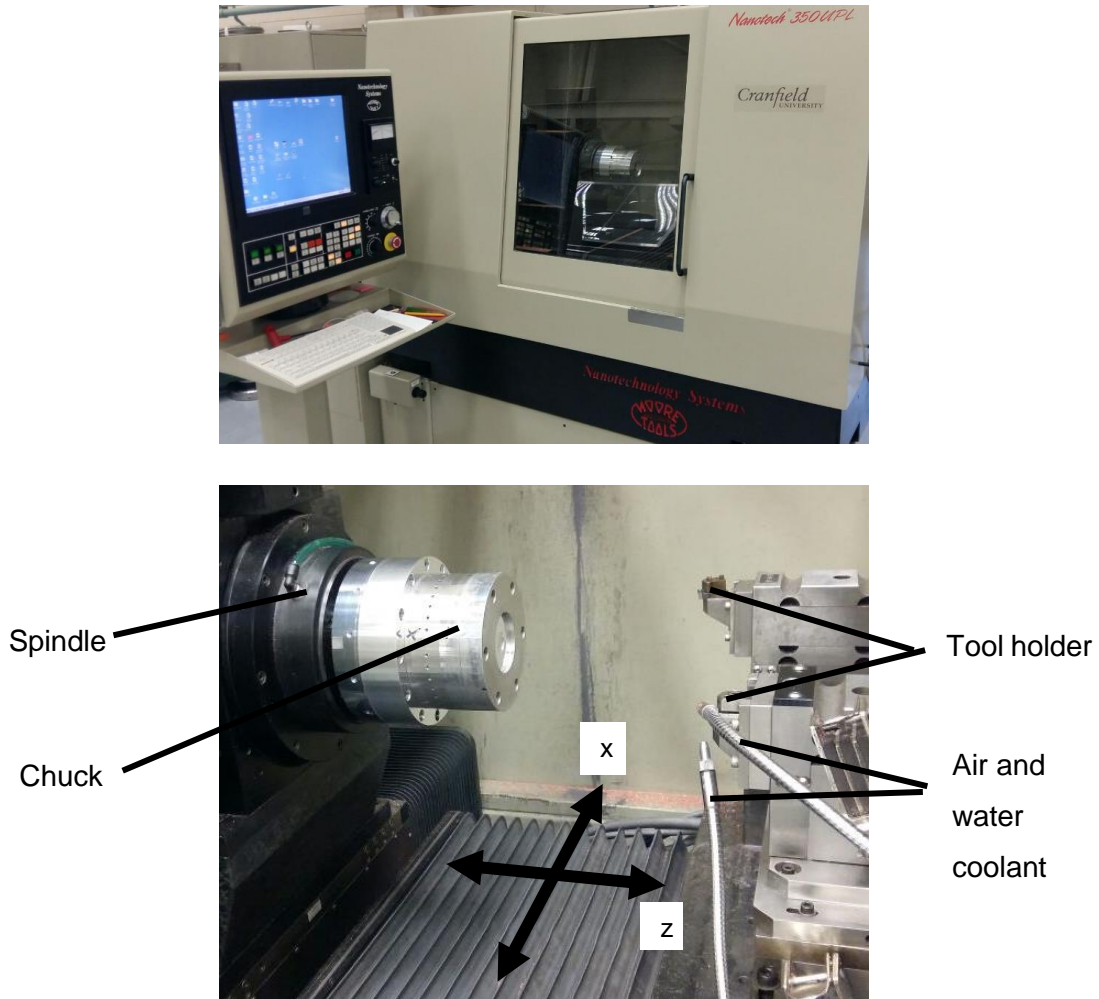


Figure 35. Moore nanotech 350UPL ultra-precision turning machine outside-look (top picture) and inside structure (bottom picture)

4.2.2 Experiments

The amplitude and wavelength of the designed sinusoidal feature are extreme small. The amplitude is even 35 times finer than wavelength. Hence the reproducibility of the machine in z direction is of utmost importance for the Integrity of the form of product. To investigate the property of machine, a series of depth of cut experiment were conducted [72].

4.2.2.1 Method

Three replicated cuts were performed at different radii of a copper workpiece with 74 mm diameter continuously (seen Figure 36). Each cut consists of four 2-mm terraces that were formed by feeding tool with four different values of cutting

depth in z direction. The values of depth of feed are 50 nm, 150 nm, 250 nm and 500 nm respectively. Also, to verify the possible effects of cutting direction, two sample with same cutting parameter design were conducted: first was cut conventionally, which was from edge to centre of the workpiece. Second sample was cut from centre to the edge of the workpiece.

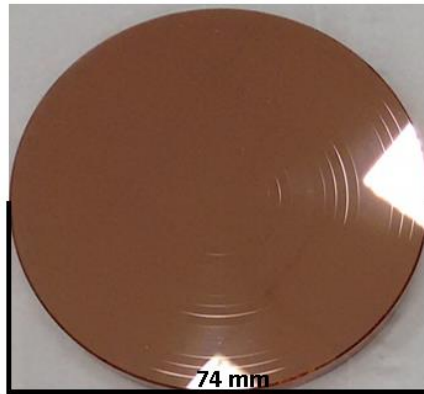


Figure 36. Depth of cut copper sample

A newly lapped diamond tool with a nose radius of 0.53 mm, rake angle 0° and clearance angle -10° was used for machining entire set of cuts. The feed rate was 4 mm/min and spindle speed were 2000 RPM.

Talysurf Series 2 profilometer (seen Figure 37), which has hemispherical tip of 2 μm radius, was employed to perform the measurement of heights of terraces and roughness of surface on each terrace due to the contact measuring method providing real surface condition. In total, four profile measurements at four different places (rationally 90° to each other, seen Figure 38) were made to avoid random measurement error when less than 3 times measurement are made. Metrology data analysis was performed using TalyMap Gold 4.1. The depth of each step was calculated as the differential height between central 1.6 mm of adjacent plateau as shown in Figure 39.

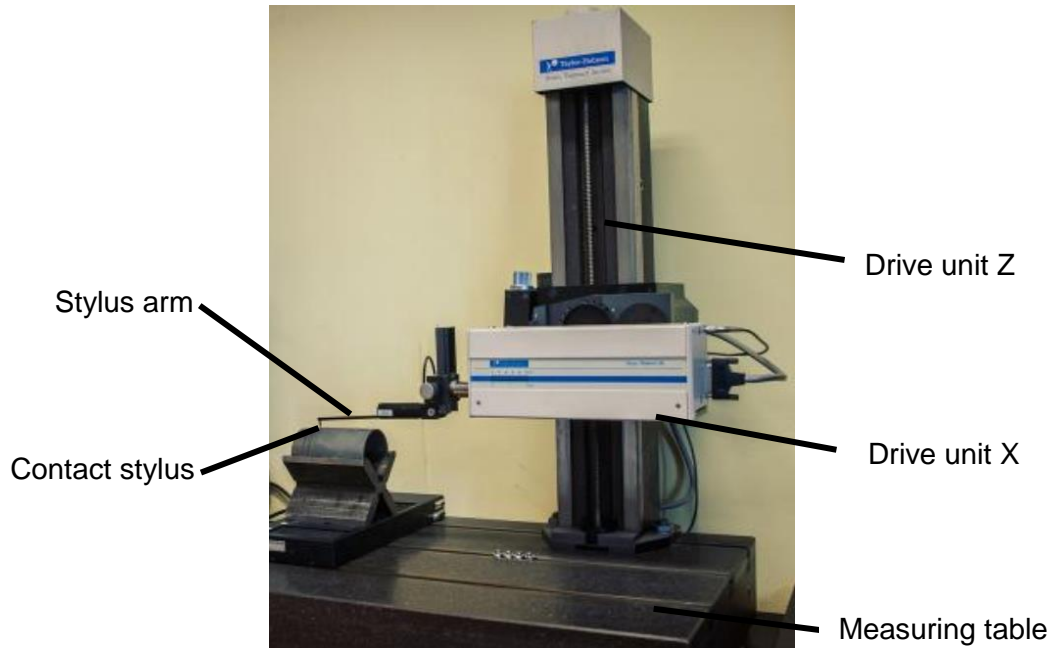


Figure 37. Talysurf Series 2 profilometer

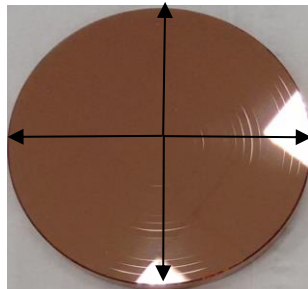


Figure 38. The arrows are the approximate measurement positions and directions

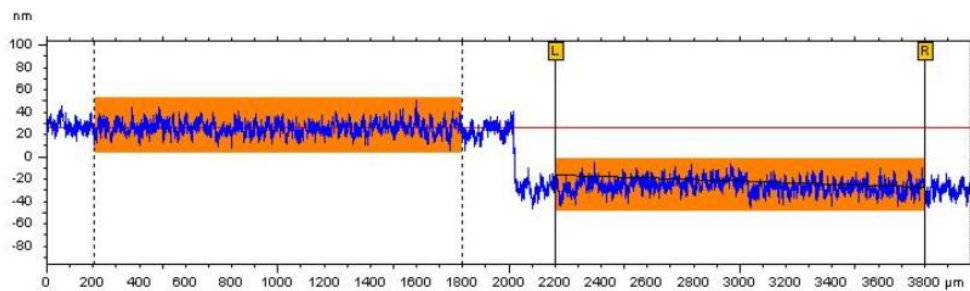


Figure 39. Data analysis on TalyMap Gold 4.1

4.2.2.2 Results

The surface finish on all terraces was of optical quality, with Ra not exceeding 5.5 nm. Table 6 and Table 7 shows the measurements and analysis results of

step height information on both samples. The same information is illustrated graphically in Figure 40.

In the Figure 40, blue error bars in first graph and the black ones in second graph, which the cuts are closer to the centre, indicates least error. The 50 nm deep cuts showed maximum uncertainty among the different depths. Error bar is experimental standard deviation of each measurement. According to the measurement result, initial judgement could be drawn that the machining process does not provide good repeatability.

Table 6. Measurement on first sample: cutting from edge to centre.

Unit: nm		P1	P2	P3	P4	Average	Std	Error
1st cut	50nm*	3.19	0.833	1.47	0.97	1.6	1.1	-48.4
	150nm	147	155	156	168	156.5	8.7	6.5
	250nm	231	244	237	233	236.3	5.7	-13.8
	500nm	525	524	527	538	528.5	6.5	28.5
2nd cut	50nm	21.1	32.8	39	31.2	31.0	7.4	-19.0
	150nm	156	163	167	183	167.3	11.4	17.3
	250nm	244	241	245	241	242.8	2.1	-7.3
	500nm	495	497	491	494	494.3	2.5	-5.8
3rd cut	50nm	51.9	42.9	58	47.4	50.1	6.4	0.1
	150nm	156	159	160	161	159.0	2.2	9.0
	250nm	235	239	244	234	238.0	4.5	-12.0
	500nm	505	497	499	500	500.3	3.4	0.3

* Profile measurement result does not show differential height.

PS: P1-P4: The first measurement to the fourth measurement.

Table 7. Measurement on second sample: cutting from centre to edge.

Unit: nm		P1	P2	P3	P4	Average	Standard Deviation	Error
1st cut	50nm	50	57.4	51.3	41.5	50.1	6.5	0.05
	150nm	153	152	151	150	151.5	1.3	1.50
	250nm	236	247	245	242	242.5	4.8	-7.50
	500nm	529	510	522	524	521.3	8.1	21.25
2nd cut	50nm*	1.52	2.59	3.7	2.21	2.5	0.9	-47.50
	150nm	147	163	156	164	157.5	7.9	7.50
	250nm	267	259	271	226	255.8	20.5	5.75
	500nm	484	487	485	477	483.3	4.3	-16.75
3rd cut	50nm*	19.4	21.3	2.15	0.451	10.8	11.0	-39.17
	150nm	120	121	126	119	121.5	3.1	-28.50
	250nm	258	244	244	247	248.3	6.7	-1.75
	500nm	508	494	499	499	500.0	5.8	0.00

* Profile measurement result does not show differential height.

PS: P1-P4: The first measurement to the fourth measurement.

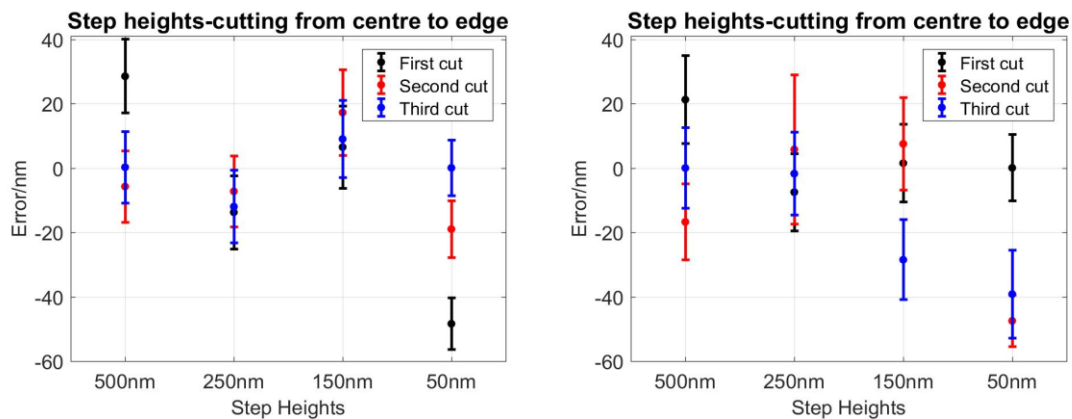


Figure 40. Error and standard uncertainty of programmed vs measured depths. First to third cut corresponds to cutting direction. Left: cutting from edge to the centre; right: cutting from centre to the edge.

4.2.2.3 Possible error sources of manufacturing

Main factors that may cause the error during manufacturing can be roughly divided into controllable and uncontrollable factors (graphical illustration shown in Figure 41). In general, it is widely agreed that the machining parameters (controlled inputs such as feed rate, depth of cut and spindle speed) and tool geometry are prevalent controlled factor [73]. There are, however, various uncontrollable factors stems from the local plastic contact between the cutting

tool and the workpiece, which, in turn, are influenced by materials microstructure as well as hard inclusions in the substrate [74]. These factors are jointly influenced by the contact stiffness and frame compliance mechanism for both machine structure loop and sample material both in static and dynamic mode. Spindle run outs are also escalated as potential problems leading to asynchronous error, which adds to chatter and vibrations despite utmost care taken in mounting the tool and workpiece on diamond turning machine.

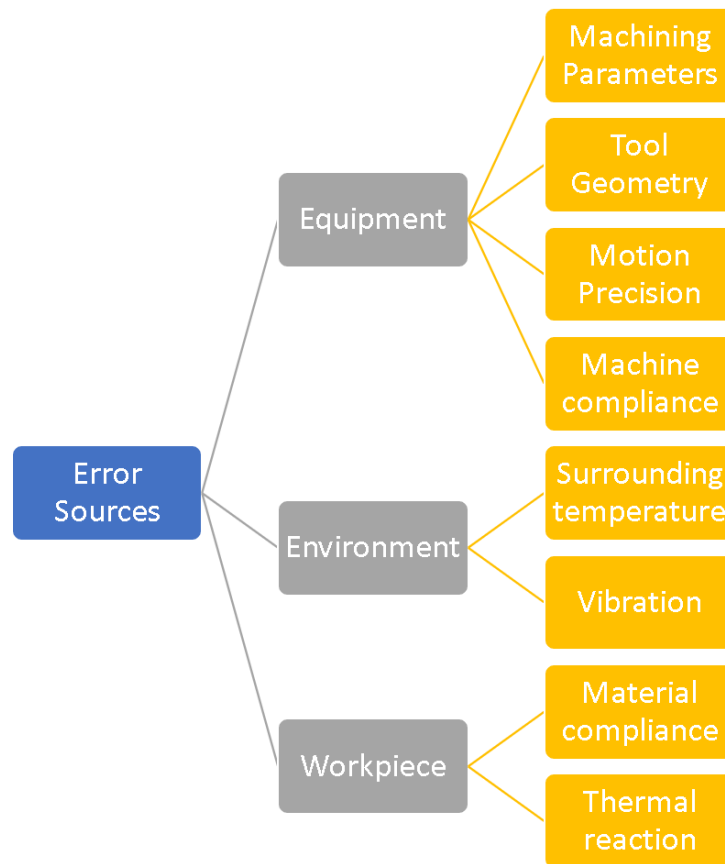


Figure 41. Possible error sources during the SPDT process

4.2.2.4 Measurement uncertainty

The measurement uncertainty is obtained by calibration of metrological characteristics of the profilometer.

To determine the amplification and linearity deviation of the profilometer [75], firstly calibrated step heights (which are 50, 100, 200, 500nm representatively, seen Figure 42) were measured in the same working range of x direction as when

the sample was measured and at different positions in the z working range, which specifically are 25%, 50% and 75% of the working rang. Equations are shown as (7) - (8). Measurement and calculated results are shown in Table 8.

$$\alpha = \frac{\sum_i^n C_i I_i}{\sum_i^n C_i^2} \quad (15)$$

Where: α is amplification coefficient, C_i is calibrated value, I_i is indicated value, n is the number of different step height standard used.

$$l = N - \alpha * N \quad (16)$$

Where: l is residual error, N is nominal value, α is amplification coefficient.



Figure 42. Calibrated step height artefact

Table 8. Measurement results of calibrated step height on different position of z working range (25%, 50% and 75% of working range representatively) Unit: nm

Mean Height	25%					Mean	error	Standard Deviation	α	Residual error
	1st	2nd	3rd	4th	5th					
500nm	436	415	423	440	430	428.8	-71.2	10	0.966445	16.78
200nm	241	217	217	215	224	222.8	22.8	11		6.71
100nm	106	108	108	107	100	105.8	5.8	3.3		3.36
50nm	42.3	40.5	44.8	38.4	37.2	40.64	-9.36	3.0		1.68

Mean Height	50%					Mean	error	Standard Deviation	α	Residual error
	1st	2nd	3rd	4th	5th					
500nm	428	429	430	430	431	429.6	-70.4	1.1	0.959715	20.14
200nm	216	212	211	209	210	211.6	11.6	2.7		8.06
100nm	107	109	109	108	108	108.2	8.2	0.84		4.03
50nm	33.2	31.5	29.4	28.8	31.9	30.96	-19.04	1.8		2.01

Mean Height	75%					Mean	error	Standard Deviation	α	Residual error
	1st	2nd	3rd	4th	5th					
500nm	422	415	409	411	427	416.8	-83.2	7.6	0.962841	18.58
200nm	236	235	224	221	220	227.2	27.2	7.7		7.43
100nm	94.7	102	107	109	103	103.14	3.14	5.5		3.72
50nm	38.8	42	40.1	37.6	32.4	38.18	-11.82	3.6		1.86

The measurement noise was assessed by measuring an optical flat (seen Figure 43). The subtraction of two profiles (measured on different position on calibrated optical flat standard) eliminated the flatness deviation of the standard.



Figure 43. Calibrated optical flat standard

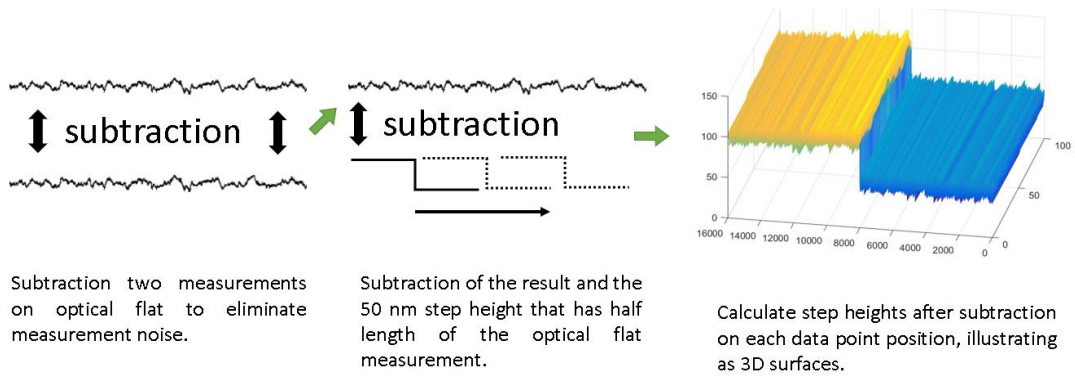


Figure 44. Assessment of flatness effect on step height measurement

The process of obtaining histogram (seen Figure 45) is shown in Figure 44. The histogram indicates that the measurement error contributed by flatness deviation, D_{Flat} , limits within 6 nm.

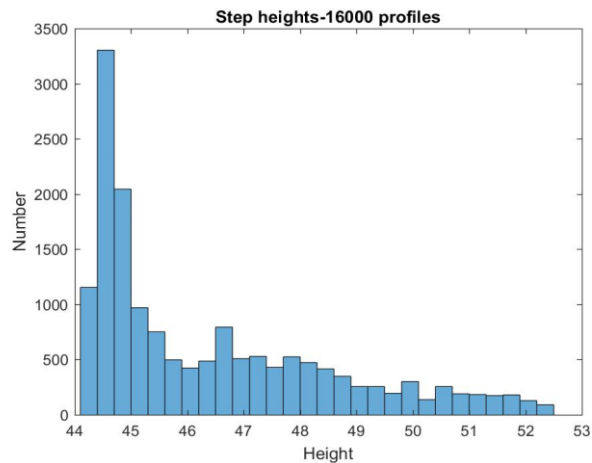


Figure 45. Histogram showing heights distribution. Around value of 44.5 nm owns most of the calculated step height

The formulas for calculating errors and uncertainties could be found below, seen equation (9) - (14).

$$\delta_{error} = \frac{|\varepsilon_{25\%} + \varepsilon_{50\%} + \varepsilon_{70\%}|}{\sqrt{3}} \quad (17)$$

Where: $\varepsilon_{25\%}$, $\varepsilon_{50\%}$, $\varepsilon_{75\%}$ stand for errors coming from measuring in different working range of z direction, which are mean values out of 5 repeated measurements minus calibrated value of the step height standard.

$$\delta_{repeat+reproduce} = \sqrt{\frac{1}{N} \sum_{i=1}^N (x_i - \mu)^2} \quad (18)$$

Where: N stands for the number of the measurements; x_i are the measured values; μ is the mean value of all the measured values, i.e. all the measurements on each position in z working range.

Considering that the distribution is propagated in a form of rectangular, hence:

$$\delta_{FLT} = \frac{D_{Flat}}{\sqrt{3}} \quad (19)$$

Where: D_{Flat} is the error contributed by flatness deviation.

$$\delta_{tracibility} = 5 \text{ nm} \quad (20)$$

The value of $\delta_{tracibility}$ is usually given by calibration of the artefact traced to primary calibration of the instrument.

Hence the combined uncertainty of the calibration metrological characteristics of the profilometer is derived as:

$$U_{combined} = \sqrt{\delta_{error}^2 + \delta_{repeat+reproduce}^2 + \delta_{FLT}^2 + \delta_{tracibility}^2} \quad (21)$$

The expanded uncertainty is calculated as (coverage factor $k=2$):

$$U_{expanded} = 2 * U_{combined} \quad (22)$$

Calculation result of measurement uncertainties are demonstrated in Table 9 below.

Table 9. Uncertainty contributed to step height measurements

Step height(nm)	δ_{error}	$\delta_{\text{repeat+reproduce}}$	δ_{FLT}	$\delta_{\text{tracibility}}$	U_{combined}	U_{expanded}
500	2.3	9.1	3.5	5	11	22
200	3.2	9.9	3.5	5	12	24
100	2.7	4.1	3.5	5	8	6
50	0.5	5	3.5	5	8	6

The measurement uncertainty of the profilometer does not exceed 30 nm. The reported expanded uncertainty is based on a standard uncertainty multiplied by a coverage factor of $k=2$, which provides a confidence level of approximately 95%.

4.3 Product measurement

4.3.1 Method

The wavelength and the amplitude of the sinusoidal feature will be evaluated to assess quality of the manufacturing process. The surface texture parameters S_a and S_q will be calculated as well.

3D mapping scanning measurements were taken on Bruker's DektakXT stylus profiler (seen Figure 46 and Figure 47), which enables 4 angstrom vertical repeatability and 1 angstrom vertical resolution. 2.5 μm radius of stylus was used. Contact force was set up to 1 mg. Lab temperature was remaining $20\text{ }^\circ\text{C} \pm 1\text{ }^\circ\text{C}$. The copper workpiece sits on the measuring table without fixture. Probing system was driving manually close to the target. Then automatically contact the workpiece. The contact force can be set up. In the measurements, 1 mg force was applied. To be able to obtain profiles through the centre of the workpiece (seen Figure 48), the 'striped-scans' were performed, seen Figure 49. According to the rotation angle, three stripes are 0° , 60° and 120° respectively. Each strip has width 20 μm , consisted of 20 single profile acquisitions with interval 1 μm , which is the closest distance the stylus could jog each time. 0° and 60° stripes were scanned once. 120° stripe was scanned three times without changing measuring parameters. Each profile could extract 6 complete waves, consisting of 6 pitches and 6 amplitudes. The centre part of sine wave was excluded. Hence each profile was separated into two parts of waves: 'left' and 'right', based on the relative position of the centre.

Measurement data was processed in surface topography analysis software TalyMap Gold 4.1. Some of the data visualization and fitting process were conducted in Matlab.



Figure 46. DektakXT overview



Figure 47. DektakXT close view

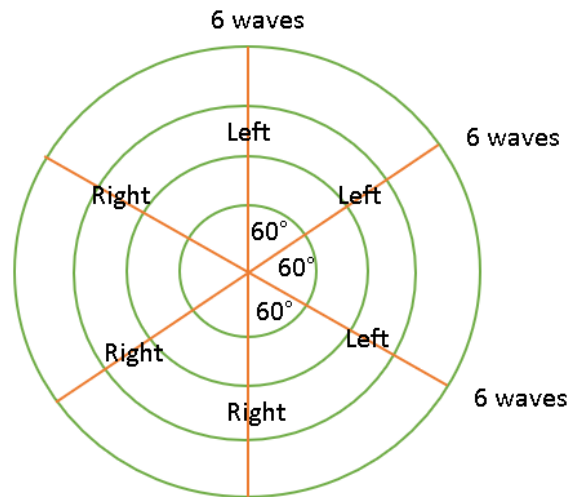


Figure 48. Extract profiles

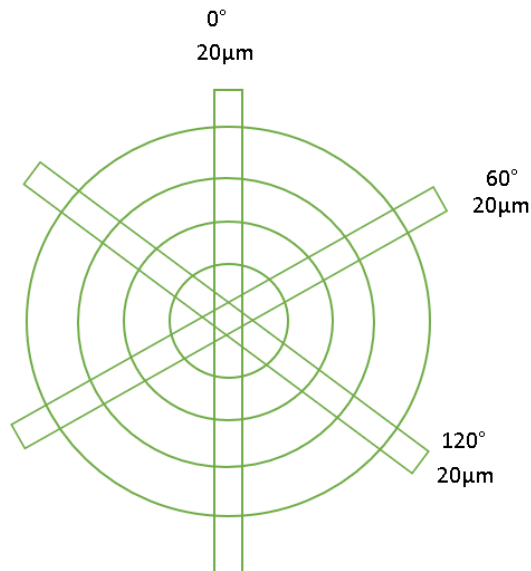


Figure 49. Striped-scans

4.3.2 Results

As an example, 60° profile is shown in Figure 50. Left (Figure 51) and right (Figure 52) side of the waves were extracted afterwards, followed by levelling operation (Figure 53) and morphological filtering (Figure 54) that deconvolves the effect of the stylus tip radius in measurement. The process was applied all the profile measurements.

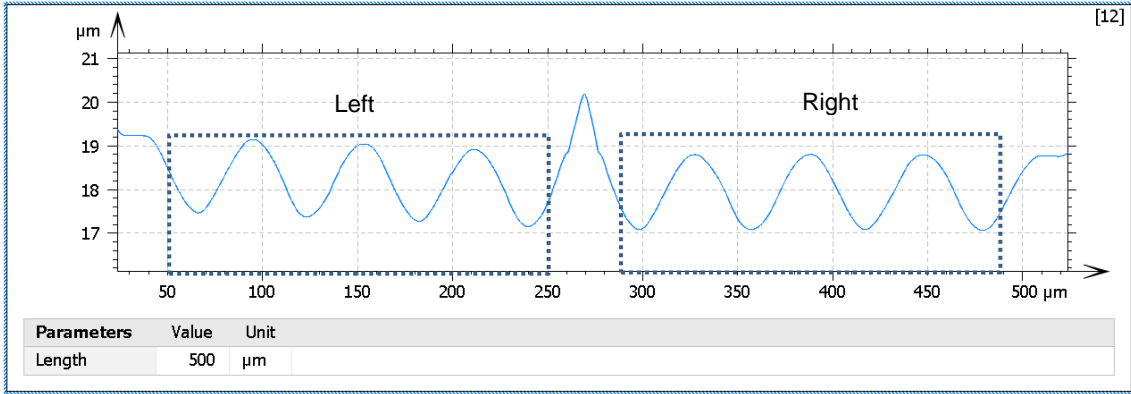


Figure 50. 60° profile measured on DexkakXT

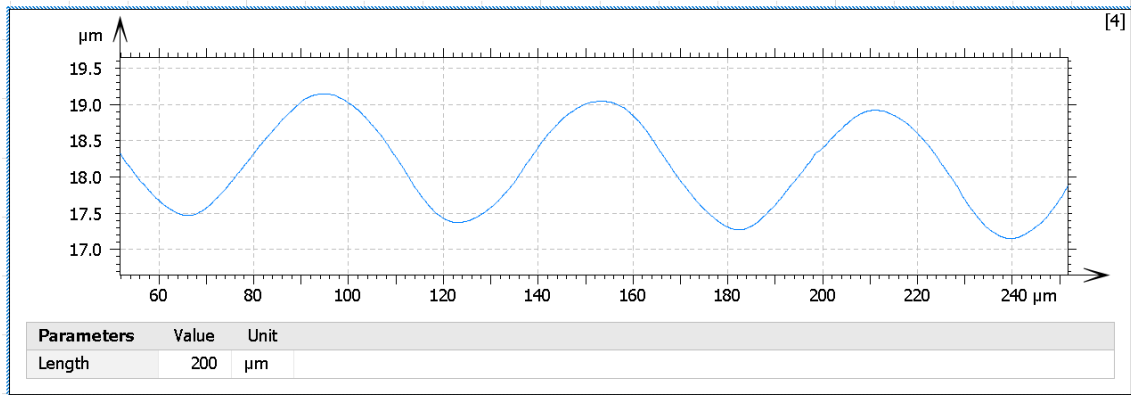


Figure 51. 60° profile, left waves

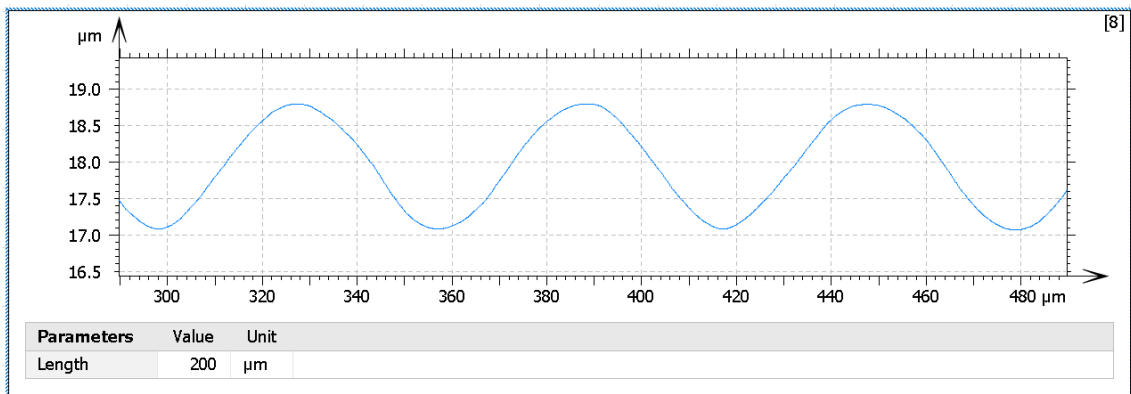


Figure 52. 60° profile, right waves

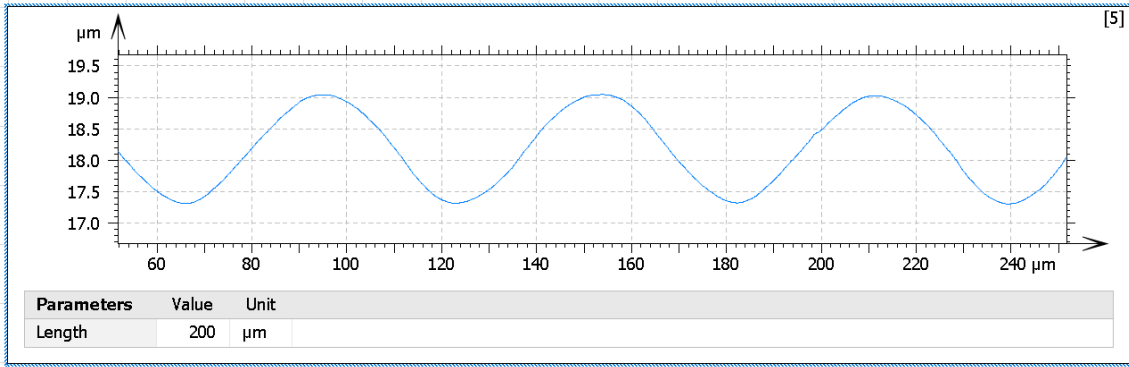


Figure 53. 60° profile, left waves, levelled

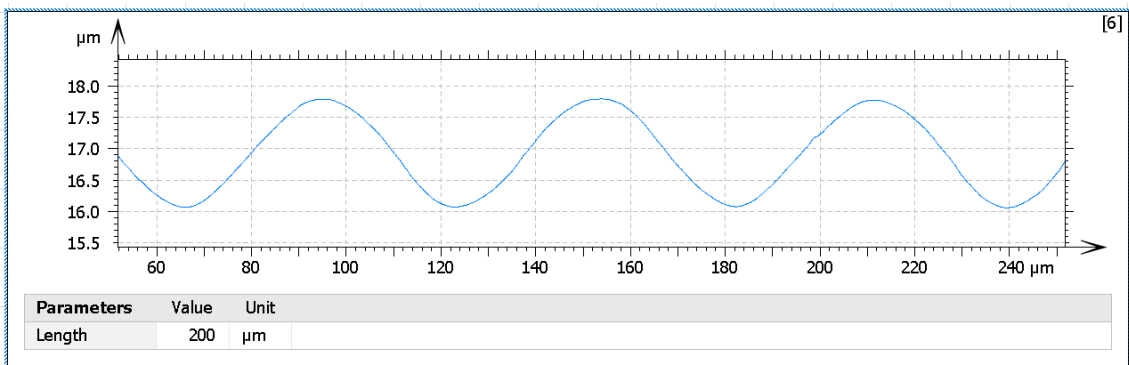


Figure 54. 60° profile, left waves, levelled, and morphological filtered

Difference between designed shape and measured shape is shown in Figure 55. It has been well known that the chosen diamond turning machine has high accurate motion on x direction, which also could be proved by CCI measurement, shown in Figure 56. Hence it indicates that the DektakXT profiler does not have calibrated lateral scale at the moment. Hence the correction of x axis scale on DektakXT would be necessary.

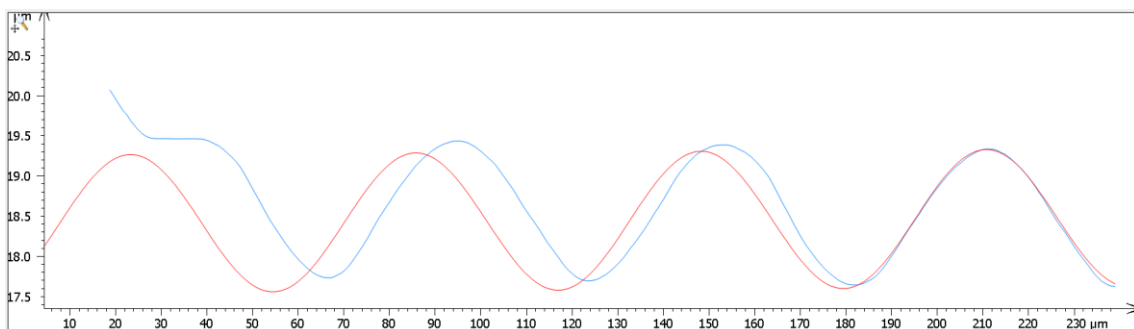


Figure 55. Subtraction between DektakXT measured 0° profile, left waves (blue) and designed waves (red).

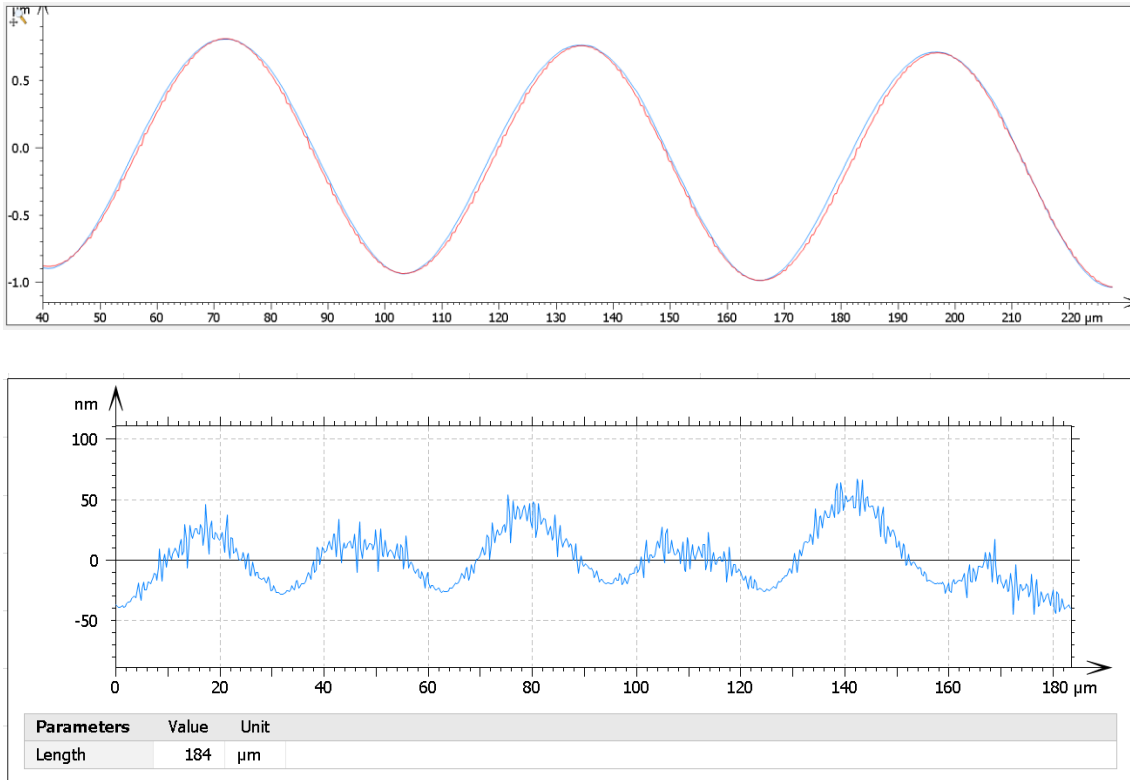


Figure 56. Above: subtraction between CCI measured profile, left waves (blue) and designed waves (red). Below: residual profile. (Ra 14.1nm, Rq 17nm)

Correction of x axis:

To establish the suitable sine function of the DektakXT measured surface, data points were fitted by sine function in Matlab. An example is shown in Figure 57. All the measured profiles were processed with the basic function:

$$y = a_1 * \sin(b_1 * x + c_1) \quad (23)$$

Results are listed in Table 10.

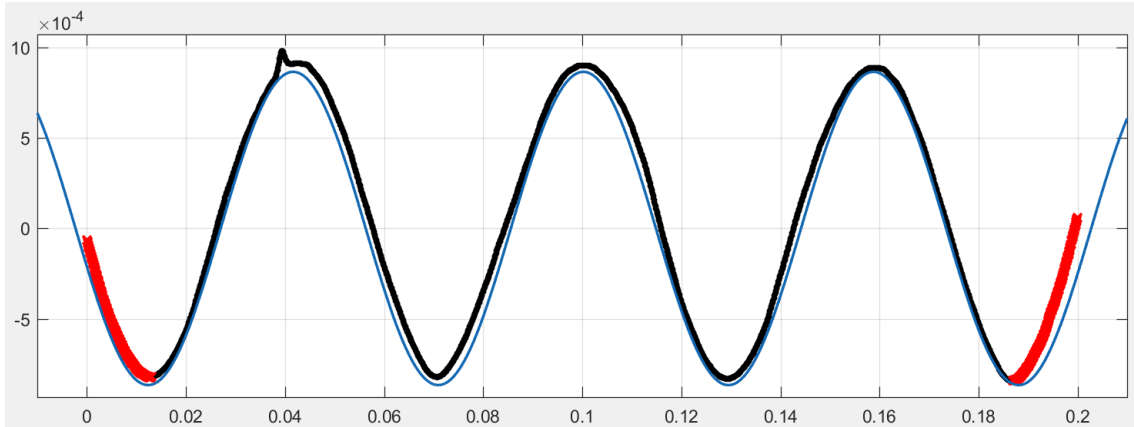


Figure 57. 120° profile, left waves fitting result. Black curve: data points; blue curve: fitting curve; red curve: excluded data points.

Table 10. Fitting results of measured profiles (unit: mm)

	a1	b1	c1
0 degree_e_L	0.000861	107.4	-2.876
0 degree_e_R	0.000863	104.4	-2.464
60 degree_e_L	0.00086	107.3	-3.012
60 degree_e_R	0.008605	103.7	-2.293
120_R1_e_L	0.000864	107.3	-2.9
120_R1_e_R	0.000863	103.6	-2.352
120_R2_e_L	0.000862	107.4	-2.913
120_R2_e_R	0.000864	103.6	-2.371
120_R3_e_L	0.000862	107.3	3.341
120_R3_e_R	0.000863	103.7	-2.408

Repeated measurements at 120° were used to estimate suitable fitting function for measured profile. Hence:

Table 11. Fitting results of 120 degree measured profiles (unit: mm)

	a1	b1	c1
120_R1_e_L	0.0008642	107.3	-2.9
120_R1_e_R	0.0008629	103.6	-2.352
120_R2_e_L	0.0008623	107.4	-2.913
120_R2_e_R	0.0008636	103.6	-2.371
120_R3_e_L	0.0008623	107.3	3.341
120_R3_e_R	0.0008634	103.7	-2.408
Mean	0.00086312	105.483333	-2.5888
Standard deviation	7.5741E-07	2.02723128	0.29075368
Standard uncertainty	3.0921E-07	0.8276137	0.130029

Hence the function for measured surface could expressed as:

$$y = 0.0008631 * \cos(105.5 * x) \quad (24)$$

Comparing with designed function:

$$y = 0.0008604 * \cos(100.5 * x) \quad (25)$$

The derived relation between DektakXT measured results and designed results is:

$$y_m = 0.9509 * y_D \quad (26)$$

where: y_m is measured and y_D is designed. Correction coefficient is fitting result. It is noted that this correction is only applied on x direction and only in this application. And deriving this correction does not consider the manufacturing error on x direction due to lack of accurate measurement of the wavelength, i.e. the correction is not reliable to be used, for reference only.

Repeated measurement of wavelength and amplitude:

According to the Table 10, the repeated measurement of wavelength and amplitude of the manufactured surface is summarized in Table 12.

Table 12. Repeated measurement of wavelength and amplitude

Features	Measurements (mm) *						Mean	Standard Deviation	Standard Uncertainty
	1	2	3	4	5	6			
Wavelength**	0.061521	0.063308	0.061626	0.063729	0.061521	0.063729	0.062572	0.001125	0.000459201
Amplitude	0.000861	0.000863	0.00086	0.000861	0.000862	0.000864	0.000862	1.58E-06	6.44291E-07
Correction	0.9509								

* 0° left, 0° right, 60° left, 60° right, 120° second repeat left, 120° second repeat right respectively.

** values are after correction

The results show that average value of manufactured wavelength is about 62.6 μm and averaged amplitude is about 0.000862 μm. Due to the lateral scale correction was establish based on the designed function, the wavelength value here cannot be used to assess manufacturing quality, which require support of more accurate measurements. The averaged amplitude shows that the manufactured surface is only few nanometres different from designed function.

Residual analysis:

Residual profiles **between fitting results and measurements** and **between different measurements** have been generated and analysis closely to explore the quality of the manufacturing process.

Figure 58 and Figure 59 illustrate the 0° profile left and right waves and their residuals from comparison of best fitting function. The same process was made for other measurements as well, seen Figure 60 to Figure 63. For each residual profile, roughness parameters Ra and Rq were calculated and listed in Table 13.

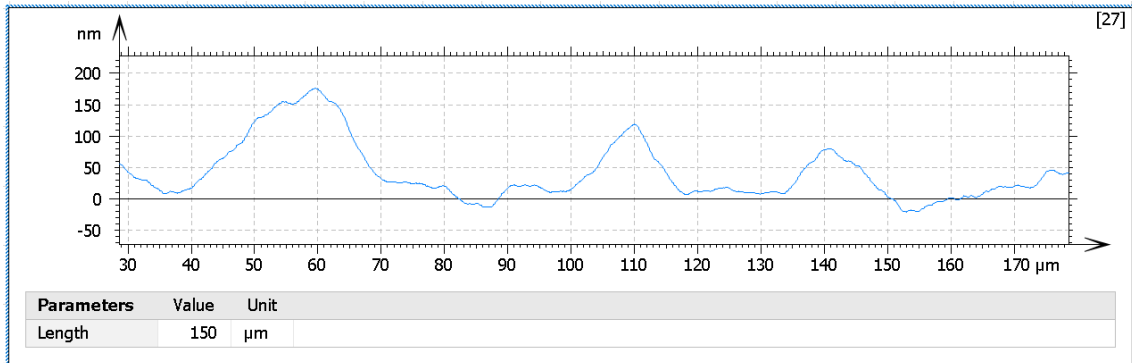
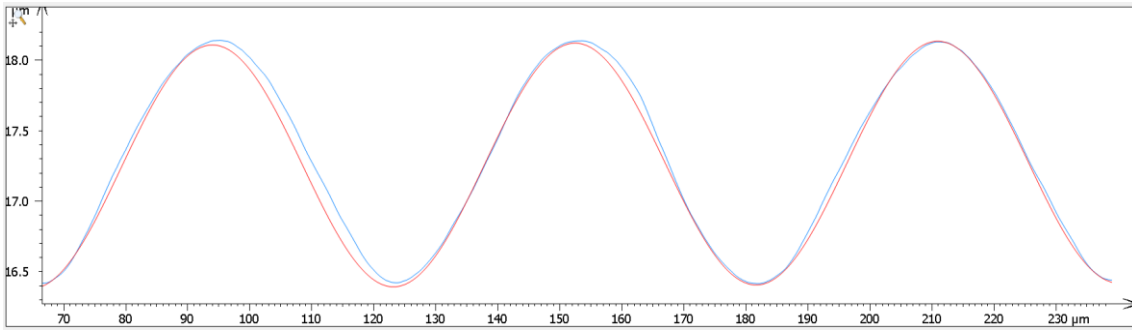


Figure 58. Above: subtraction between measured 0° profile, left waves (blue) and best fitting result (red). Below: residual profile.

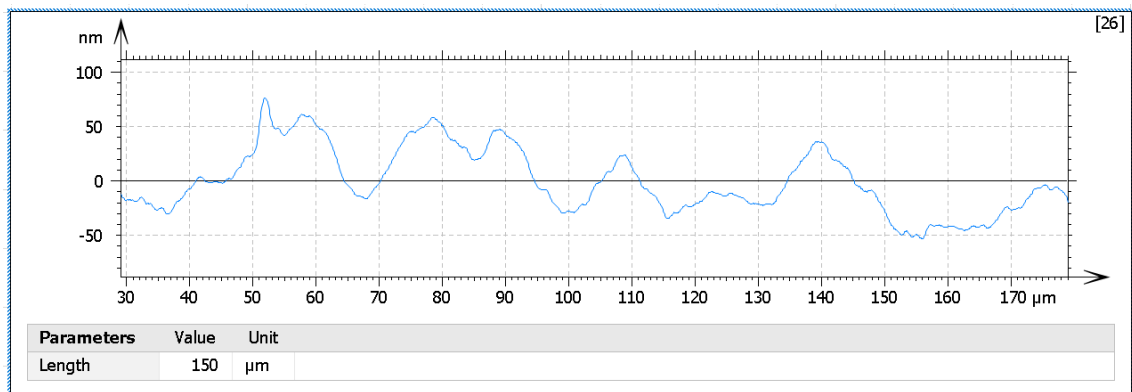
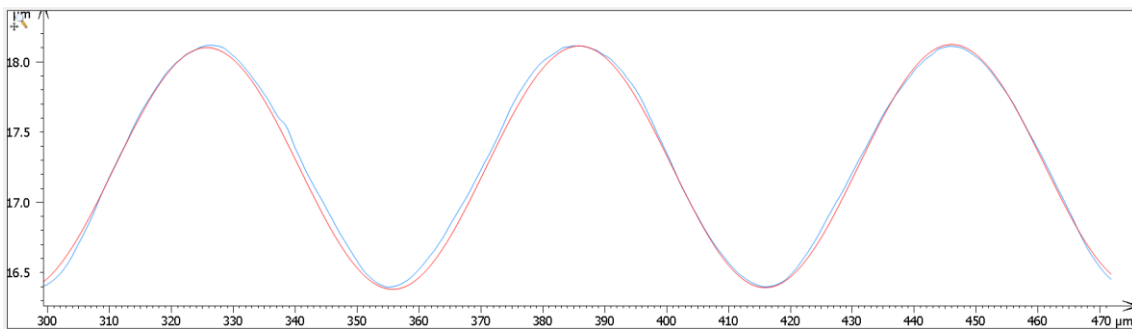


Figure 59. Above: subtraction between measured 0° profile, right waves (blue) and best fitting result (red). Below: residual profile.

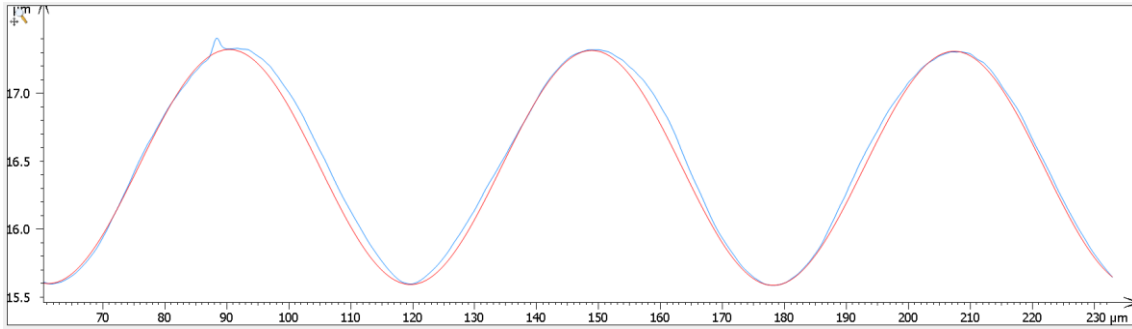


Figure 60. Subtraction between measured 120° profile, second measurement, left waves (blue) and best fitting result (red).

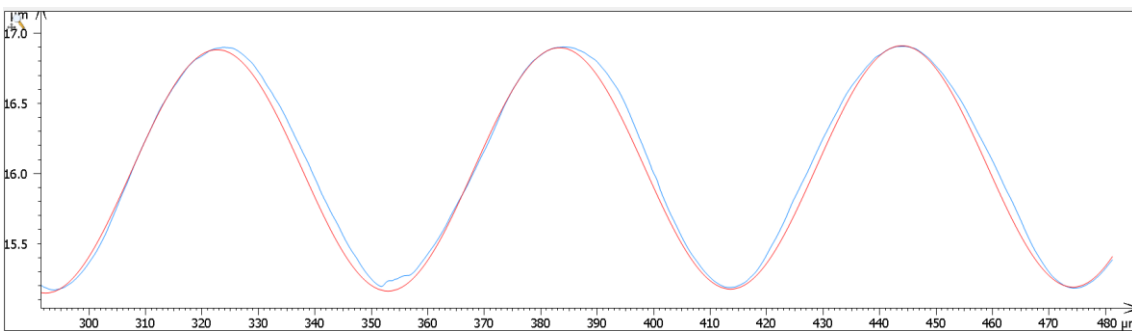


Figure 61. Subtraction between measured 120° profile, second measurement, right waves (blue) and best fitting result (red).

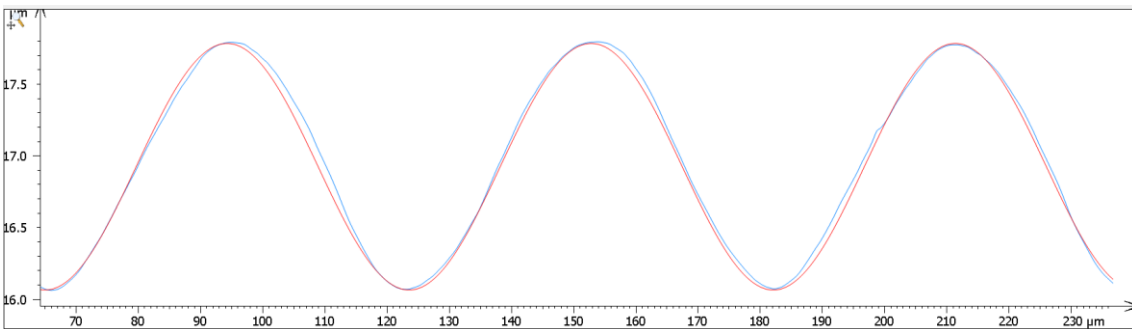


Figure 62. Subtraction between measured 60° profile, left waves (blue) and best fitting result (red).

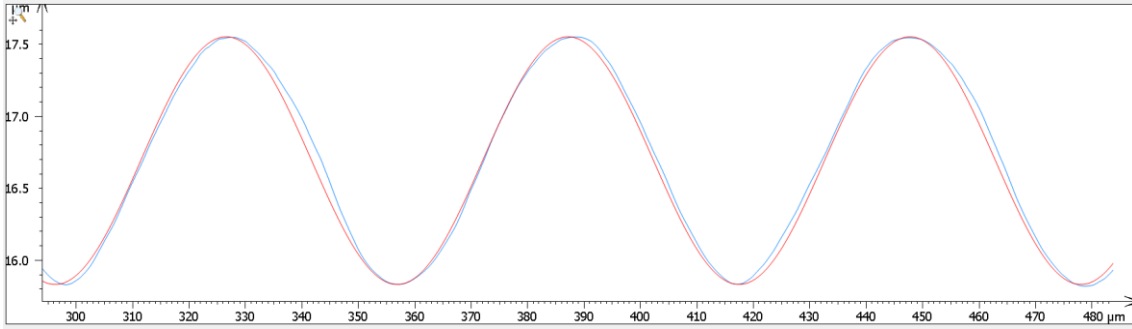


Figure 63. Subtraction between measured 60° profile, right waves (blue) and best fitting result (red).

Table 13. Roughness parameters of residual profiles between residual profiles and best fitting result

Unit: nm	Left		Right	
	Ra	Rq	Ra	Rq
0 degree	35	41.3	19.4	22.9
60 degree	23.8	31.2	30.4	38.9
120_R2	33.9	39.2	34.9	41.6

What is shown clearly in subtraction process is that for almost all peaks, right flanks have been left materials that is supposed to be removed. The most possible reason could be the tool wear. It may also due to the motion of the machine motion. The same reason may also suitable for imperfection valley in Figure 61. Considering the measuring instrument instability in x axis, dynamic error during measurement may also be a reason of the difference between measured profile and designed profile. Also, there is a protrusion near the first peak shown in Figure 60. It may be a dirt on the surface during measurement since similar object does not show anywhere else.

Beforehand, measurement noise has been assessed by subtracting two repeated measurement at 120° stripe (Seen Figure 64). Rq value is about 3.82 nm and Ra values is about 3 nm. Table 13 summarizes the surface roughness of the residual profiles. It indicates that the error mainly caused by tool is no more than 40 nm, considering measurement noise of the instrument. This error could be compensated by considering tool waviness geometry in the machining program.

To obtain geometry of the tool waviness, the waviness-controlled tool could be used, or measure the tool with unknow waviness.

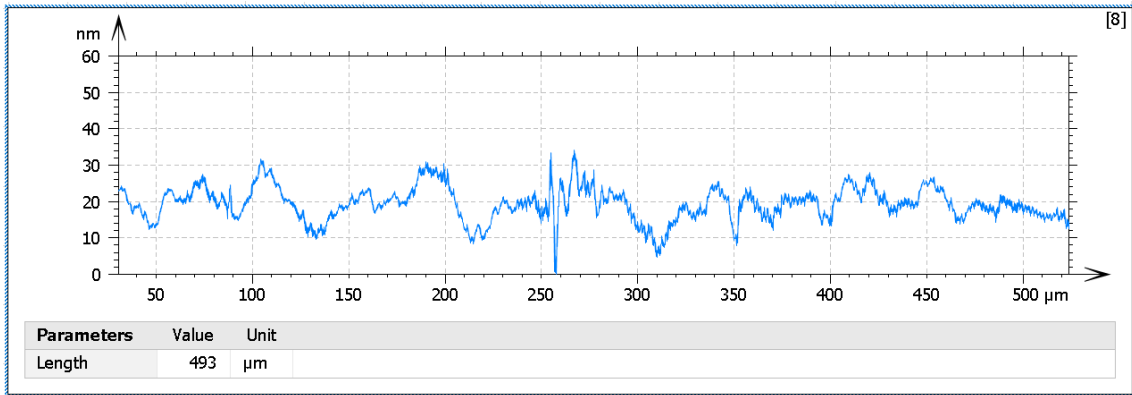


Figure 64. Subtraction of 120° profile, left waves, first and second measurements.

Moreover, residuals between different measurements were obtained. Examples are shown in Figure 65 and Figure 66. Residual profiles roughness parameters are calculated and summarized in Table 14.

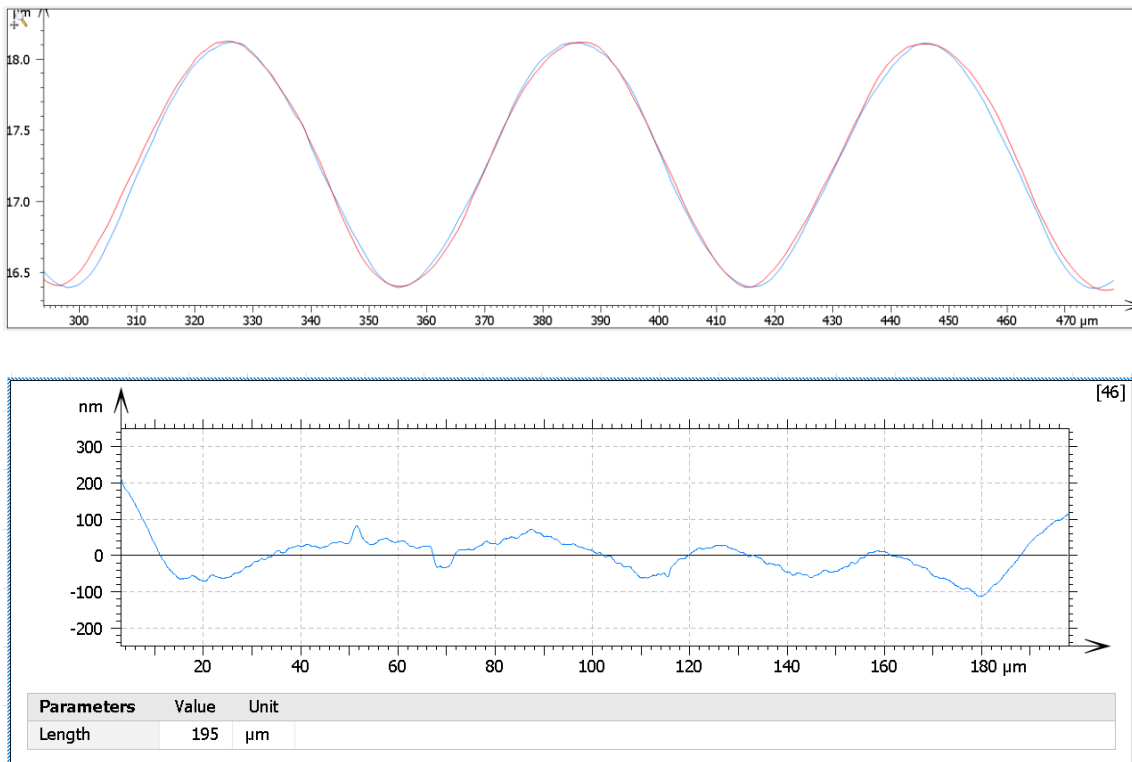


Figure 65. Above: subtraction between measured 0° profile, right waves (blue) and 60° profile, right waves (red). Below: residual profile.

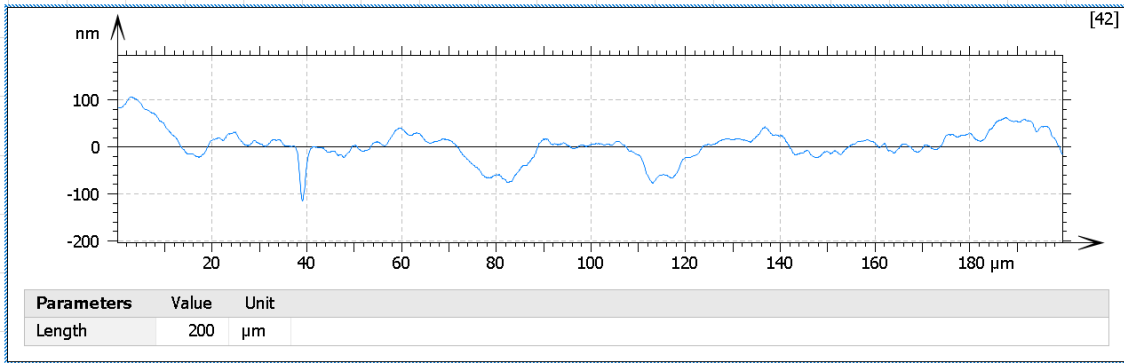
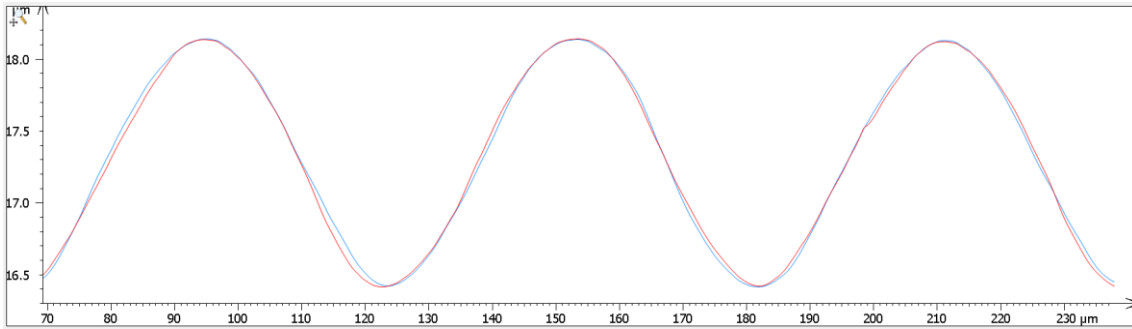


Figure 66. Above: subtraction between measured 0° profile, left waves (blue) and 60° profile, left waves (red). Below: residual profile.

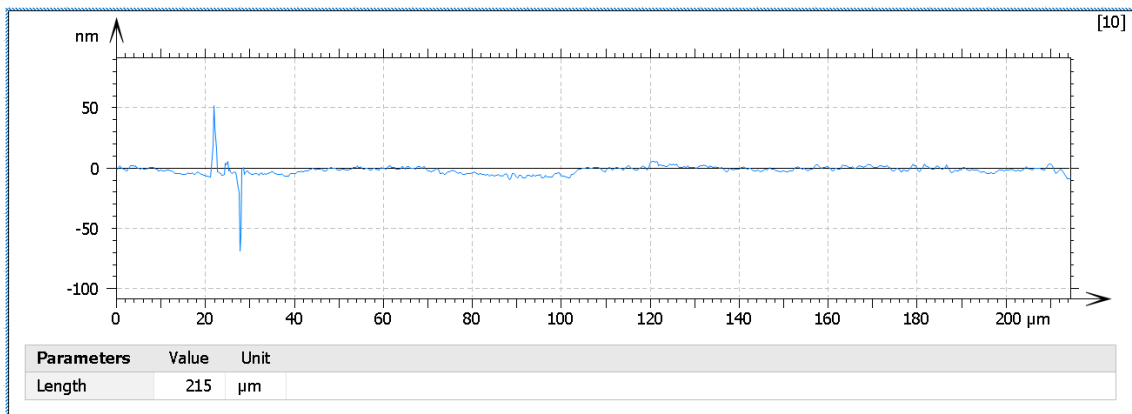


Figure 67. Residual profile of subtraction between 0° profile, left waves and 60° profile, left waves measured by CCI. (Ra 1.71 nm; Rq 2.06 nm)

Table 14. Residual of subtractions between different measurements

Unit: nm	Ra	Rq
0_L-60_L*	22.9	29.7
0_R-60_R	17.5	20.6
0_L-120_L	23.7	28.4
0_R-120_R	21.5	27.6
60_L-120_L	25	31.2
60_R-120_R	27.1	33.2

* 0 degree left waves minus 60 degree left waves.

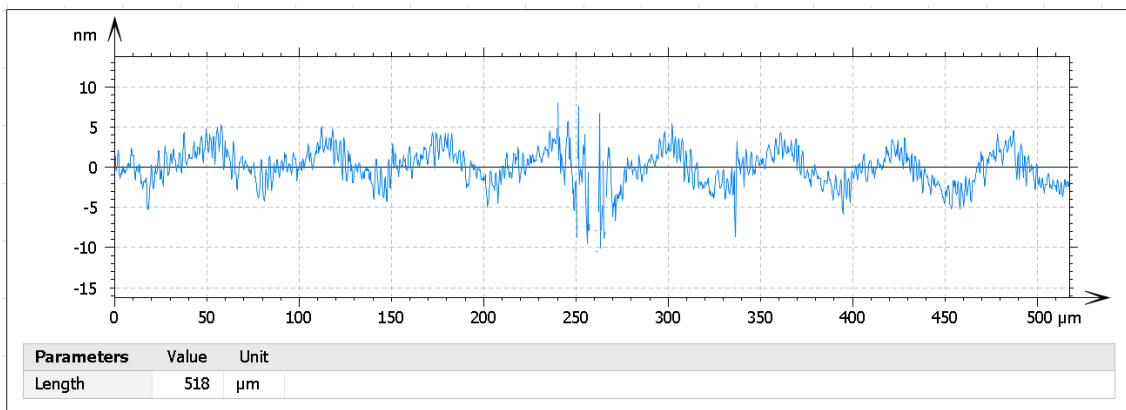


Figure 68. Subtraction of two profiles extracted from two repeated measurement of CCI. Geometry influence in the middle was thresholded. (Ra 1.82 nm, Rq 2.36 nm)

The difference between different measurements mainly comes from the error effect coming from spindle rotation. Depending on the roundness accuracy of the spindle rotation, workpiece may deform slightly or wobbling following spindle. The difference may also be caused by unstable tool assembly or material behaviour. The roughness parameters in Table 14 shows that the error given is about 30 nm, with consideration of the measurement noise that is about 3 nm.

5 Measurement uncertainty

According to international standard guidance about estimation of uncertainty in product verification [76] and good practice guide for calibration areal stylus instrument [75], measurement uncertainty estimation of manufactured radial sinusoidal shape is demonstrated below.

Table 15. Uncertainty sources of measurement

Task: functionality evaluation of the product					
NO.	Designation	Designation	Uncertainty Components	Comments	Axis
1	u_{Re}	u_{Re-W}	Repeatability of wavelength measurement	Type A evaluation. Determined from repeated measurements of the sample.	X
		u_{Re-A}	Repeatability of amplitude measurement		Z
2	u_{Re-In}		Repeatability of instrument	Type B evaluation. According to specification of the measuring instrument.	Z
3	u_F		Measuring force	Type B evaluation. Based on Hertz contact law: a sphere with a half plane	Z
4	u_{FLT}		Flatness	Type A evaluation. Determined from measurements of the optical flat. Surface texture parameter Sz.	Z
5	u_A	u_{A-xy}	Amplification	Type A evaluation. Determined from measurements of the periodical sinusoidal shape.	X
		u_{A-z}		Type A evaluation. Determined from measurements of the step heights.	Z
6	u_L	u_{L-xy}	Linearity	Type A evaluation. Determined from measurements of the cross grating.	X
		u_{L-z}		Type A evaluation. Determined from measurements of the step heights.	Z
7	u_{trace}	$u_{trace-flat}$	Traceability	Type B evaluation. Obtained from calibration certificates of used standard	Z
		$u_{trace-sine}$			X
		$u_{trace-step}$			Z

Amplitude measurement:

- 1) Repeatability of amplitude measurement - u_{Re-A}

According to Table 12,

$$u_{Re-A} = 0.644 \text{ nm} \quad (27)$$

- 2) Repeatability of instrument - u_{Re-In}

The manufacturing specification gives step height repeatability:

$$u_{Re-In} = 0.4 \text{ nm} \quad (28)$$

- 3) Measuring force - u_F

According to Hertz contact theory of sphere contacting with plane substrate, the depth of indentation is given by equation [77]:

$$d \cong \left(\frac{16F^2}{9E_*^2 * R} \right)^{\frac{1}{3}} \quad (29)$$

Where:

$$\frac{1}{E_*} = \frac{1}{2} \left(\frac{1 - \nu_1^2}{E_1} + \frac{1 - \nu_2^2}{E_2} \right) \quad (30)$$

E_1 and E_2 are elastic moduli of contacting materials, ν_1 and ν_2 are Poisson's ratios. R is radius of sphere, F is force.

In the measurement from DektakXT profiler, 2.5 μm radius stylus was used, measuring force was 0.5 mg (considering gravity $g=9.780 \text{ m/s}^2$). Young's modulus of diamond stylus is about 1220 GPa and Poisson's ratio is about 0.2 [78]. The young's modulus of cooper is about 130 GPa and Poisson's ratio is about 0.34 [79]. Hence the variance limit a is:

$$a = d \cong \left(\frac{16F^2}{9E_*^2 * R} \right)^{\frac{1}{3}} = 2.2014 * 10^{-4} (\mu\text{m}) \quad (31)$$

The contribution of measuring force to the measuring uncertainty is propagated in form of rectangular distribution. Hence the standard uncertainty is calculated as:

$$u_F = a * b = 5.0399 * 10^{-4} * \frac{1}{\sqrt{3}} = 3.4945 * 10^{-4} (\mu\text{m}) \quad (32)$$

4) Flatness - u_{FLT}

Flatness of the reference plane of instrument is evaluated by measuring optical flat with calibrated surface. Considering the measurement of sample has length no more than 0.6 mm, the optical flat will be measured 1 mm length 5 times at different positions. Surface roughness parameter S_z will be introduced for the evaluation of the flatness. Measurement results are shown in Table 16.

Table 16. Flatness measurements

Measurements	Sz (nm)
1	10
2	41.2
3	5.57
4	24.2
5	8.23
Average	17.84
σ	14.92070541
Standard uncertainty	6.67274 2315

5) Amplification and linearity of z direction - u_{Step}

Evaluation of amplification and linearity of z direction could be done by using a series of step heights with various height values. The sample has amplification not beyond 2 μm , hence the calibrated step heights 500 nm, 1 μm and 2 μm were chosen. The calibrated standard was placed on the same area on xy plane where the sample was measured, and the measuring force kept the same as when measured the sample. Five times measurements were made by driving stylus on y direction. Measurement results are shown in Table 17.

Table 17. Step height measurement and uncertainty contribution

Step heights (μm)	Measurements					Average	α	Error	σ	u_e	u_{repeat}	u_{trace}	$u_{combine}$	U (k=2)
	1	2	3	4	5									
0.5	0.437	0.433	0.438	0.428	0.432	0.4336	0.972419	0.0046	0.004037	0.001806	0.001805547	0.005	0.007258	0.014516
1	0.91	0.907	0.909	0.909	0.907	0.9084		0.0084	0.001342	0.000600	0.0006	0.005	0.009812	0.019624
2	1.99	1.99	1.99	1.99	1.99	1.99		0.01	2.483E-16	1.110E-16	1.11022E-16	0.005	0.01118	0.022361

Hence the uncertainty contributed by step height measurement does not beyond 22.4 nm.

Combined uncertainty:

$$u_{c-A} = \sqrt{u_{Re-A}^2 + u_{Re-In}^2 + u_F^2 + u_{FLT}^2 + u_{Step}^2} \quad (33)$$

$$u_{c-A} = \sqrt{0.644^2 + 0.4^2 + 0.349^2 + 6.673^2 + 22.4^2} = 23.39 \text{ nm} \quad (34)$$

$$U_{expand-A} = 13.06 * 2 = 46.78 \text{ nm} \quad (35)$$

The reported expanded uncertainty is based on a standard uncertainty multiplied by a coverage factor of $k=2$, which provides a confidence level of approximately 95%.

Wavelength measurement:

- 1) Repeatability of wavelength measurement - u_{Re-W}

According to Table 12,

$$u_{Re-W} = 459.2 \text{ nm} \quad (36)$$

- 2) Amplification of x direction

Periodical sinusoidal shape (seen Figure 69) was chosen for evaluating amplification of x direction, which the parameter PSm (Mean width of the profile elements) is the evaluated measurand. The nominal period is 100 μm . As the scanning length of the product is 600 μm on both directions (x and y), six-periods length of the calibrated standard shape should be evaluated along the x direction. And five times measurements on the different positions of the artefact would be conducted. However, we do not have this type of calibration standard at the moment. Hence, the wavelength measurement uncertainty contributed by amplification of x axis of measuring instrument could not be assessed.

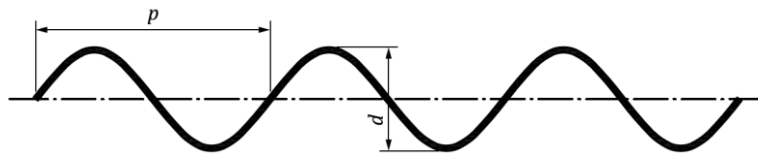


Figure 69. Periodical sinusoidal shape (Type PPS) [9]. p: period; d: amplitude.

3) Linearity of x direction

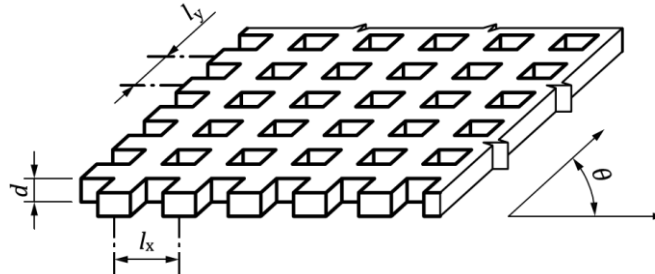


Figure 70. Cross grating (Type ACG) [9]. l_x, l_y : pitch in x and y axis; θ : angle between x and y axes; d : depth of the pits.

Generally, the calibration standard is used for evaluate linearity deviation of the measurement device is cross grating. By measuring the distance between each pit, the linearity deviation on x axis could be determined. The NPL calibrated cross grating standard with 100 μm pitch was chosen to be used (seen Figure 17). In total, 5 measurements would be taken at different position of the artefact. Then the pits centre would be found. The measurement of distance between pits centre would be conducted.

For the DextakXT profiler, the lateral resolution could be defined by user. Specifically, user defines the running time (s), the measuring length (μm) and the number of measuring points (pts). Then the system determines the lateral resolution ($\mu\text{m}/\text{pt}$). The advantage is that user could choose desired resolution within a big range. However, the drawback is that the instability and the uncertainty of x scale becomes large due to the calculation process. Moreover, it does not have distance inspection in x drive unit. Hence, the evaluation of the linearity deviation of the instrument requires relatively complicated and systematic assessment.

Essentially, cross grating could also be used for determination of the amplification in x axis by measuring the average value of the pitches in x axis. One of the disadvantage of using cross grating instead of periodical sinusoidal shape is that

during the measuring process, stylus is moving with a certain speed, due to the steep slope of the pit wall, stylus would not be able to touch the wall and give the accurate measurement. Moreover, the gravity centre of each pit needs to be located by applying specified algorithm in order to carry on the average calculation. It would introduce more source of measurement uncertainty. Hence, if only amplification was required, best choice of calibration standard would be periodical sinusoidal shape.

Combined uncertainty:

Hence, for now the combined uncertainty of the wavelength measurement is derived by:

$$u_{c-W} = \sqrt{u_{Re-W}^2} = 459.2 \text{ nm} \quad (37)$$

$$U_{expand-B} = 459.4 * 2 = 918.8 \text{ nm} \quad (38)$$

The reported expanded uncertainty is based on a standard uncertainty multiplied by a coverage factor of $k=2$, which provides a confidence level of approximately 95%.

6 Application of the product

The product was also repeatedly measured by white light interferometer CCI 6000 (shown in Figure 71) that produced by Taylor Hobson, with 50x magnification lens, NA 0.7 and field of view 0.36 mm². The maximum pixel mode XY (1024 pixels) was applied. X and Y drive unit range of the instrument is about 150x150 mm. The product was placed in the middle of the range, which the location is about 75x75 mm. Five positions are chosen in z working range of instrument: 10%, 30%, 50%, 70%, 90%. Sample was measured 5 times at each position. An example of measurement result is shown in Figure 72. Calculated values of Sa and Sq are shown in Table 18. It is noted that the Sa and Sq values were derived by the extracted area of each measurement, seen Figure 73. The reason is to calculate Sa and Sq value as the same dimension as the designed surface, seen in Figure 74. The Sa and Sq value of the designed shape are 0.525 μm and 0.588 μm respectively.

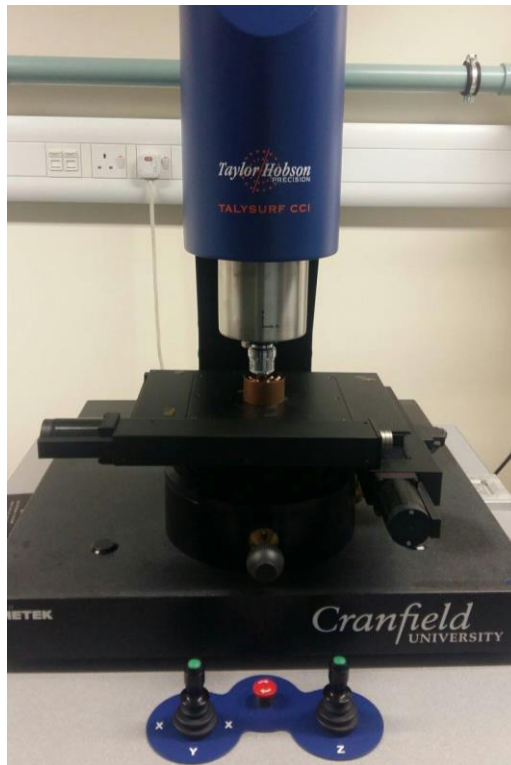


Figure 71. Taylor Hobson CCI 6000

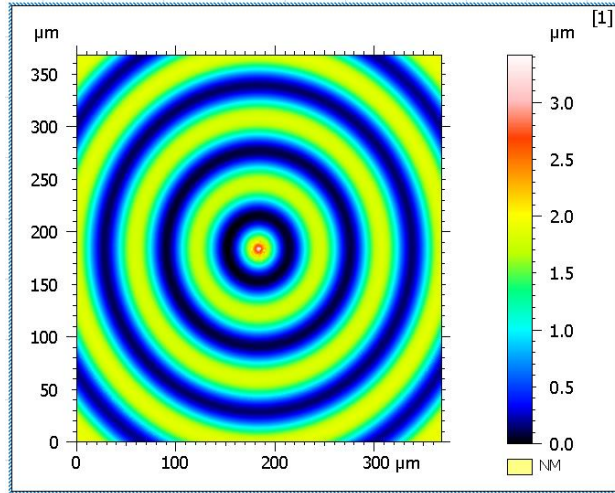


Figure 72. Example of measurement from CCI

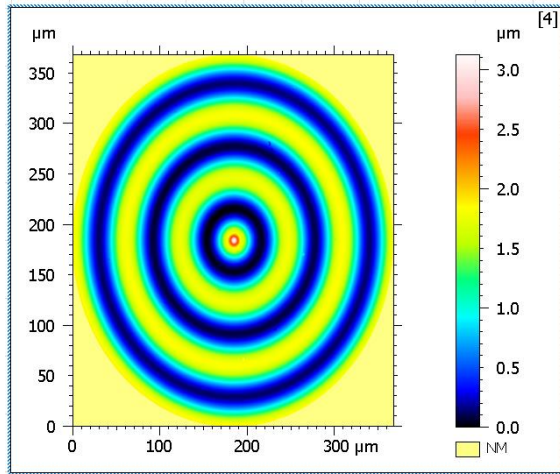


Figure 73. Extracted area of repeated measurement from CCI

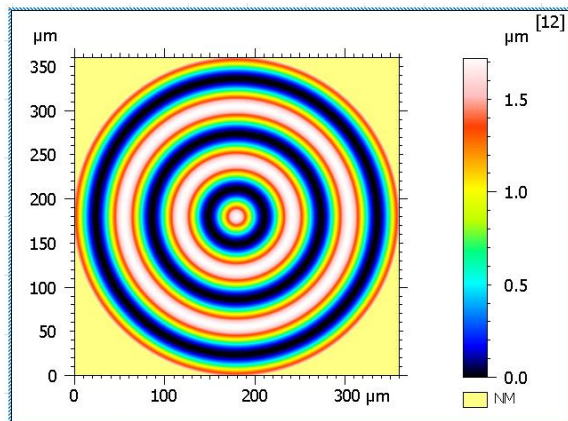


Figure 74. Designed radial sinusoidal shape, imported in Talymap.

Table 18. Repeated measurement results of the product on CCI

Positions	Parameters (nm)	Number of repeated measurements					Average Sa	Average Sq	σ (Sa)	σ (Sq)	$u(Sa)$	$u(Sq)$
		1	2	3	4	5						
10%	Sa	545	544	542	542	542	543	605	1.2207	1.2207	0.2441	0.2441
	Sq	607	606	604	604	604						
30%	Sa	542	544	542	544	542						
	Sq	604	606	604	606	604						
50%	Sa	545	544	543	543	544						
	Sq	607	606	605	605	606						
70%	Sa	543	544	543	546	546						
	Sq	605	606	605	608	608						
90%	Sa	543	543	543	543	542						
	Sq	605	605	605	605	604						

Calculated results show that in the same field of view the Sa and Sq values of the measured surface are about 20 nm bigger than the values of designed surface. Most possible reason could be the protrusion that is higher than the designed amplitude in the middle of the product. However, in the middle of the designed surface, it should be a sinusoidal peak. Besides, other elements such as positioning, levelling operation, filtering in the software, etc. may contribute the difference. Also, the standard uncertainty of Sa and Sq measurements are less than nanometre, which shows that the CCI provides satisfied measurement repeatability.

7 Summary

1. A protrusion stands in the centre of the product in every manufacturing trial. The comparison of roughness parameters calculation result between the measured shape from CCI and the designed shape indicates that the protrusion is the main reason to cause the calculation difference.
2. The comparison between the designed radial sinusoidal shape with DektakXT profiler measurement of the machined shape shows that the amplitude was produced by the turning machine with the error within few nanometres.
3. The comparison between designed radial sinusoidal shape and CCI measurement of the machined shape shows that the DektakXT profiler has large amount systematic error in x scale. The profiler did not provide accurate result to wavelength/pitch measurements. Therefore, the machine motion accuracy on x direction could not be evaluated systematically. The CCI measurement result was introduced for comparison, which it indicates that the errors from machine motion and tool wear is sub-micro level. The machine motion accuracy could be improved by programming machining process in incremental mode.
4. The tool geometry could be the most possible reason that causes large imperfection of the product surface.
5. Step height experiments indicates that the chosen diamond turning machine does not have satisfied repeatability on z direction when it feeds less than 100 nm, while the repeatability becomes better when it feeds bigger than 100 nm. The result of the product amplitude measurements proves that the machine has reliable producibility on z direction when the feed is micro level.

8 Conclusion

1. SPDT (Single point diamond turning) technique has been used for manufacturing type ARS (Radial Sinusoidal Shape) material measure that is capable to test overall performance of surface topography measuring instrument.

2. The chosen diamond turning machine achieved desired surface finishing and accuracy of the form in this machining task. The result indicates that x, y and z axis of the machine is cooperatively working overall with nanometre level accuracy. The only issue of the machine is that the protrusion appears in the middle of the workpiece, which could be eliminate by applying on-machine measurement. Besides, tool geometry is another main contribution to the imperfection of the surface.
3. Profiler was used to measure amplitude and wavelength of the product. In amplitude direction, the manufacturing error is under 2 nm. In wavelength direction, the manufacturing error is under hundred nanometres. White light interferometer was employed to measure areal surface roughness parameters Sa and Sq that have error about 20 nm.

9 Future work

1. To minimise the effect of the mounting process to the centre alignment of the tool, on-machine measurement could be introduced in to measure the workpiece after machining without unload the workpiece. The realization of the accurate on-machine measurement could increase quality of the final product dramatically.
2. The machine motion error on x axis could be reduced by programming in incremental movement command, which eliminate the superimposition of the error in each feed. Moreover, tool geometry needs to be considered in the program, especially for the relatively smaller feature than the tool radius.
3. In terms of the presenting work, calibration of the DektakXT profiler needs to be completed comprehensively in order to give better measurement result.

REFERENCES

- [1] T. Hobson and G. PRECISION'S, "Exploring Surface Texture: A fundamental guide to the measurement of surface finish," *Leicester–Inglaterra, 4th Ed. ed. Taylor Hobson Ltda*, vol. 100, 2003.
- [2] "ISO 25178-6:2010 Geometrical product specifications (GPS) -- Surface texture: Areal -- Part 6: Classification of methods for measuring surface texture," 2010.
- [3] J. E. Harvey, N. Choi, S. Schroeder, and A. Duparré, "Total integrated scatter from surfaces with arbitrary roughness, correlation widths, and incident angles," *Opt. Eng.*, vol. 51, no. 1, p. 13402, 2012.
- [4] S. Schröder, T. Herffurth, H. Blaschke, and A. Duparré, "Angle-resolved scattering: an effective method for characterizing thin-film coatings," *Appl. Opt.*, vol. 50, no. 9, pp. C164–C171, 2011.
- [5] R. E. Reason, "Surface finish and its measurement," *J. Inst. Prod. Eng.*, vol. 23, no. 10, pp. 347–372, 1944.
- [6] J. JCGM, "200: 2012—International Vocabulary of Metrology—Basic and General Concepts and Associated Terms (VIM)," Technical Report, 2012.
- [7] *ISO 25178-600 specification (GPS)-Surface texture: Areal part 600: Metrological characteristics for areal-topography measuring methods.* 2017.
- [8] R. Leach, *Optical measurement of surface topography*, vol. 14. Springer, 2011.
- [9] *ISO 25178-70:2014 Geometrical product specification (GPS) -- Surface texture: Areal -- Part 70: Material measures. .*
- [10] "ISO 25178-701:2010 Geometrical product specifications (GPS) -- Surface texture: Areal -- Part 701: Calibration and measurement standards for contact (stylus) instruments," 2010.

- [11] M. Eifler, J. Hering, G. von Freymann, and J. Seewig, "Manufacturing of the ISO 25178-70 material measures with direct laser writing-a feasibility study," *Surf. Topogr. Metrol. Prop.*, 2018.
- [12] M. Stedman, "Mapping the performance of surface-measuring instruments," in *Micromachining of Elements with Optical and Other Submicrometer Dimensional and Surface Specifications*, 1987, vol. 803, pp. 138–144.
- [13] R. Leach, *Fundamental principles of engineering nanometrology*. Elsevier, 2014.
- [14] M. Stedman, "Limits of surface measurement by optical probes," in *Surface Measurement and Characterization*, 1989, vol. 1009, pp. 62–68.
- [15] M. Stedman and K. Lindsey, "Limits of surface measurement by stylus instruments," in *Surface Measurement and Characterization*, 1989, vol. 1009, pp. 56–62.
- [16] S. Rosén, T. R. Thomas, and B.-G. Rosén, "The Stedman diagram revisited," *Surf. Topogr. Metrol. Prop.*, vol. 2, no. 1, p. 14005, 2013.
- [17] S. Rosén, T. R. Thomas, and B. G. Rosén, "The Stedman diagram revisited," *Surf. Topogr. Metrol. Prop.*, vol. 2, no. 1, 2014.
- [18] "ISO 5436-1:2000 Geometrical Product Specifications (GPS) -- Surface texture: Profile method; Measurement standards -- Part 1: Material measures," 2000.
- [19] K. Nemoto *et al.*, "Development of a roughness measurement standard with irregular surface topography for improving 3D surface texture measurement," *Meas. Sci. Technol.*, vol. 20, no. 8, p. 84023, 2009.
- [20] K. Nemoto, K. Yanagi, M. Aketagawa, D. Kanda, I. Yoshida, and M. Uchidate, "A study on surface material measures for areal surface texture measuring instruments - Measuring conditions for the areal profiling," *Key Eng. Mater.*, vol. 381–382, pp. 241–244, 2008.

- [21] J. Frühauf, R. Krüger-Sehm, A. Felgner, and T. Dziomba, *Areal roughness standards*, vol. 1. 2012.
- [22] H. H. Gatzert and R. Krüger-Sehm, "Roughness standards for the calibration of SPM—from design to comparison measurement," in *5th Seminar on Quantitative Microscopy and 1st Seminar on Nanoscale Calibration Standards and Methods*, 2001.
- [23] J. Seewig, M. Eifler, F. Schneider, and J. C. Aurich, "Design and verification of geometric roughness standards by reverse engineering," *Procedia CIRP*, vol. 45, pp. 259–262, 2016.
- [24] M. Eifler, F. Schneider, J. Seewig, B. Kirsch, and J. C. Aurich, "Manufacturing of new roughness standards for the linearity of the vertical axis—Feasibility study and optimization," *Eng. Sci. Technol. an Int. J.*, vol. 19, no. 4, pp. 1993–2001, 2016.
- [25] Y. Chen, X. Zhang, T. Luo, X. Liu, and W. Huang, "Fabrication and characterization of areal roughness specimens for applications in scanning probe microscopy," *Meas. Sci. Technol.*, vol. 24, no. 5, p. 55402, 2013.
- [26] "VLSI Standards, Inc.," <http://www.vlsistandards.com/>.
- [27] C. L. Giusca, R. K. Leach, and F. Helery, "Calibration of the scales of areal surface topography measuring instruments: Part 2. Amplification, linearity and squareness," *Meas. Sci. Technol.*, vol. 23, no. 6, 2012.
- [28] L. De Chiffre, L. Carli, and R. S. Eriksen, "Multiple height calibration artefact for 3D microscopy," *CIRP Ann. - Manuf. Technol.*, vol. 60, no. 1, pp. 535–538, 2011.
- [29] R. Koops, M. Van Veghel, and A. Van De Nes, "A dedicated calibration standard for nanoscale areal surface texture measurements," *Microelectron. Eng.*, vol. 141, pp. 250–255, 2015.
- [30] R. K. Leach, C. L. Giusca, and P. Rubert, "A single set of material measures for the calibration of areal surface topography measuring instruments: the

- NPL Areal Bento Box,” *Proc. Met. Props*, pp. 406–413, 2013.
- [31] U. Hubner *et al.*, “Fabrication of calibration standards for the in-situ-determination of AFM tip-shapes,” in *5th Seminar on Quantitative Mircroscopy and 1st Seminar on Nanoscale Calibration Standards and Methods*, 2001.
- [32] N. G. Orji, R. G. Dixon, J. Fu, and T. V. Vorburger, “Traceable pico-meter level step height metrology,” *Wear*, vol. 257, no. 12, pp. 1264–1269, 2004.
- [33] “Anfatec Instruments AG,” http://www.anfatec.de/accessories/afm_gratings.html. .
- [34] “Pelco Security Cameras and Surveillance Systems,” <https://www.pelco.com/>. .
- [35] “Veeco Instruments,” <http://www.veeco.com/>. .
- [36] “MikroMasch,” <https://www.spmtips.com/>. .
- [37] “NTT Advanced Techn.,” <http://www.ntt-at.com/>. .
- [38] U. Brand, T. Kleine-Besten, and H. Schwenke, “Development of a special CMM for dimensional metrology on microsystem components,” in *Proceedings of the 15th Annual Meeting of the American Society for Precision Engineering, Scottsdale, AZ, USA*, 2000, vol. 2227.
- [39] R. Leach, C. Giusca, M. Guttmann, P. J. Jakobs, and P. Rubert, “Development of low-cost material measures for calibration of the metrological characteristics of areal surface texture instruments,” *CIRP Ann. - Manuf. Technol.*, vol. 64, no. 1, pp. 545–548, 2015.
- [40] “NPL Areal Standard,” <http://www.npl.co.uk/upload/pdf/instruments-areal-standard-flyer.pdf>. .
- [41] J. Seewig, M. Eifler, and G. Wiora, “Unambiguous evaluation of a chirp measurement standard,” *Surf. Topogr. Metrol. Prop.*, vol. 2, no. 4, p. 45003, 2014.

- [42] R. Krüger-Sehm, P. Bakucz, L. Jung, and H. Wilhelms, "Chirp-Kalibriernormale für Oberflächenmessgeräte (Chirp Calibration Standards for Surface Measuring Instruments)," *Tech. Mess.*, vol. 74, no. 11, pp. 572–576, 2007.
- [43] A. Fujii, H. Suzuki, and K. Yanagi, "Development of measurement standards for verifying functional performance of surface texture measuring instruments," *J. Phys. Conf. Ser.*, vol. 311, no. 1, 2011.
- [44] L. Koenders and G. Wilkening, "Review on available calibration artefacts," in *Proceedings of the 5th Seminar on Quantitative Microscopy and 1st Seminar on Nanoscale Calibration Standards and Methods, Braunschweig, Germany, PTB-F-44 (Braunschweig, 2001)*, 2001, pp. 50–60.
- [45] C. L. Giusca, R. K. Leach, and F. Helery, "Calibration of the scales of areal surface topography measuring instruments: part 2. Amplification, linearity and squareness," *Meas. Sci. Technol.*, vol. 23, no. 6, p. 65005, 2012.
- [46] "NANOSENSORS," <http://www.nanosensors.com/> .
- [47] "SIS Surface Imaging Systems GmbH," <http://www.sis-gmbh.com/> .
- [48] "Ibsen Photonics," <https://ibsen.com/> .
- [49] A. Alburayt, W. P. Syam, and R. K. Leach, "Lateral scale calibration for focus variation microscopy," *Meas. Sci. Technol.*, 2018.
- [50] "Advanced Surface Microscopy," <https://www.asmicro.com/> .
- [51] "MOXTEK Optical and X-ray Components Manufacturer," <http://moxtek.com/> .
- [52] V. G. Badami, J. Liesener, C. J. Evans, and P. de Groot, "Evaluation of the measurement performance of a coherence scanning microscope using roughness specimens," in *Proceedings of ASPE Annual Meeting*, 2011, pp. 23–26.
- [53] C. L. Giusca and R. K. Leach, "Calibration of the scales of areal surface topography measuring instruments: Part 3. Resolution," *Meas. Sci.*

Technol., vol. 24, no. 10, 2013.

- [54] K. R. Williams, K. Gupta, and M. Wasilik, "Etch rates for micromachining processing-Part II," *J. microelectromechanical Syst.*, vol. 12, no. 6, pp. 761–778, 2003.
- [55] S. Reyntjens and R. Puers, "A review of focused ion beam applications in microsystem technology," *J. micromechanics microengineering*, vol. 11, no. 4, p. 287, 2001.
- [56] F. Watt, A. A. Bettiol, J. A. Van Kan, E. J. Teo, and M. B. H. Breese, "Ion beam lithography and nanofabrication: a review," *Int. J. Nanosci.*, vol. 4, no. 03, pp. 269–286, 2005.
- [57] K. H. Ho and S. T. Newman, "State of the art electrical discharge machining (EDM)," *Int. J. Mach. Tools Manuf.*, vol. 43, no. 13, pp. 1287–1300, 2003.
- [58] J. A. McGeough, M. C. Leu, K. P. Rajurkar, A. K. M. De Silva, and Q. Liu, "Electroforming process and application to micro/macro manufacturing," *CIRP Ann.*, vol. 50, no. 2, pp. 499–514, 2001.
- [59] G. Chryssolouris, *Laser machining: theory and practice*. Springer Science & Business Media, 2013.
- [60] U. Klotzbach, A. F. Lasagni, M. Panzner, and V. Franke, "Laser micromachining," in *Fabrication and Characterization in the Micro-Nano Range*, Springer, 2011, pp. 29–46.
- [61] P. Thakur, "Electron beam machining," <https://www.slideshare.net/Prashantthakur13/electron-beam-machining>, 2015. .
- [62] "Electron Beam Machining : Principle, Working, Equipment's, Application, Advantages and Disadvantages," <http://www.mech4study.com/2017/03/electron-beam-machining-principle-working-equipment-application-advantages-and-disadvantages.html>, 2017. .

- [63] T. C. G. Lo-A-Foe, "Single-point diamond turning," *Dr. Thesis TUE*, 1989.
- [64] E. Paul, C. J. Evans, A. Mangamelli, M. L. McGlaufflin, and R. S. Polvani, "Chemical aspects of tool wear in single point diamond turning," *Precis. Eng.*, vol. 18, no. 1, pp. 4–19, 1996.
- [65] M. Tauhiduzzaman and S. C. Veldhuis, "Effect of material microstructure and tool geometry on surface generation in single point diamond turning," *Precis. Eng.*, vol. 38, no. 3, pp. 481–491, 2014.
- [66] Z. J. Yuan, M. Zhou, and S. Dong, "Effect of diamond tool sharpness on minimum cutting thickness and cutting surface integrity in ultraprecision machining," *J. Mater. Process. Technol.*, vol. 62, no. 4, pp. 327–330, 1996.
- [67] J. F. Cuttino, A. C. Miller, and D. E. Schinstock, "Performance optimization of a fast tool servo for single-point diamond turning machines," *IEEE/ASME Trans. mechatronics*, vol. 4, no. 2, pp. 169–179, 1999.
- [68] C. F. Cheung and W. B. Lee, "Characterisation of nanosurface generation in single-point diamond turning," *Int. J. Mach. Tools Manuf.*, vol. 41, no. 6, pp. 851–875, 2001.
- [69] "ISO 4288:1996(en) Geometrical Product Specifications (GPS) — Surface texture: Profile method — Rules and procedures for the assessment of surface texture," 1996.
- [70] "ISO 25178-2:2012 Geometrical product specifications (GPS) -- Surface texture: Areal -- Part 2: Terms, definitions and surface texture parameters," 2012.
- [71] S. Goel, X. Luo, P. Comley, R. L. Reuben, and A. Cox, "Brittle–ductile transition during diamond turning of single crystal silicon carbide," *Int. J. Mach. Tools Manuf.*, vol. 65, pp. 15–21, 2013.
- [72] J. Zhao, C. Giusca, and S. Goel, "Manufacturing uncertainty: How reproducible is the depth of cut during diamond turning of OFHC copper?," in *EUSPEN 18th International Conference & Exhibition*, 2018.

- [73] V. Mishra, N. Khatri, K. Nand, K. Singh, and R. V Sarepaka, "Experimental investigation on uncontrollable parameters for surface finish during diamond turning," *Mater. Manuf. Process.*, vol. 30, no. 2, pp. 232–240, 2015.
- [74] A. Sharma, D. Datta, and R. Balasubramaniam, "An investigation of tool and hard particle interaction in nanoscale cutting of copper beryllium," *Comput. Mater. Sci.*, vol. 145, pp. 208–223, 2018.
- [75] C. L. Giusca and R. K. Leach, "GPG 129: Calibration of the metrological characteristics of contact stylus instruments," 2013.
- [76] "ISO 14253-2:2011 Geometrical product specifications (GPS) -- Inspection by measurement of workpieces and measuring equipment -- Part 2: Guidance for the estimation of uncertainty in GPS measurement, in calibration of measuring equipment and in product ver," 2011.
- [77] D. A. H. Hanaor, Y. Gan, and I. Einav, "Contact mechanics of fractal surfaces by spline assisted discretisation," *Int. J. Solids Struct.*, vol. 59, pp. 121–131, 2015.
- [78] K. E. Spear and J. P. Dismukes, *Synthetic diamond: emerging CVD science and technology*, vol. 25. John Wiley & Sons, 1994.
- [79] L. Ben Freund and S. Suresh, *Thin film materials: stress, defect formation and surface evolution*. Cambridge University Press, 2004.

APPENDICES

Appendix A G-code for radial sinusoidal shape

G00G71G90G40G94	G01X-0.253187Z0.0000F0.03	G01X-0.246780Z-0.000023F0.03
T0202	G01X-0.252808Z0.0000F0.03	G01X-0.246591Z-0.000025F0.03
G56	G01X-0.252430Z0.0000F0.03	G01X-0.246402Z-0.000028F0.03
/M04S2000	G01X-0.252051Z0.0000F0.03	G01X-0.246212Z-0.000031F0.03
G01X-0.260000Z10.000000F500	G01X-0.251673Z0.0000F0.03	G01X-0.246023Z-0.000034F0.03
G01X-0.260000Z1.000000F200	G01X-0.251294Z0.0000F0.03	G01X-0.245833Z-0.000038F0.03
G01X-0.260000Z0.01F10	G01X-0.250916Z0.0000F0.03	G01X-0.245644Z-0.000041F0.03
M01	G01X-0.250537Z0.0000F0.03	G01X-0.245455Z-0.000045F0.03
M28	G01X-0.250159Z0.0000F0.03	G01X-0.245265Z-0.000049F0.03
G01X-0.260000Z0.0000F0.03	G01X-0.250000Z0.000000F0.03	G01X-0.245076Z-0.000053F0.03
G01X-0.259621Z0.0000F0.03	G04X1	G01X-0.244886Z-0.000057F0.03
G01X-0.259243Z0.0000F0.03	G01X-0.249811Z-0.000000F0.03	G01X-0.244697Z-0.000061F0.03
G01X-0.258864Z0.0000F0.03	G01X-0.249621Z-0.000000F0.03	G01X-0.244508Z-0.000066F0.03
G01X-0.258486Z0.0000F0.03	G01X-0.249432Z-0.000001F0.03	G01X-0.244318Z-0.000070F0.03
G01X-0.258107Z0.0000F0.03	G01X-0.249242Z-0.000001F0.03	G01X-0.244129Z-0.000075F0.03
G01X-0.257729Z0.0000F0.03	G01X-0.249053Z-0.000002F0.03	G01X-0.243939Z-0.000080F0.03
G01X-0.257350Z0.0000F0.03	G01X-0.248864Z-0.000003F0.03	G01X-0.243750Z-0.000085F0.03
G01X-0.256972Z0.0000F0.03	G01X-0.248674Z-0.000004F0.03	G01X-0.243561Z-0.000090F0.03
G01X-0.256593Z0.0000F0.03	G01X-0.248485Z-0.000005F0.03	G01X-0.243371Z-0.000095F0.03
G01X-0.256215Z0.0000F0.03	G01X-0.248295Z-0.000006F0.03	G01X-0.243182Z-0.000101F0.03
G01X-0.255836Z0.0000F0.03	G01X-0.248106Z-0.000008F0.03	G01X-0.242992Z-0.000107F0.03
G01X-0.255458Z0.0000F0.03	G01X-0.247917Z-0.000009F0.03	G01X-0.242803Z-0.000112F0.03
G01X-0.255079Z0.0000F0.03	G01X-0.247727Z-0.000011F0.03	G01X-0.242614Z-0.000118F0.03
G01X-0.254701Z0.0000F0.03	G01X-0.247538Z-0.000013F0.03	G01X-0.242424Z-0.000125F0.03
G01X-0.254322Z0.0000F0.03	G01X-0.247348Z-0.000015F0.03	G01X-0.242235Z-0.000131F0.03
G01X-0.253944Z0.0000F0.03	G01X-0.247159Z-0.000018F0.03	G01X-0.242045Z-0.000137F0.03
G01X-0.253565Z0.0000F0.03	G01X-0.246970Z-0.000020F0.03	G01X-0.241856Z-0.000144F0.03

G01X-0.241667Z-0.000150F0.03	G01X-0.235985Z-0.000419F0.03	G01X-0.230303Z-0.000807F0.03
G01X-0.241477Z-0.000157F0.03	G01X-0.235795Z-0.000431F0.03	G01X-0.230114Z-0.000821F0.03
G01X-0.241288Z-0.000164F0.03	G01X-0.235606Z-0.000442F0.03	G01X-0.229924Z-0.000836F0.03
G01X-0.241098Z-0.000172F0.03	G01X-0.235417Z-0.000453F0.03	G01X-0.229735Z-0.000851F0.03
G01X-0.240909Z-0.000179F0.03	G01X-0.235227Z-0.000465F0.03	G01X-0.229545Z-0.000866F0.03
G01X-0.240720Z-0.000186F0.03	G01X-0.235038Z-0.000476F0.03	G01X-0.229356Z-0.000881F0.03
G01X-0.240530Z-0.000194F0.03	G01X-0.234848Z-0.000488F0.03	G01X-0.229167Z-0.000896F0.03
G01X-0.240341Z-0.000202F0.03	G01X-0.234659Z-0.000500F0.03	G01X-0.228977Z-0.000911F0.03
G01X-0.240152Z-0.000210F0.03	G01X-0.234470Z-0.000512F0.03	G01X-0.228788Z-0.000927F0.03
G01X-0.239962Z-0.000218F0.03	G01X-0.234280Z-0.000524F0.03	G01X-0.228598Z-0.000942F0.03
G01X-0.239773Z-0.000226F0.03	G01X-0.234091Z-0.000536F0.03	G01X-0.228409Z-0.000957F0.03
G01X-0.239583Z-0.000234F0.03	G01X-0.233902Z-0.000549F0.03	G01X-0.228220Z-0.000973F0.03
G01X-0.239394Z-0.000243F0.03	G01X-0.233712Z-0.000561F0.03	G01X-0.228030Z-0.000988F0.03
G01X-0.239205Z-0.000251F0.03	G01X-0.233523Z-0.000574F0.03	G01X-0.227841Z-0.001004F0.03
G01X-0.239015Z-0.000260F0.03	G01X-0.233333Z-0.000587F0.03	G01X-0.227652Z-0.001020F0.03
G01X-0.238826Z-0.000269F0.03	G01X-0.233144Z-0.000600F0.03	G01X-0.227462Z-0.001036F0.03
G01X-0.238636Z-0.000278F0.03	G01X-0.232955Z-0.000613F0.03	G01X-0.227273Z-0.001052F0.03
G01X-0.238447Z-0.000287F0.03	G01X-0.232765Z-0.000626F0.03	G01X-0.227083Z-0.001067F0.03
G01X-0.238258Z-0.000296F0.03	G01X-0.232576Z-0.000639F0.03	G01X-0.226894Z-0.001083F0.03
G01X-0.238068Z-0.000306F0.03	G01X-0.232386Z-0.000653F0.03	G01X-0.226705Z-0.001099F0.03
G01X-0.237879Z-0.000316F0.03	G01X-0.232197Z-0.000666F0.03	G01X-0.226515Z-0.001116F0.03
G01X-0.237689Z-0.000325F0.03	G01X-0.232008Z-0.000680F0.03	G01X-0.226326Z-0.001132F0.03
G01X-0.237500Z-0.000335F0.03	G01X-0.231818Z-0.000693F0.03	G01X-0.226136Z-0.001148F0.03
G01X-0.237311Z-0.000345F0.03	G01X-0.231629Z-0.000707F0.03	G01X-0.225947Z-0.001164F0.03
G01X-0.237121Z-0.000355F0.03	G01X-0.231439Z-0.000721F0.03	G01X-0.225758Z-0.001180F0.03
G01X-0.236932Z-0.000366F0.03	G01X-0.231250Z-0.000735F0.03	G01X-0.225568Z-0.001197F0.03
G01X-0.236742Z-0.000376F0.03	G01X-0.231061Z-0.000749F0.03	G01X-0.225379Z-0.001213F0.03
G01X-0.236553Z-0.000387F0.03	G01X-0.230871Z-0.000763F0.03	G01X-0.225189Z-0.001229F0.03
G01X-0.236364Z-0.000398F0.03	G01X-0.230682Z-0.000778F0.03	G01X-0.225000Z-0.001246F0.03
G01X-0.236174Z-0.000408F0.03	G01X-0.230492Z-0.000792F0.03	G01X-0.224811Z-0.001262F0.03

G01X-0.224621Z-0.001278F0.03	G01X-0.218939Z-0.001716F0.03	G01X-0.213258Z-0.001311F0.03
G01X-0.224432Z-0.001295F0.03	G01X-0.218750Z-0.001721F0.03	G01X-0.213068Z-0.001295F0.03
G01X-0.224242Z-0.001311F0.03	G01X-0.218561Z-0.001716F0.03	G01X-0.212879Z-0.001278F0.03
G01X-0.224053Z-0.001328F0.03	G01X-0.218371Z-0.001708F0.03	G01X-0.212689Z-0.001262F0.03
G01X-0.223864Z-0.001344F0.03	G01X-0.218182Z-0.001698F0.03	G01X-0.212500Z-0.001246F0.03
G01X-0.223674Z-0.001360F0.03	G01X-0.217992Z-0.001687F0.03	G01X-0.212311Z-0.001229F0.03
G01X-0.223485Z-0.001377F0.03	G01X-0.217803Z-0.001676F0.03	G01X-0.212121Z-0.001213F0.03
G01X-0.223295Z-0.001393F0.03	G01X-0.217614Z-0.001663F0.03	G01X-0.211932Z-0.001197F0.03
G01X-0.223106Z-0.001409F0.03	G01X-0.217424Z-0.001651F0.03	G01X-0.211742Z-0.001180F0.03
G01X-0.222917Z-0.001425F0.03	G01X-0.217235Z-0.001637F0.03	G01X-0.211553Z-0.001164F0.03
G01X-0.222727Z-0.001441F0.03	G01X-0.217045Z-0.001624F0.03	G01X-0.211364Z-0.001148F0.03
G01X-0.222538Z-0.001457F0.03	G01X-0.216856Z-0.001610F0.03	G01X-0.211174Z-0.001132F0.03
G01X-0.222348Z-0.001473F0.03	G01X-0.216667Z-0.001595F0.03	G01X-0.210985Z-0.001116F0.03
G01X-0.222159Z-0.001489F0.03	G01X-0.216477Z-0.001581F0.03	G01X-0.210795Z-0.001099F0.03
G01X-0.221970Z-0.001505F0.03	G01X-0.216288Z-0.001566F0.03	G01X-0.210606Z-0.001083F0.03
G01X-0.221780Z-0.001520F0.03	G01X-0.216098Z-0.001551F0.03	G01X-0.210417Z-0.001067F0.03
G01X-0.221591Z-0.001536F0.03	G01X-0.215909Z-0.001536F0.03	G01X-0.210227Z-0.001052F0.03
G01X-0.221402Z-0.001551F0.03	G01X-0.215720Z-0.001520F0.03	G01X-0.210038Z-0.001036F0.03
G01X-0.221212Z-0.001566F0.03	G01X-0.215530Z-0.001505F0.03	G01X-0.209848Z-0.001020F0.03
G01X-0.221023Z-0.001581F0.03	G01X-0.215341Z-0.001489F0.03	G01X-0.209659Z-0.001004F0.03
G01X-0.220833Z-0.001595F0.03	G01X-0.215152Z-0.001473F0.03	G01X-0.209470Z-0.000988F0.03
G01X-0.220644Z-0.001610F0.03	G01X-0.214962Z-0.001457F0.03	G01X-0.209280Z-0.000973F0.03
G01X-0.220455Z-0.001624F0.03	G01X-0.214773Z-0.001441F0.03	G01X-0.209091Z-0.000957F0.03
G01X-0.220265Z-0.001637F0.03	G01X-0.214583Z-0.001425F0.03	G01X-0.208902Z-0.000942F0.03
G01X-0.220076Z-0.001651F0.03	G01X-0.214394Z-0.001409F0.03	G01X-0.208712Z-0.000927F0.03
G01X-0.219886Z-0.001663F0.03	G01X-0.214205Z-0.001393F0.03	G01X-0.208523Z-0.000911F0.03
G01X-0.219697Z-0.001676F0.03	G01X-0.214015Z-0.001377F0.03	G01X-0.208333Z-0.000896F0.03
G01X-0.219508Z-0.001687F0.03	G01X-0.213826Z-0.001360F0.03	G01X-0.208144Z-0.000881F0.03
G01X-0.219318Z-0.001698F0.03	G01X-0.213636Z-0.001344F0.03	G01X-0.207955Z-0.000866F0.03
G01X-0.219129Z-0.001708F0.03	G01X-0.213447Z-0.001328F0.03	G01X-0.207765Z-0.000851F0.03

G01X-0.207576Z-0.000836F0.03	G01X-0.201894Z-0.000442F0.03	G01X-0.196212Z-0.000164F0.03
G01X-0.207386Z-0.000821F0.03	G01X-0.201705Z-0.000431F0.03	G01X-0.196023Z-0.000157F0.03
G01X-0.207197Z-0.000807F0.03	G01X-0.201515Z-0.000419F0.03	G01X-0.195833Z-0.000150F0.03
G01X-0.207008Z-0.000792F0.03	G01X-0.201326Z-0.000408F0.03	G01X-0.195644Z-0.000144F0.03
G01X-0.206818Z-0.000778F0.03	G01X-0.201136Z-0.000398F0.03	G01X-0.195455Z-0.000137F0.03
G01X-0.206629Z-0.000763F0.03	G01X-0.200947Z-0.000387F0.03	G01X-0.195265Z-0.000131F0.03
G01X-0.206439Z-0.000749F0.03	G01X-0.200758Z-0.000376F0.03	G01X-0.195076Z-0.000125F0.03
G01X-0.206250Z-0.000735F0.03	G01X-0.200568Z-0.000366F0.03	G01X-0.194886Z-0.000118F0.03
G01X-0.206061Z-0.000721F0.03	G01X-0.200379Z-0.000355F0.03	G01X-0.194697Z-0.000112F0.03
G01X-0.205871Z-0.000707F0.03	G01X-0.200189Z-0.000345F0.03	G01X-0.194508Z-0.000107F0.03
G01X-0.205682Z-0.000693F0.03	G01X-0.200000Z-0.000335F0.03	G01X-0.194318Z-0.000101F0.03
G01X-0.205492Z-0.000680F0.03	G01X-0.199811Z-0.000325F0.03	G01X-0.194129Z-0.000095F0.03
G01X-0.205303Z-0.000666F0.03	G01X-0.199621Z-0.000316F0.03	G01X-0.193939Z-0.000090F0.03
G01X-0.205114Z-0.000653F0.03	G01X-0.199432Z-0.000306F0.03	G01X-0.193750Z-0.000085F0.03
G01X-0.204924Z-0.000639F0.03	G01X-0.199242Z-0.000296F0.03	G01X-0.193561Z-0.000080F0.03
G01X-0.204735Z-0.000626F0.03	G01X-0.199053Z-0.000287F0.03	G01X-0.193371Z-0.000075F0.03
G01X-0.204545Z-0.000613F0.03	G01X-0.198864Z-0.000278F0.03	G01X-0.193182Z-0.000070F0.03
G01X-0.204356Z-0.000600F0.03	G01X-0.198674Z-0.000269F0.03	G01X-0.192992Z-0.000066F0.03
G01X-0.204167Z-0.000587F0.03	G01X-0.198485Z-0.000260F0.03	G01X-0.192803Z-0.000061F0.03
G01X-0.203977Z-0.000574F0.03	G01X-0.198295Z-0.000251F0.03	G01X-0.192614Z-0.000057F0.03
G01X-0.203788Z-0.000561F0.03	G01X-0.198106Z-0.000243F0.03	G01X-0.192424Z-0.000053F0.03
G01X-0.203598Z-0.000549F0.03	G01X-0.197917Z-0.000234F0.03	G01X-0.192235Z-0.000049F0.03
G01X-0.203409Z-0.000536F0.03	G01X-0.197727Z-0.000226F0.03	G01X-0.192045Z-0.000045F0.03
G01X-0.203220Z-0.000524F0.03	G01X-0.197538Z-0.000218F0.03	G01X-0.191856Z-0.000041F0.03
G01X-0.203030Z-0.000512F0.03	G01X-0.197348Z-0.000210F0.03	G01X-0.191667Z-0.000038F0.03
G01X-0.202841Z-0.000500F0.03	G01X-0.197159Z-0.000202F0.03	G01X-0.191477Z-0.000034F0.03
G01X-0.202652Z-0.000488F0.03	G01X-0.196970Z-0.000194F0.03	G01X-0.191288Z-0.000031F0.03
G01X-0.202462Z-0.000476F0.03	G01X-0.196780Z-0.000186F0.03	G01X-0.191098Z-0.000028F0.03
G01X-0.202273Z-0.000465F0.03	G01X-0.196591Z-0.000179F0.03	G01X-0.190909Z-0.000025F0.03
G01X-0.202083Z-0.000453F0.03	G01X-0.196402Z-0.000172F0.03	G01X-0.190720Z-0.000023F0.03

G01X-0.190530Z-0.000020F0.03	G01X-0.185038Z-0.000013F0.03	G01X-0.179356Z-0.000144F0.03
G01X-0.190341Z-0.000018F0.03	G01X-0.184848Z-0.000015F0.03	G01X-0.179167Z-0.000150F0.03
G01X-0.190152Z-0.000015F0.03	G01X-0.184659Z-0.000018F0.03	G01X-0.178977Z-0.000157F0.03
G01X-0.189962Z-0.000013F0.03	G01X-0.184470Z-0.000020F0.03	G01X-0.178788Z-0.000164F0.03
G01X-0.189773Z-0.000011F0.03	G01X-0.184280Z-0.000023F0.03	G01X-0.178598Z-0.000172F0.03
G01X-0.189583Z-0.000009F0.03	G01X-0.184091Z-0.000025F0.03	G01X-0.178409Z-0.000179F0.03
G01X-0.189394Z-0.000008F0.03	G01X-0.183902Z-0.000028F0.03	G01X-0.178220Z-0.000186F0.03
G01X-0.189205Z-0.000006F0.03	G01X-0.183712Z-0.000031F0.03	G01X-0.178030Z-0.000194F0.03
G01X-0.189015Z-0.000005F0.03	G01X-0.183523Z-0.000034F0.03	G01X-0.177841Z-0.000202F0.03
G01X-0.188826Z-0.000004F0.03	G01X-0.183333Z-0.000038F0.03	G01X-0.177652Z-0.000210F0.03
G01X-0.188636Z-0.000003F0.03	G01X-0.183144Z-0.000041F0.03	G01X-0.177462Z-0.000218F0.03
G01X-0.188447Z-0.000002F0.03	G01X-0.182955Z-0.000045F0.03	G01X-0.177273Z-0.000226F0.03
G01X-0.188258Z-0.000001F0.03	G01X-0.182765Z-0.000049F0.03	G01X-0.177083Z-0.000234F0.03
G01X-0.188068Z-0.000001F0.03	G01X-0.182576Z-0.000053F0.03	G01X-0.176894Z-0.000243F0.03
G01X-0.187879Z-0.000000F0.03	G01X-0.182386Z-0.000057F0.03	G01X-0.176705Z-0.000251F0.03
G01X-0.187689Z-0.000000F0.03	G01X-0.182197Z-0.000061F0.03	G01X-0.176515Z-0.000260F0.03
G01X-0.187500Z-0.000000F0.03	G01X-0.182008Z-0.000066F0.03	G01X-0.176326Z-0.000269F0.03
G04X1	G01X-0.181818Z-0.000070F0.03	G01X-0.176136Z-0.000278F0.03
G01X-0.187311Z-0.000000F0.03	G01X-0.181629Z-0.000075F0.03	G01X-0.175947Z-0.000287F0.03
G01X-0.187121Z-0.000000F0.03	G01X-0.181439Z-0.000080F0.03	G01X-0.175758Z-0.000296F0.03
G01X-0.186932Z-0.000001F0.03	G01X-0.181250Z-0.000085F0.03	G01X-0.175568Z-0.000306F0.03
G01X-0.186742Z-0.000001F0.03	G01X-0.181061Z-0.000090F0.03	G01X-0.175379Z-0.000316F0.03
G01X-0.186553Z-0.000002F0.03	G01X-0.180871Z-0.000095F0.03	G01X-0.175189Z-0.000325F0.03
G01X-0.186364Z-0.000003F0.03	G01X-0.180682Z-0.000101F0.03	G01X-0.175000Z-0.000335F0.03
G01X-0.186174Z-0.000004F0.03	G01X-0.180492Z-0.000107F0.03	G01X-0.174811Z-0.000345F0.03
G01X-0.185985Z-0.000005F0.03	G01X-0.180303Z-0.000112F0.03	G01X-0.174621Z-0.000355F0.03
G01X-0.185795Z-0.000006F0.03	G01X-0.180114Z-0.000118F0.03	G01X-0.174432Z-0.000366F0.03
G01X-0.185606Z-0.000008F0.03	G01X-0.179924Z-0.000125F0.03	G01X-0.174242Z-0.000376F0.03
G01X-0.185417Z-0.000009F0.03	G01X-0.179735Z-0.000131F0.03	G01X-0.174053Z-0.000387F0.03
G01X-0.185227Z-0.000011F0.03	G01X-0.179545Z-0.000137F0.03	G01X-0.173864Z-0.000398F0.03

G01X-0.173674Z-0.000408F0.03	G01X-0.167992Z-0.000792F0.03	G01X-0.162311Z-0.001262F0.03
G01X-0.173485Z-0.000419F0.03	G01X-0.167803Z-0.000807F0.03	G01X-0.162121Z-0.001278F0.03
G01X-0.173295Z-0.000431F0.03	G01X-0.167614Z-0.000821F0.03	G01X-0.161932Z-0.001295F0.03
G01X-0.173106Z-0.000442F0.03	G01X-0.167424Z-0.000836F0.03	G01X-0.161742Z-0.001311F0.03
G01X-0.172917Z-0.000453F0.03	G01X-0.167235Z-0.000851F0.03	G01X-0.161553Z-0.001328F0.03
G01X-0.172727Z-0.000465F0.03	G01X-0.167045Z-0.000866F0.03	G01X-0.161364Z-0.001344F0.03
G01X-0.172538Z-0.000476F0.03	G01X-0.166856Z-0.000881F0.03	G01X-0.161174Z-0.001360F0.03
G01X-0.172348Z-0.000488F0.03	G01X-0.166667Z-0.000896F0.03	G01X-0.160985Z-0.001377F0.03
G01X-0.172159Z-0.000500F0.03	G01X-0.166477Z-0.000911F0.03	G01X-0.160795Z-0.001393F0.03
G01X-0.171970Z-0.000512F0.03	G01X-0.166288Z-0.000927F0.03	G01X-0.160606Z-0.001409F0.03
G01X-0.171780Z-0.000524F0.03	G01X-0.166098Z-0.000942F0.03	G01X-0.160417Z-0.001425F0.03
G01X-0.171591Z-0.000536F0.03	G01X-0.165909Z-0.000957F0.03	G01X-0.160227Z-0.001441F0.03
G01X-0.171402Z-0.000549F0.03	G01X-0.165720Z-0.000973F0.03	G01X-0.160038Z-0.001457F0.03
G01X-0.171212Z-0.000561F0.03	G01X-0.165530Z-0.000988F0.03	G01X-0.159848Z-0.001473F0.03
G01X-0.171023Z-0.000574F0.03	G01X-0.165341Z-0.001004F0.03	G01X-0.159659Z-0.001489F0.03
G01X-0.170833Z-0.000587F0.03	G01X-0.165152Z-0.001020F0.03	G01X-0.159470Z-0.001505F0.03
G01X-0.170644Z-0.000600F0.03	G01X-0.164962Z-0.001036F0.03	G01X-0.159280Z-0.001520F0.03
G01X-0.170455Z-0.000613F0.03	G01X-0.164773Z-0.001052F0.03	G01X-0.159091Z-0.001536F0.03
G01X-0.170265Z-0.000626F0.03	G01X-0.164583Z-0.001067F0.03	G01X-0.158902Z-0.001551F0.03
G01X-0.170076Z-0.000639F0.03	G01X-0.164394Z-0.001083F0.03	G01X-0.158712Z-0.001566F0.03
G01X-0.169886Z-0.000653F0.03	G01X-0.164205Z-0.001099F0.03	G01X-0.158523Z-0.001581F0.03
G01X-0.169697Z-0.000666F0.03	G01X-0.164015Z-0.001116F0.03	G01X-0.158333Z-0.001595F0.03
G01X-0.169508Z-0.000680F0.03	G01X-0.163826Z-0.001132F0.03	G01X-0.158144Z-0.001610F0.03
G01X-0.169318Z-0.000693F0.03	G01X-0.163636Z-0.001148F0.03	G01X-0.157955Z-0.001624F0.03
G01X-0.169129Z-0.000707F0.03	G01X-0.163447Z-0.001164F0.03	G01X-0.157765Z-0.001637F0.03
G01X-0.168939Z-0.000721F0.03	G01X-0.163258Z-0.001180F0.03	G01X-0.157576Z-0.001651F0.03
G01X-0.168750Z-0.000735F0.03	G01X-0.163068Z-0.001197F0.03	G01X-0.157386Z-0.001663F0.03
G01X-0.168561Z-0.000749F0.03	G01X-0.162879Z-0.001213F0.03	G01X-0.157197Z-0.001676F0.03
G01X-0.168371Z-0.000763F0.03	G01X-0.162689Z-0.001229F0.03	G01X-0.157008Z-0.001687F0.03
G01X-0.168182Z-0.000778F0.03	G01X-0.162500Z-0.001246F0.03	G01X-0.156818Z-0.001698F0.03

G01X-0.156629Z-0.001708F0.03	G01X-0.150947Z-0.001328F0.03	G01X-0.145265Z-0.000851F0.03
G01X-0.156439Z-0.001716F0.03	G01X-0.150758Z-0.001311F0.03	G01X-0.145076Z-0.000836F0.03
G01X-0.156250Z-0.001721F0.03	G01X-0.150568Z-0.001295F0.03	G01X-0.144886Z-0.000821F0.03
G01X-0.156061Z-0.001716F0.03	G01X-0.150379Z-0.001278F0.03	G01X-0.144697Z-0.000807F0.03
G01X-0.155871Z-0.001708F0.03	G01X-0.150189Z-0.001262F0.03	G01X-0.144508Z-0.000792F0.03
G01X-0.155682Z-0.001698F0.03	G01X-0.150000Z-0.001246F0.03	G01X-0.144318Z-0.000778F0.03
G01X-0.155492Z-0.001687F0.03	G01X-0.149811Z-0.001229F0.03	G01X-0.144129Z-0.000763F0.03
G01X-0.155303Z-0.001676F0.03	G01X-0.149621Z-0.001213F0.03	G01X-0.143939Z-0.000749F0.03
G01X-0.155114Z-0.001663F0.03	G01X-0.149432Z-0.001197F0.03	G01X-0.143750Z-0.000735F0.03
G01X-0.154924Z-0.001651F0.03	G01X-0.149242Z-0.001180F0.03	G01X-0.143561Z-0.000721F0.03
G01X-0.154735Z-0.001637F0.03	G01X-0.149053Z-0.001164F0.03	G01X-0.143371Z-0.000707F0.03
G01X-0.154545Z-0.001624F0.03	G01X-0.148864Z-0.001148F0.03	G01X-0.143182Z-0.000693F0.03
G01X-0.154356Z-0.001610F0.03	G01X-0.148674Z-0.001132F0.03	G01X-0.142992Z-0.000680F0.03
G01X-0.154167Z-0.001595F0.03	G01X-0.148485Z-0.001116F0.03	G01X-0.142803Z-0.000666F0.03
G01X-0.153977Z-0.001581F0.03	G01X-0.148295Z-0.001099F0.03	G01X-0.142614Z-0.000653F0.03
G01X-0.153788Z-0.001566F0.03	G01X-0.148106Z-0.001083F0.03	G01X-0.142424Z-0.000639F0.03
G01X-0.153598Z-0.001551F0.03	G01X-0.147917Z-0.001067F0.03	G01X-0.142235Z-0.000626F0.03
G01X-0.153409Z-0.001536F0.03	G01X-0.147727Z-0.001052F0.03	G01X-0.142045Z-0.000613F0.03
G01X-0.153220Z-0.001520F0.03	G01X-0.147538Z-0.001036F0.03	G01X-0.141856Z-0.000600F0.03
G01X-0.153030Z-0.001505F0.03	G01X-0.147348Z-0.001020F0.03	G01X-0.141667Z-0.000587F0.03
G01X-0.152841Z-0.001489F0.03	G01X-0.147159Z-0.001004F0.03	G01X-0.141477Z-0.000574F0.03
G01X-0.152652Z-0.001473F0.03	G01X-0.146970Z-0.000988F0.03	G01X-0.141288Z-0.000561F0.03
G01X-0.152462Z-0.001457F0.03	G01X-0.146780Z-0.000973F0.03	G01X-0.141098Z-0.000549F0.03
G01X-0.152273Z-0.001441F0.03	G01X-0.146591Z-0.000957F0.03	G01X-0.140909Z-0.000536F0.03
G01X-0.152083Z-0.001425F0.03	G01X-0.146402Z-0.000942F0.03	G01X-0.140720Z-0.000524F0.03
G01X-0.151894Z-0.001409F0.03	G01X-0.146212Z-0.000927F0.03	G01X-0.140530Z-0.000512F0.03
G01X-0.151705Z-0.001393F0.03	G01X-0.146023Z-0.000911F0.03	G01X-0.140341Z-0.000500F0.03
G01X-0.151515Z-0.001377F0.03	G01X-0.145833Z-0.000896F0.03	G01X-0.140152Z-0.000488F0.03
G01X-0.151326Z-0.001360F0.03	G01X-0.145644Z-0.000881F0.03	G01X-0.139962Z-0.000476F0.03
G01X-0.151136Z-0.001344F0.03	G01X-0.145455Z-0.000866F0.03	G01X-0.139773Z-0.000465F0.03

G01X-0.139583Z-0.000453F0.03	G01X-0.133902Z-0.000172F0.03	G01X-0.128220Z-0.000023F0.03
G01X-0.139394Z-0.000442F0.03	G01X-0.133712Z-0.000164F0.03	G01X-0.128030Z-0.000020F0.03
G01X-0.139205Z-0.000431F0.03	G01X-0.133523Z-0.000157F0.03	G01X-0.127841Z-0.000018F0.03
G01X-0.139015Z-0.000419F0.03	G01X-0.133333Z-0.000150F0.03	G01X-0.127652Z-0.000015F0.03
G01X-0.138826Z-0.000408F0.03	G01X-0.133144Z-0.000144F0.03	G01X-0.127462Z-0.000013F0.03
G01X-0.138636Z-0.000398F0.03	G01X-0.132955Z-0.000137F0.03	G01X-0.127273Z-0.000011F0.03
G01X-0.138447Z-0.000387F0.03	G01X-0.132765Z-0.000131F0.03	G01X-0.127083Z-0.000009F0.03
G01X-0.138258Z-0.000376F0.03	G01X-0.132576Z-0.000125F0.03	G01X-0.126894Z-0.000008F0.03
G01X-0.138068Z-0.000366F0.03	G01X-0.132386Z-0.000118F0.03	G01X-0.126705Z-0.000006F0.03
G01X-0.137879Z-0.000355F0.03	G01X-0.132197Z-0.000112F0.03	G01X-0.126515Z-0.000005F0.03
G01X-0.137689Z-0.000345F0.03	G01X-0.132008Z-0.000107F0.03	G01X-0.126326Z-0.000004F0.03
G01X-0.137500Z-0.000335F0.03	G01X-0.131818Z-0.000101F0.03	G01X-0.126136Z-0.000003F0.03
G01X-0.137311Z-0.000325F0.03	G01X-0.131629Z-0.000095F0.03	G01X-0.125947Z-0.000002F0.03
G01X-0.137121Z-0.000316F0.03	G01X-0.131439Z-0.000090F0.03	G01X-0.125758Z-0.000001F0.03
G01X-0.136932Z-0.000306F0.03	G01X-0.131250Z-0.000085F0.03	G01X-0.125568Z-0.000001F0.03
G01X-0.136742Z-0.000296F0.03	G01X-0.131061Z-0.000080F0.03	G01X-0.125379Z-0.000000F0.03
G01X-0.136553Z-0.000287F0.03	G01X-0.130871Z-0.000075F0.03	G01X-0.125189Z-0.000000F0.03
G01X-0.136364Z-0.000278F0.03	G01X-0.130682Z-0.000070F0.03	G01X-0.125000Z0.000000F0.03
G01X-0.136174Z-0.000269F0.03	G01X-0.130492Z-0.000066F0.03	G04X1
G01X-0.135985Z-0.000260F0.03	G01X-0.130303Z-0.000061F0.03	G01X-0.124811Z-0.000000F0.03
G01X-0.135795Z-0.000251F0.03	G01X-0.130114Z-0.000057F0.03	G01X-0.124621Z-0.000000F0.03
G01X-0.135606Z-0.000243F0.03	G01X-0.129924Z-0.000053F0.03	G01X-0.124432Z-0.000001F0.03
G01X-0.135417Z-0.000234F0.03	G01X-0.129735Z-0.000049F0.03	G01X-0.124242Z-0.000001F0.03
G01X-0.135227Z-0.000226F0.03	G01X-0.129545Z-0.000045F0.03	G01X-0.124053Z-0.000002F0.03
G01X-0.135038Z-0.000218F0.03	G01X-0.129356Z-0.000041F0.03	G01X-0.123864Z-0.000003F0.03
G01X-0.134848Z-0.000210F0.03	G01X-0.129167Z-0.000038F0.03	G01X-0.123674Z-0.000004F0.03
G01X-0.134659Z-0.000202F0.03	G01X-0.128977Z-0.000034F0.03	G01X-0.123485Z-0.000005F0.03
G01X-0.134470Z-0.000194F0.03	G01X-0.128788Z-0.000031F0.03	G01X-0.123295Z-0.000006F0.03
G01X-0.134280Z-0.000186F0.03	G01X-0.128598Z-0.000028F0.03	G01X-0.123106Z-0.000008F0.03
G01X-0.134091Z-0.000179F0.03	G01X-0.128409Z-0.000025F0.03	G01X-0.122917Z-0.000009F0.03

G01X-0.122727Z-0.000011F0.03	G01X-0.117045Z-0.000137F0.03	G01X-0.111364Z-0.000398F0.03
G01X-0.122538Z-0.000013F0.03	G01X-0.116856Z-0.000144F0.03	G01X-0.111174Z-0.000408F0.03
G01X-0.122348Z-0.000015F0.03	G01X-0.116667Z-0.000150F0.03	G01X-0.110985Z-0.000419F0.03
G01X-0.122159Z-0.000018F0.03	G01X-0.116477Z-0.000157F0.03	G01X-0.110795Z-0.000431F0.03
G01X-0.121970Z-0.000020F0.03	G01X-0.116288Z-0.000164F0.03	G01X-0.110606Z-0.000442F0.03
G01X-0.121780Z-0.000023F0.03	G01X-0.116098Z-0.000172F0.03	G01X-0.110417Z-0.000453F0.03
G01X-0.121591Z-0.000025F0.03	G01X-0.115909Z-0.000179F0.03	G01X-0.110227Z-0.000465F0.03
G01X-0.121402Z-0.000028F0.03	G01X-0.115720Z-0.000186F0.03	G01X-0.110038Z-0.000476F0.03
G01X-0.121212Z-0.000031F0.03	G01X-0.115530Z-0.000194F0.03	G01X-0.109848Z-0.000488F0.03
G01X-0.121023Z-0.000034F0.03	G01X-0.115341Z-0.000202F0.03	G01X-0.109659Z-0.000500F0.03
G01X-0.120833Z-0.000038F0.03	G01X-0.115152Z-0.000210F0.03	G01X-0.109470Z-0.000512F0.03
G01X-0.120644Z-0.000041F0.03	G01X-0.114962Z-0.000218F0.03	G01X-0.109280Z-0.000524F0.03
G01X-0.120455Z-0.000045F0.03	G01X-0.114773Z-0.000226F0.03	G01X-0.109091Z-0.000536F0.03
G01X-0.120265Z-0.000049F0.03	G01X-0.114583Z-0.000234F0.03	G01X-0.108902Z-0.000549F0.03
G01X-0.120076Z-0.000053F0.03	G01X-0.114394Z-0.000243F0.03	G01X-0.108712Z-0.000561F0.03
G01X-0.119886Z-0.000057F0.03	G01X-0.114205Z-0.000251F0.03	G01X-0.108523Z-0.000574F0.03
G01X-0.119697Z-0.000061F0.03	G01X-0.114015Z-0.000260F0.03	G01X-0.108333Z-0.000587F0.03
G01X-0.119508Z-0.000066F0.03	G01X-0.113826Z-0.000269F0.03	G01X-0.108144Z-0.000600F0.03
G01X-0.119318Z-0.000070F0.03	G01X-0.113636Z-0.000278F0.03	G01X-0.107955Z-0.000613F0.03
G01X-0.119129Z-0.000075F0.03	G01X-0.113447Z-0.000287F0.03	G01X-0.107765Z-0.000626F0.03
G01X-0.118939Z-0.000080F0.03	G01X-0.113258Z-0.000296F0.03	G01X-0.107576Z-0.000639F0.03
G01X-0.118750Z-0.000085F0.03	G01X-0.113068Z-0.000306F0.03	G01X-0.107386Z-0.000653F0.03
G01X-0.118561Z-0.000090F0.03	G01X-0.112879Z-0.000316F0.03	G01X-0.107197Z-0.000666F0.03
G01X-0.118371Z-0.000095F0.03	G01X-0.112689Z-0.000325F0.03	G01X-0.107008Z-0.000680F0.03
G01X-0.118182Z-0.000101F0.03	G01X-0.112500Z-0.000335F0.03	G01X-0.106818Z-0.000693F0.03
G01X-0.117992Z-0.000107F0.03	G01X-0.112311Z-0.000345F0.03	G01X-0.106629Z-0.000707F0.03
G01X-0.117803Z-0.000112F0.03	G01X-0.112121Z-0.000355F0.03	G01X-0.106439Z-0.000721F0.03
G01X-0.117614Z-0.000118F0.03	G01X-0.111932Z-0.000366F0.03	G01X-0.106250Z-0.000735F0.03
G01X-0.117424Z-0.000125F0.03	G01X-0.111742Z-0.000376F0.03	G01X-0.106061Z-0.000749F0.03
G01X-0.117235Z-0.000131F0.03	G01X-0.111553Z-0.000387F0.03	G01X-0.105871Z-0.000763F0.03

G01X-0.105682Z-0.000778F0.03	G01X-0.100000Z-0.001246F0.03	G01X-0.094318Z-0.001698F0.03
G01X-0.105492Z-0.000792F0.03	G01X-0.099811Z-0.001262F0.03	G01X-0.094129Z-0.001708F0.03
G01X-0.105303Z-0.000807F0.03	G01X-0.099621Z-0.001278F0.03	G01X-0.093939Z-0.001716F0.03
G01X-0.105114Z-0.000821F0.03	G01X-0.099432Z-0.001295F0.03	G01X-0.093750Z-0.001721F0.03
G01X-0.104924Z-0.000836F0.03	G01X-0.099242Z-0.001311F0.03	G01X-0.093561Z-0.001716F0.03
G01X-0.104735Z-0.000851F0.03	G01X-0.099053Z-0.001328F0.03	G01X-0.093371Z-0.001708F0.03
G01X-0.104545Z-0.000866F0.03	G01X-0.098864Z-0.001344F0.03	G01X-0.093182Z-0.001698F0.03
G01X-0.104356Z-0.000881F0.03	G01X-0.098674Z-0.001360F0.03	G01X-0.092992Z-0.001687F0.03
G01X-0.104167Z-0.000896F0.03	G01X-0.098485Z-0.001377F0.03	G01X-0.092803Z-0.001676F0.03
G01X-0.103977Z-0.000911F0.03	G01X-0.098295Z-0.001393F0.03	G01X-0.092614Z-0.001663F0.03
G01X-0.103788Z-0.000927F0.03	G01X-0.098106Z-0.001409F0.03	G01X-0.092424Z-0.001651F0.03
G01X-0.103598Z-0.000942F0.03	G01X-0.097917Z-0.001425F0.03	G01X-0.092235Z-0.001637F0.03
G01X-0.103409Z-0.000957F0.03	G01X-0.097727Z-0.001441F0.03	G01X-0.092045Z-0.001624F0.03
G01X-0.103220Z-0.000973F0.03	G01X-0.097538Z-0.001457F0.03	G01X-0.091856Z-0.001610F0.03
G01X-0.103030Z-0.000988F0.03	G01X-0.097348Z-0.001473F0.03	G01X-0.091667Z-0.001595F0.03
G01X-0.102841Z-0.001004F0.03	G01X-0.097159Z-0.001489F0.03	G01X-0.091477Z-0.001581F0.03
G01X-0.102652Z-0.001020F0.03	G01X-0.096970Z-0.001505F0.03	G01X-0.091288Z-0.001566F0.03
G01X-0.102462Z-0.001036F0.03	G01X-0.096780Z-0.001520F0.03	G01X-0.091098Z-0.001551F0.03
G01X-0.102273Z-0.001052F0.03	G01X-0.096591Z-0.001536F0.03	G01X-0.090909Z-0.001536F0.03
G01X-0.102083Z-0.001067F0.03	G01X-0.096402Z-0.001551F0.03	G01X-0.090720Z-0.001520F0.03
G01X-0.101894Z-0.001083F0.03	G01X-0.096212Z-0.001566F0.03	G01X-0.090530Z-0.001505F0.03
G01X-0.101705Z-0.001099F0.03	G01X-0.096023Z-0.001581F0.03	G01X-0.090341Z-0.001489F0.03
G01X-0.101515Z-0.001116F0.03	G01X-0.095833Z-0.001595F0.03	G01X-0.090152Z-0.001473F0.03
G01X-0.101326Z-0.001132F0.03	G01X-0.095644Z-0.001610F0.03	G01X-0.089962Z-0.001457F0.03
G01X-0.101136Z-0.001148F0.03	G01X-0.095455Z-0.001624F0.03	G01X-0.089773Z-0.001441F0.03
G01X-0.100947Z-0.001164F0.03	G01X-0.095265Z-0.001637F0.03	G01X-0.089583Z-0.001425F0.03
G01X-0.100758Z-0.001180F0.03	G01X-0.095076Z-0.001651F0.03	G01X-0.089394Z-0.001409F0.03
G01X-0.100568Z-0.001197F0.03	G01X-0.094886Z-0.001663F0.03	G01X-0.089205Z-0.001393F0.03
G01X-0.100379Z-0.001213F0.03	G01X-0.094697Z-0.001676F0.03	G01X-0.089015Z-0.001377F0.03
G01X-0.100189Z-0.001229F0.03	G01X-0.094508Z-0.001687F0.03	G01X-0.088826Z-0.001360F0.03

G01X-0.088636Z-0.001344F0.03	G01X-0.082955Z-0.000866F0.03	G01X-0.077273Z-0.000465F0.03
G01X-0.088447Z-0.001328F0.03	G01X-0.082765Z-0.000851F0.03	G01X-0.077083Z-0.000453F0.03
G01X-0.088258Z-0.001311F0.03	G01X-0.082576Z-0.000836F0.03	G01X-0.076894Z-0.000442F0.03
G01X-0.088068Z-0.001295F0.03	G01X-0.082386Z-0.000821F0.03	G01X-0.076705Z-0.000431F0.03
G01X-0.087879Z-0.001278F0.03	G01X-0.082197Z-0.000807F0.03	G01X-0.076515Z-0.000419F0.03
G01X-0.087689Z-0.001262F0.03	G01X-0.082008Z-0.000792F0.03	G01X-0.076326Z-0.000408F0.03
G01X-0.087500Z-0.001246F0.03	G01X-0.081818Z-0.000778F0.03	G01X-0.076136Z-0.000398F0.03
G01X-0.087311Z-0.001229F0.03	G01X-0.081629Z-0.000763F0.03	G01X-0.075947Z-0.000387F0.03
G01X-0.087121Z-0.001213F0.03	G01X-0.081439Z-0.000749F0.03	G01X-0.075758Z-0.000376F0.03
G01X-0.086932Z-0.001197F0.03	G01X-0.081250Z-0.000735F0.03	G01X-0.075568Z-0.000366F0.03
G01X-0.086742Z-0.001180F0.03	G01X-0.081061Z-0.000721F0.03	G01X-0.075379Z-0.000355F0.03
G01X-0.086553Z-0.001164F0.03	G01X-0.080871Z-0.000707F0.03	G01X-0.075189Z-0.000345F0.03
G01X-0.086364Z-0.001148F0.03	G01X-0.080682Z-0.000693F0.03	G01X-0.075000Z-0.000335F0.03
G01X-0.086174Z-0.001132F0.03	G01X-0.080492Z-0.000680F0.03	G01X-0.074811Z-0.000325F0.03
G01X-0.085985Z-0.001116F0.03	G01X-0.080303Z-0.000666F0.03	G01X-0.074621Z-0.000316F0.03
G01X-0.085795Z-0.001099F0.03	G01X-0.080114Z-0.000653F0.03	G01X-0.074432Z-0.000306F0.03
G01X-0.085606Z-0.001083F0.03	G01X-0.079924Z-0.000639F0.03	G01X-0.074242Z-0.000296F0.03
G01X-0.085417Z-0.001067F0.03	G01X-0.079735Z-0.000626F0.03	G01X-0.074053Z-0.000287F0.03
G01X-0.085227Z-0.001052F0.03	G01X-0.079545Z-0.000613F0.03	G01X-0.073864Z-0.000278F0.03
G01X-0.085038Z-0.001036F0.03	G01X-0.079356Z-0.000600F0.03	G01X-0.073674Z-0.000269F0.03
G01X-0.084848Z-0.001020F0.03	G01X-0.079167Z-0.000587F0.03	G01X-0.073485Z-0.000260F0.03
G01X-0.084659Z-0.001004F0.03	G01X-0.078977Z-0.000574F0.03	G01X-0.073295Z-0.000251F0.03
G01X-0.084470Z-0.000988F0.03	G01X-0.078788Z-0.000561F0.03	G01X-0.073106Z-0.000243F0.03
G01X-0.084280Z-0.000973F0.03	G01X-0.078598Z-0.000549F0.03	G01X-0.072917Z-0.000234F0.03
G01X-0.084091Z-0.000957F0.03	G01X-0.078409Z-0.000536F0.03	G01X-0.072727Z-0.000226F0.03
G01X-0.083902Z-0.000942F0.03	G01X-0.078220Z-0.000524F0.03	G01X-0.072538Z-0.000218F0.03
G01X-0.083712Z-0.000927F0.03	G01X-0.078030Z-0.000512F0.03	G01X-0.072348Z-0.000210F0.03
G01X-0.083523Z-0.000911F0.03	G01X-0.077841Z-0.000500F0.03	G01X-0.072159Z-0.000202F0.03
G01X-0.083333Z-0.000896F0.03	G01X-0.077652Z-0.000488F0.03	G01X-0.071970Z-0.000194F0.03
G01X-0.083144Z-0.000881F0.03	G01X-0.077462Z-0.000476F0.03	G01X-0.071780Z-0.000186F0.03

G01X-0.071591Z-0.000179F0.03	G01X-0.065909Z-0.000025F0.03	G01X-0.060417Z-0.000009F0.03
G01X-0.071402Z-0.000172F0.03	G01X-0.065720Z-0.000023F0.03	G01X-0.060227Z-0.000011F0.03
G01X-0.071212Z-0.000164F0.03	G01X-0.065530Z-0.000020F0.03	G01X-0.060038Z-0.000013F0.03
G01X-0.071023Z-0.000157F0.03	G01X-0.065341Z-0.000018F0.03	G01X-0.059848Z-0.000015F0.03
G01X-0.070833Z-0.000150F0.03	G01X-0.065152Z-0.000015F0.03	G01X-0.059659Z-0.000018F0.03
G01X-0.070644Z-0.000144F0.03	G01X-0.064962Z-0.000013F0.03	G01X-0.059470Z-0.000020F0.03
G01X-0.070455Z-0.000137F0.03	G01X-0.064773Z-0.000011F0.03	G01X-0.059280Z-0.000023F0.03
G01X-0.070265Z-0.000131F0.03	G01X-0.064583Z-0.000009F0.03	G01X-0.059091Z-0.000025F0.03
G01X-0.070076Z-0.000125F0.03	G01X-0.064394Z-0.000008F0.03	G01X-0.058902Z-0.000028F0.03
G01X-0.069886Z-0.000118F0.03	G01X-0.064205Z-0.000006F0.03	G01X-0.058712Z-0.000031F0.03
G01X-0.069697Z-0.000112F0.03	G01X-0.064015Z-0.000005F0.03	G01X-0.058523Z-0.000034F0.03
G01X-0.069508Z-0.000107F0.03	G01X-0.063826Z-0.000004F0.03	G01X-0.058333Z-0.000038F0.03
G01X-0.069318Z-0.000101F0.03	G01X-0.063636Z-0.000003F0.03	G01X-0.058144Z-0.000041F0.03
G01X-0.069129Z-0.000095F0.03	G01X-0.063447Z-0.000002F0.03	G01X-0.057955Z-0.000045F0.03
G01X-0.068939Z-0.000090F0.03	G01X-0.063258Z-0.000001F0.03	G01X-0.057765Z-0.000049F0.03
G01X-0.068750Z-0.000085F0.03	G01X-0.063068Z-0.000001F0.03	G01X-0.057576Z-0.000053F0.03
G01X-0.068561Z-0.000080F0.03	G01X-0.062879Z-0.000000F0.03	G01X-0.057386Z-0.000057F0.03
G01X-0.068371Z-0.000075F0.03	G01X-0.062689Z-0.000000F0.03	G01X-0.057197Z-0.000061F0.03
G01X-0.068182Z-0.000070F0.03	G01X-0.062500Z0.000000F0.03	G01X-0.057008Z-0.000066F0.03
G01X-0.067992Z-0.000066F0.03	G04X1	G01X-0.056818Z-0.000070F0.03
G01X-0.067803Z-0.000061F0.03	G01X-0.062311Z-0.000000F0.03	G01X-0.056629Z-0.000075F0.03
G01X-0.067614Z-0.000057F0.03	G01X-0.062121Z-0.000000F0.03	G01X-0.056439Z-0.000080F0.03
G01X-0.067424Z-0.000053F0.03	G01X-0.061932Z-0.000001F0.03	G01X-0.056250Z-0.000085F0.03
G01X-0.067235Z-0.000049F0.03	G01X-0.061742Z-0.000001F0.03	G01X-0.056061Z-0.000090F0.03
G01X-0.067045Z-0.000045F0.03	G01X-0.061553Z-0.000002F0.03	G01X-0.055871Z-0.000095F0.03
G01X-0.066856Z-0.000041F0.03	G01X-0.061364Z-0.000003F0.03	G01X-0.055682Z-0.000101F0.03
G01X-0.066667Z-0.000038F0.03	G01X-0.061174Z-0.000004F0.03	G01X-0.055492Z-0.000107F0.03
G01X-0.066477Z-0.000034F0.03	G01X-0.060985Z-0.000005F0.03	G01X-0.055303Z-0.000112F0.03
G01X-0.066288Z-0.000031F0.03	G01X-0.060795Z-0.000006F0.03	G01X-0.055114Z-0.000118F0.03
G01X-0.066098Z-0.000028F0.03	G01X-0.060606Z-0.000008F0.03	G01X-0.054924Z-0.000125F0.03

G01X-0.054735Z-0.000131F0.03	G01X-0.049053Z-0.000387F0.03	G01X-0.043371Z-0.000763F0.03
G01X-0.054545Z-0.000137F0.03	G01X-0.048864Z-0.000398F0.03	G01X-0.043182Z-0.000778F0.03
G01X-0.054356Z-0.000144F0.03	G01X-0.048674Z-0.000408F0.03	G01X-0.042992Z-0.000792F0.03
G01X-0.054167Z-0.000150F0.03	G01X-0.048485Z-0.000419F0.03	G01X-0.042803Z-0.000807F0.03
G01X-0.053977Z-0.000157F0.03	G01X-0.048295Z-0.000431F0.03	G01X-0.042614Z-0.000821F0.03
G01X-0.053788Z-0.000164F0.03	G01X-0.048106Z-0.000442F0.03	G01X-0.042424Z-0.000836F0.03
G01X-0.053598Z-0.000172F0.03	G01X-0.047917Z-0.000453F0.03	G01X-0.042235Z-0.000851F0.03
G01X-0.053409Z-0.000179F0.03	G01X-0.047727Z-0.000465F0.03	G01X-0.042045Z-0.000866F0.03
G01X-0.053220Z-0.000186F0.03	G01X-0.047538Z-0.000476F0.03	G01X-0.041856Z-0.000881F0.03
G01X-0.053030Z-0.000194F0.03	G01X-0.047348Z-0.000488F0.03	G01X-0.041667Z-0.000896F0.03
G01X-0.052841Z-0.000202F0.03	G01X-0.047159Z-0.000500F0.03	G01X-0.041477Z-0.000911F0.03
G01X-0.052652Z-0.000210F0.03	G01X-0.046970Z-0.000512F0.03	G01X-0.041288Z-0.000927F0.03
G01X-0.052462Z-0.000218F0.03	G01X-0.046780Z-0.000524F0.03	G01X-0.041098Z-0.000942F0.03
G01X-0.052273Z-0.000226F0.03	G01X-0.046591Z-0.000536F0.03	G01X-0.040909Z-0.000957F0.03
G01X-0.052083Z-0.000234F0.03	G01X-0.046402Z-0.000549F0.03	G01X-0.040720Z-0.000973F0.03
G01X-0.051894Z-0.000243F0.03	G01X-0.046212Z-0.000561F0.03	G01X-0.040530Z-0.000988F0.03
G01X-0.051705Z-0.000251F0.03	G01X-0.046023Z-0.000574F0.03	G01X-0.040341Z-0.001004F0.03
G01X-0.051515Z-0.000260F0.03	G01X-0.045833Z-0.000587F0.03	G01X-0.040152Z-0.001020F0.03
G01X-0.051326Z-0.000269F0.03	G01X-0.045644Z-0.000600F0.03	G01X-0.039962Z-0.001036F0.03
G01X-0.051136Z-0.000278F0.03	G01X-0.045455Z-0.000613F0.03	G01X-0.039773Z-0.001052F0.03
G01X-0.050947Z-0.000287F0.03	G01X-0.045265Z-0.000626F0.03	G01X-0.039583Z-0.001067F0.03
G01X-0.050758Z-0.000296F0.03	G01X-0.045076Z-0.000639F0.03	G01X-0.039394Z-0.001083F0.03
G01X-0.050568Z-0.000306F0.03	G01X-0.044886Z-0.000653F0.03	G01X-0.039205Z-0.001099F0.03
G01X-0.050379Z-0.000316F0.03	G01X-0.044697Z-0.000666F0.03	G01X-0.039015Z-0.001116F0.03
G01X-0.050189Z-0.000325F0.03	G01X-0.044508Z-0.000680F0.03	G01X-0.038826Z-0.001132F0.03
G01X-0.050000Z-0.000335F0.03	G01X-0.044318Z-0.000693F0.03	G01X-0.038636Z-0.001148F0.03
G01X-0.049811Z-0.000345F0.03	G01X-0.044129Z-0.000707F0.03	G01X-0.038447Z-0.001164F0.03
G01X-0.049621Z-0.000355F0.03	G01X-0.043939Z-0.000721F0.03	G01X-0.038258Z-0.001180F0.03
G01X-0.049432Z-0.000366F0.03	G01X-0.043750Z-0.000735F0.03	G01X-0.038068Z-0.001197F0.03
G01X-0.049242Z-0.000376F0.03	G01X-0.043561Z-0.000749F0.03	G01X-0.037879Z-0.001213F0.03

G01X-0.037689Z-0.001229F0.03	G01X-0.032008Z-0.001687F0.03	G01X-0.026326Z-0.001360F0.03
G01X-0.037500Z-0.001246F0.03	G01X-0.031818Z-0.001698F0.03	G01X-0.026136Z-0.001344F0.03
G01X-0.037311Z-0.001262F0.03	G01X-0.031629Z-0.001708F0.03	G01X-0.025947Z-0.001328F0.03
G01X-0.037121Z-0.001278F0.03	G01X-0.031439Z-0.001716F0.03	G01X-0.025758Z-0.001311F0.03
G01X-0.036932Z-0.001295F0.03	G01X-0.031250Z-0.001721F0.03	G01X-0.025568Z-0.001295F0.03
G01X-0.036742Z-0.001311F0.03	G01X-0.031061Z-0.001716F0.03	G01X-0.025379Z-0.001278F0.03
G01X-0.036553Z-0.001328F0.03	G01X-0.030871Z-0.001708F0.03	G01X-0.025189Z-0.001262F0.03
G01X-0.036364Z-0.001344F0.03	G01X-0.030682Z-0.001698F0.03	G01X-0.025000Z-0.001246F0.03
G01X-0.036174Z-0.001360F0.03	G01X-0.030492Z-0.001687F0.03	G01X-0.024811Z-0.001229F0.03
G01X-0.035985Z-0.001377F0.03	G01X-0.030303Z-0.001676F0.03	G01X-0.024621Z-0.001213F0.03
G01X-0.035795Z-0.001393F0.03	G01X-0.030114Z-0.001663F0.03	G01X-0.024432Z-0.001197F0.03
G01X-0.035606Z-0.001409F0.03	G01X-0.029924Z-0.001651F0.03	G01X-0.024242Z-0.001180F0.03
G01X-0.035417Z-0.001425F0.03	G01X-0.029735Z-0.001637F0.03	G01X-0.024053Z-0.001164F0.03
G01X-0.035227Z-0.001441F0.03	G01X-0.029545Z-0.001624F0.03	G01X-0.023864Z-0.001148F0.03
G01X-0.035038Z-0.001457F0.03	G01X-0.029356Z-0.001610F0.03	G01X-0.023674Z-0.001132F0.03
G01X-0.034848Z-0.001473F0.03	G01X-0.029167Z-0.001595F0.03	G01X-0.023485Z-0.001116F0.03
G01X-0.034659Z-0.001489F0.03	G01X-0.028977Z-0.001581F0.03	G01X-0.023295Z-0.001099F0.03
G01X-0.034470Z-0.001505F0.03	G01X-0.028788Z-0.001566F0.03	G01X-0.023106Z-0.001083F0.03
G01X-0.034280Z-0.001520F0.03	G01X-0.028598Z-0.001551F0.03	G01X-0.022917Z-0.001067F0.03
G01X-0.034091Z-0.001536F0.03	G01X-0.028409Z-0.001536F0.03	G01X-0.022727Z-0.001052F0.03
G01X-0.033902Z-0.001551F0.03	G01X-0.028220Z-0.001520F0.03	G01X-0.022538Z-0.001036F0.03
G01X-0.033712Z-0.001566F0.03	G01X-0.028030Z-0.001505F0.03	G01X-0.022348Z-0.001020F0.03
G01X-0.033523Z-0.001581F0.03	G01X-0.027841Z-0.001489F0.03	G01X-0.022159Z-0.001004F0.03
G01X-0.033333Z-0.001595F0.03	G01X-0.027652Z-0.001473F0.03	G01X-0.021970Z-0.000988F0.03
G01X-0.033144Z-0.001610F0.03	G01X-0.027462Z-0.001457F0.03	G01X-0.021780Z-0.000973F0.03
G01X-0.032955Z-0.001624F0.03	G01X-0.027273Z-0.001441F0.03	G01X-0.021591Z-0.000957F0.03
G01X-0.032765Z-0.001637F0.03	G01X-0.027083Z-0.001425F0.03	G01X-0.021402Z-0.000942F0.03
G01X-0.032576Z-0.001651F0.03	G01X-0.026894Z-0.001409F0.03	G01X-0.021212Z-0.000927F0.03
G01X-0.032386Z-0.001663F0.03	G01X-0.026705Z-0.001393F0.03	G01X-0.021023Z-0.000911F0.03
G01X-0.032197Z-0.001676F0.03	G01X-0.026515Z-0.001377F0.03	G01X-0.020833Z-0.000896F0.03

G01X-0.020644Z-0.000881F0.03	G01X-0.014962Z-0.000476F0.03	G01X-0.009280Z-0.000186F0.03
G01X-0.020455Z-0.000866F0.03	G01X-0.014773Z-0.000465F0.03	G01X-0.009091Z-0.000179F0.03
G01X-0.020265Z-0.000851F0.03	G01X-0.014583Z-0.000453F0.03	G01X-0.008902Z-0.000172F0.03
G01X-0.020076Z-0.000836F0.03	G01X-0.014394Z-0.000442F0.03	G01X-0.008712Z-0.000164F0.03
G01X-0.019886Z-0.000821F0.03	G01X-0.014205Z-0.000431F0.03	G01X-0.008523Z-0.000157F0.03
G01X-0.019697Z-0.000807F0.03	G01X-0.014015Z-0.000419F0.03	G01X-0.008333Z-0.000150F0.03
G01X-0.019508Z-0.000792F0.03	G01X-0.013826Z-0.000408F0.03	G01X-0.008144Z-0.000144F0.03
G01X-0.019318Z-0.000778F0.03	G01X-0.013636Z-0.000398F0.03	G01X-0.007955Z-0.000137F0.03
G01X-0.019129Z-0.000763F0.03	G01X-0.013447Z-0.000387F0.03	G01X-0.007765Z-0.000131F0.03
G01X-0.018939Z-0.000749F0.03	G01X-0.013258Z-0.000376F0.03	G01X-0.007576Z-0.000125F0.03
G01X-0.018750Z-0.000735F0.03	G01X-0.013068Z-0.000366F0.03	G01X-0.007386Z-0.000118F0.03
G01X-0.018561Z-0.000721F0.03	G01X-0.012879Z-0.000355F0.03	G01X-0.007197Z-0.000112F0.03
G01X-0.018371Z-0.000707F0.03	G01X-0.012689Z-0.000345F0.03	G01X-0.007008Z-0.000107F0.03
G01X-0.018182Z-0.000693F0.03	G01X-0.012500Z-0.000335F0.03	G01X-0.006818Z-0.000101F0.03
G01X-0.017992Z-0.000680F0.03	G01X-0.012311Z-0.000325F0.03	G01X-0.006629Z-0.000095F0.03
G01X-0.017803Z-0.000666F0.03	G01X-0.012121Z-0.000316F0.03	G01X-0.006439Z-0.000090F0.03
G01X-0.017614Z-0.000653F0.03	G01X-0.011932Z-0.000306F0.03	G01X-0.006250Z-0.000085F0.03
G01X-0.017424Z-0.000639F0.03	G01X-0.011742Z-0.000296F0.03	G01X-0.006061Z-0.000080F0.03
G01X-0.017235Z-0.000626F0.03	G01X-0.011553Z-0.000287F0.03	G01X-0.005871Z-0.000075F0.03
G01X-0.017045Z-0.000613F0.03	G01X-0.011364Z-0.000278F0.03	G01X-0.005682Z-0.000070F0.03
G01X-0.016856Z-0.000600F0.03	G01X-0.011174Z-0.000269F0.03	G01X-0.005492Z-0.000066F0.03
G01X-0.016667Z-0.000587F0.03	G01X-0.010985Z-0.000260F0.03	G01X-0.005303Z-0.000061F0.03
G01X-0.016477Z-0.000574F0.03	G01X-0.010795Z-0.000251F0.03	G01X-0.005114Z-0.000057F0.03
G01X-0.016288Z-0.000561F0.03	G01X-0.010606Z-0.000243F0.03	G01X-0.004924Z-0.000053F0.03
G01X-0.016098Z-0.000549F0.03	G01X-0.010417Z-0.000234F0.03	G01X-0.004735Z-0.000049F0.03
G01X-0.015909Z-0.000536F0.03	G01X-0.010227Z-0.000226F0.03	G01X-0.004545Z-0.000045F0.03
G01X-0.015720Z-0.000524F0.03	G01X-0.010038Z-0.000218F0.03	G01X-0.004356Z-0.000041F0.03
G01X-0.015530Z-0.000512F0.03	G01X-0.009848Z-0.000210F0.03	G01X-0.004167Z-0.000038F0.03
G01X-0.015341Z-0.000500F0.03	G01X-0.009659Z-0.000202F0.03	G01X-0.003977Z-0.000034F0.03
G01X-0.015152Z-0.000488F0.03	G01X-0.009470Z-0.000194F0.03	G01X-0.003788Z-0.000031F0.03

G01X-0.003598Z-0.000028F0.03	G01X-0.001894Z-0.000008F0.03	G01X-0.000189Z-0.000000F0.03
G01X-0.003409Z-0.000025F0.03	G01X-0.001705Z-0.000006F0.03	G01X0.000000Z0.000000F0.03
G01X-0.003220Z-0.000023F0.03	G01X-0.001515Z-0.000005F0.03	G04X1
G01X-0.003030Z-0.000020F0.03	G01X-0.001326Z-0.000004F0.03	G01X0.000000Z15F100
G01X-0.002841Z-0.000018F0.03	G01X-0.001136Z-0.000003F0.03	M29
G01X-0.002652Z-0.000015F0.03	G01X-0.000947Z-0.000002F0.03	M01
G01X-0.002462Z-0.000013F0.03	G01X-0.000758Z-0.000001F0.03	G01X0.000000Z100F500
G01X-0.002273Z-0.000011F0.03	G01X-0.000568Z-0.000001F0.03	M05
G01X-0.002083Z-0.000009F0.03	G01X-0.000379Z-0.000000F0.03	M30